universität wien

DIPLOMARBEIT

Titel der Diplomarbeit

The use of strontium isotope ratio measurements by MC-ICP-MS for fundamental studies on diagenesis and for the reconstruction of animal migration at the Celtic excavation site Roseldorf

Verfasserin

Sarah Theiner

angestrebter akademischer Grad

Magistra der Naturwissenschaften (Mag. rer. nat.)

Wien, 2011

Studienkennzahl lt. Studienblatt:	A 419
Studienrichtung lt. Studienblatt:	Diplomstudium Chemie
Betreuer:	Ao. Univ. Prof. DI Dr. Thomas Prohaska

‘Nescire autem quid ante quam natus sis acciderit,

id est semper esse puerum.

Quid enim est aetas hominis,

nisi ea memoria rerum veterum cum superiorum aetate contexitur?’

Cicero, Orator, 34, 120

‘Omnis illa, quae appellatur curiositas, quid aliud quaerit, quam de rerum cognitione laetitiam?’

Augustinus, De vera religione 94

Table of contents

Acknowledgments 6
Abstract 7
Zusammenfassung 8
1. Introduction and theoretical aspects 10
1.1. The strontium isotopic system 10
1.1.1. Sr isotope ratio measurements for (pre-) historic animal migration studies 13
1.2. Elements serving as dietary indicators 14
1.3. Isotope mapping – the concept of 'Isoscapes' 15
1.3.1. Oxygen and hydrogen based isoscapes 15
1.3.2. Carbon based isoscapes 16
1.3.3. Strontium based isoscapes 17
1.3.4. Global isotope databases for hydrogen and oxygen 18
1.3.5. Limitations, challenges and future perspectives of isoscapes 19
1.3.6. Objective of this study 19
1.4. Diagenesis of bone and tooth matrices 20
1.4.1. Solubility profile methods 21
1.4.2. Chemical imaging and spectroscopic techniques 23
1.4.3. Objective of this study 23
1.5. Human and animal dentition 24
1.5.1. Dental structure of humans 25
1.5.2. Dental structure of ruminants 26
1.5.3. Dental structure of horses 27
1.5.4. The potential of animal teeth for studying ecological processes 28
1.6. Bone structure and elemental turnover 29
1.6.1. Objective of this study 29
1.7. The Celtic settlement site Roseldorf 31
1.7.1. The 'sanctuaries' of Roseldorf 32
1.7.2. Archaeozoological studies of Roseldorf's animal remains 34
1.7.3. Objective of this study 34
1.8. Strontium isotope ratio measurements by ICP-MS 35

1.8.1. Inductively Coupled Plasma-Mass Spectrometry (ICP-MS) 35
1.8.2. Interferences in ICP-MS on the example of Sr 37
2. Materials and Methods 39
2.1. Reagents and Materials 39
2.2. Sample material 40
2.2.1. Tooth material for the diagenesis study 40
2.2.2. Recent sheep hard tissues for the investigation of Sr turnover 41
2.2.3. Sample material from Roseldorf 42
2.3. Sample preparation 48
2.3.1. Diagenesis study and sequential leaching procedure 48
2.3.2. The investigation of Sr turnover in sheep hard tissues 49
2.3.3. Roseldorf 49
2.3.4. Sr/matrix separation 51
2.4. Instrumentation 52
2.4.1. The ICP-QMS instrument (ICP-QMS ELAN DRC e) 52
2.4.2. The multiple collector sector field instrument (MC-ICP-SFMS Nu Plasma) 54
2.4.3. Data processing 56
3. Results and Discussion 58
3.1. Diagenesis study of tooth and bone matrices 58
3.1.1. Human tooth dentine and enamel 58
3.1.2. Animal tooth dentine and bone 63
3.1.3. General observations 69
3.2. Investigation of Sr turnover in sheep hard tissues 73
3.2.1. Jaw bone of the sheep ‘Stronzi’ 73
3.2.2. Jaw bone of the ^{86}Sr spiked sheep ‘Anja’ 75
3.3. The Celtic excavation site Roseldorf 78
3.3.1. Sr isotope mapping 78
3.3.2. The local range of the Celtic settlement site Roseldorf 83
3.3.3. Human and animal tooth samples of the Celtic excavation site Roseldorf 85
3.3.4. Multielemental analysis 93
4. Summary and Conclusion 95
4.1. Diagenesis study of tooth and bone matrices 95

4.2. Sr turnover in sheep hard tissues....96
4.3. The Celtic excavation site Roseldorf....96
5. Future perspectives....99
5.1. Diagenesis study of teeth and bone matrices....99
5.2. Investigation of Sr turnover in sheep hard tissues....99
5.3. The Celtic excavation site Roseldorf....100
6. Bibliographies....101
7. Appendix....117
7.1 Certificates of Analysis....117
7.2. Measurement results....119
7.2.1. Diagenesis study of teeth and bone matrices....119
7.2.2. $^{87}Sr/^{86}Sr$ ratios of sheeps....138
7.2.3. $^{87}Sr/^{86}Sr$ ratios Roseldorf....139
7.2.4. Multielementdata Roseldorf....143
7.4. List of Tables....147
7.5. List of Figures....148
7.6. List of Abbreviations....150

Acknowledgments

Primarily, I would like thank my supervisor Thomas Prohaska who enabled me to work on an interesting and challenging diploma thesis where I was able to combine my favorite research fields of analytical chemistry and history. He created a group with a great and enjoyable working atmosphere. I have gained a lot of new experiences and developed myself further in the last months due to scientific exchange, the numerous presentations and the cooperative working spirit. It was a pleasure to be part of the VIRIS group.
Many thanks to the whole VIRIS team including Johanna, Kathi, Lubna, Moni, Regina, Steffi, Christopher for his patience by my measurements, Andi for just being Andi and Dominique for her help in the lab and her mental support.
Especially Johanna needs to be pointed out as she has been my supervisor, my mentor and my greatest support during all the months of my work for my diploma thesis. Johanna has always had an open ear for me, she explained me everything and has never lost the patience with me asking numerous questions.

Furthermore, I would like to thank Maria Teschler-Nicola and Erich Pucher from the Natural History Museum of Vienna who not only provided archaeological sample material to me, but who also gave me an interesting insight in the completely different research fields of anthropology and archaeozoology.

Many thanks go to my best friends Eva and Karim for listening and just being there.
I would also like to express my thanks to my chemistry teacher Erwin Klein – it was because of him that I came up with the crazy idea to study chemistry.

Special thanks to my family, grandmothers and grandfathers, aunts and uncles, cousins… for their mental and also financial support.

Above all, I want to say thank you to Karin and Gerhard, my parents who have guided me through all the stages of my life, no matter how difficult they were. They have always stood behind me and my decisions and I can be sure about their help and support!

Abstract

The application of strontium isotope ratio measurements in anthropological and archaeological research offers the possibility to elucidate historical questions including human and animal migration, the reconstruction of ancient trade routes and may shed light on cultic practises and social concepts of (pre-) historic societies.

The ubiquity of strontium in the environment, the natural variation and regional differences of its isotopic composition permit tracing the origin of e.g. human and animal individuals.

The Celtic central settlement site Roseldorf (Lower Austria) represents a very important and impressive find spot of Latène culture (approx. 300 BC) in Austria. Not only the dimension of the settlement and the amount of unique archaeological findings (e.g. weapons, coins, iron crown), but also several settlement structures, identified as sanctuaries and comprising huge amounts of fragmented animal and human skeletal remains are of particular concern for the reconstruction of ritual behaviour of Celts in this region. Archaeozoological morphology studies of cattle and horse bone material seem to indicate the presence of non-autochthonous animals in Roseldorf and point to their Italian provenance. The topic of this diploma thesis was to determine strontium isotope ratios of cattle, horse and human tooth samples using Multiple Collector-Inductively Coupled Plasma-Mass Spectrometry (MC-ICP-MS) which were compared to the local strontium signal represented by environmental samples from area in and around the excavation site close to Roseldorf. The characteristic strontium isotope signatures have the potential to give an indication about the origin of the examined individuals in order to assess animal and human mobility and to draw conclusions about possible trading contacts practised by the Celtic settlers of Roseldorf.

When analysing archaeological fossils, problems have emerged concerning the alteration of the investigated material due to interactions with the burial environment and the availability of biological strontium (diagenesis). A sequential leaching technique, involving weak acid, was tested in order to remove diagenetic strontium of human and animal dental and bone material derived from the medieval excavation site Gars Thunau (Lower Austria).

Additionally, the turnover rate and metabolism of strontium in biological tissues was investigated by monitoring the incorporation of strontium into bone of recent sheep.

Zusammenfassung

Die Anwendung von Strontiumisotopenmessungen im Bereich der anthropologischen und archäologischen Forschung bietet die Möglichkeit, Aufschlüsse über historische Fragestellungen zu erlangen, die Migrationsbewegungen von Menschen und Tieren und die Rekonstruktion von antiken Handelsrouten beinhalten, und somit Licht auf kultische Praktiken und soziale Konzepte (prä-) historischer Gesellschaften werfen. Die Ubiquität von Strontium in der Umwelt, die natürliche Variation und die regionalen Unterschiede seiner Isotopenzusammensetzung erlauben die Herkunft und Wanderungen von zum Beispiel Menschen und tierischen Individuen nachzuverfolgen.

Die keltische Zentralsiedlung Roseldorf (Niederösterreich) repräsentiert einen sehr wichtigen und beeindruckenden Fundort der Latène-Kultur (ca. 300 v. Chr.) in Österreich. Nicht nur die Dimension der Siedlung und die Menge an einzigartigem archäologischem Fundmaterial (z.B. Waffen, Münzen, Eisenkrone), sondern auch einige Siedlungsstrukturen, die als Heiligtümer identifiziert wurden und große Mengen an fragmentierten tierischen und menschlichen Skelettüberresten beinhalten, sind von großer Bedeutung für die Rekonstruktion von rituellen Praktiken der Kelten in dieser Region. Archäozoologische Studien, die Morphologie von Knochenmaterial von Rindern und Pferden betreffend, scheinen auf das Vorhandensein von nicht autochthonen Tieren in Roseldorf und deren italienischen Ursprung hinzuweisen.

Die Strontiumisotopenverhältnisse von Rinder-, Pferden- und Menschenzahnproben wurden im Rahmen dieser Arbeit mittels Multi Kollektor-Induktiv Gekoppeltes Plasma-Massenspektrometrie (MC-ICP-MS) bestimmt und mit dem lokalen Strontiumsignal, das von Umweltproben aus Roseldorf selbst, aber auch aus seiner Umgebung, repräsentiert wird, verglichen. Die charakteristischen Strontiumsignaturen können einen Hinweis über die Herkunft des untersuchten Individuums geben, um die Wanderungsbewegung von Menschen und Tieren einschätzen und um Rückschlüsse über mögliche Handelskontakte der keltischen Siedler in Roseldorf ziehen zu können.

Bei der Analyse von archäologischen Fossilien können Probleme bezüglich der Veränderung des Probenmaterials aufgrund von Interaktionen mit der Grabungsumgebung und der Verfügbarkeit von biologischem Strontium auftreten (Diagenese). Ein sequentielles „Extraktionsverfahren“ mittels einer schwachen Säure wurde getestet, um diagenetisches

Strontium aus dem Zahn- und Knochenmaterial von Menschen und Tieren der mittelalterlichen Ausgrabung Gars Thunau (Niederösterreich) zu entfernen.

Zusätzlich wurde die Umsatzrate und der Metabolismus von Strontium in biologischem Gewebe durch die Beobachtung des Einbaus von Strontium in Knochen von rezenten Schafen untersucht.

1. Introduction and theoretical aspects

1.1. The strontium isotopic system

Strontium (Sr) is an alkaline earth element with four naturally occurring isotopes including the three non–radiogenic ^{84}Sr, ^{86}Sr and ^{88}Sr and the radiogenic ^{87}Sr. The isotopes of the alkali metal rubidium (Rb) are ^{85}Rb and ^{87}Rb (Capo et al. 1998).

The relative abundances set by the International Union of Pure and Applied Chemistry (IUPAC) of the Sr and Rb isotopes are shown in Table 1 (Capo et al. 1998).

Isotope	Abundance
^{84}Sr	0.56
^{86}Sr	9.87
^{87}Sr	7.04
^{88}Sr	82.53
^{85}Rb	72.17
^{87}Rb	27.83

Tab. 1 Isotope abundances of Sr and Rb

The isotope ^{87}Sr is formed as a daughter nuclide by the radioactive β^- decay of ^{87}Rb with a half-life of about 48.8×10^9 years (Steiger and Jaeger 1977). This reaction leads to a natural variation of the $^{87}Sr/^{86}Sr$ ratio in rocks which is dependent on the (initial) relative Rb content and the age of the geological material. Strontium isotopic signatures are conveyed through weathering processes from the rocks into the soil and the stream- and groundwater and enter the human and animal food chain via water, plants and animals. The fact that the ionic radius of Sr (1.18 Å) is similar to that of calcium (1.00 Å) permits e.g. the substitution of Sr for Ca in hydroxyapatite $Ca_{10}(PO_4)_6(OH)_2$ and leads to the incorporation of Sr into human and animal hard tissues (Capo et al. 1998). The biologically available Sr pool in soil is mostly influenced by mineral weathering and by ground and stream waters, atmospheric deposition and fertilizers (Bentley 2006).

Due to the relatively small differences between the isotope masses of heavy elements, no significant Sr isotope fractionation occurs during cycling through biogeochemical processes, compared with the amount of fractionation of isotopes from lighter elements such as oxygen, carbon and nitrogen (Capo et al. 1998). The correlation of the bioavailable strontium isotopic composition of the geological area and the diet with the strontium ratios of skeletal tissues allows the distinction of migrants from local individuals (Bentley 2006).

The unique properties of strontium including its ubiquity and its behaviour within the natural cycle, offer its application as a tracer in various scientific disciplines. Strontium isotope ratio measurements are a versatile and commonly used tool in anthropological, archaeological and archaeozoological research for the investigation of population dynamic processes including human migration (Huemer 2008; Schweissing and Grupe 2003; Irrgeher et al. 2010; Teschler-Nicola et al. 1999) and animal mobility (Balasse et al. 2002; Viner et al. 2010). In Table 2 recent studies are listed that are dealing with human migration and the identification of local and non-local individuals using Sr isotope ratio measurements. Strontium isotope analyses can also reveal information about animal husbandry techniques (Evans et al. 2007), ancient trade routes (Walton et al. 2009), dietary patterns and thus the lifestyle of prehistoric societies (Chenery et al. 2010; Smits et al. 2010). Applications include the provenance of ancient artefacts such as wood (Horsky 2010) and metal objects (Balcaen et al. 2010), food authenticity studies (Brunner 2007; Rodrigues et al. 2011) and the investigation of ecological systems using fish and its migration pattern (Sturm 2008; Zitek et al. 2010). ICP-MS instruments serve as analytical method for the determination of Sr isotope ratios (see chapter 1.8.) (Prohaska et al. 2002; Latkoczy et al. 1998).

time period	**investigated area**	**literature reference**
Roman period	Britain	(Chenery et al. 2011)
Iron Age	Thailand	(Cox et al. 2011)
600 – 1000 AD	Beringa, Peru	(Knudson and Tung 2011)
Neolithic period	Japan	(Kusaka et al. 2011)
Roman period	Britain	(Müldner et al. 2011)
600 – 1000 AD	Conchopata, Peru	(Tung and Knudson 2011)
Roman period	Britain	(Chenery et al. 2010)

Classic Maya period	Copan, Honduras	(Price et al. 2010)
900-1000 AD	Gars/Thunau, Lower Austria	(Prohaska et al. 2010)
~1500 BC	Bismarck Archipelago	(Shaw et al. 2010)
Neolithic period	Rhine Basin, Germany	(Smits et al. 2010)
Maya period	Guatemala	(Wright et al. 2010)
Inca period	Valley of Cuzco, Peru	(Andrushko et al. 2009)
0-1500 AD	Nasca, Peru	(Conlee et al. 2009)
Roman period	York, Britain	(Leach et al. 2009)
$11^{th}/12^{th}$ century AD	Near and Middle East	(Mitchell and Millard 2009)
Neolithic period	Germany	(Nehlich et al. 2009)
Byzanthic period	Jordan	(Perry et al. 2009)
~1500 BC	Bismarck Archipelago	(Shaw et al. 2009)
17^{th} – 19^{th} century	Barbados	(Schroeder et al. 2009)
Middle Holocene	Lake Baikal, Sibiria	(Haverkort et al. 2008)
500 – 1100 AD	Peru	(Knudson 2008)
Mycenaean period	Crete, Greece	(Nafplioti 2008)
200 – 300 AD	Western Jordan	(Perry et al. 2008)
Neanderthal	Lakonis, Greece	(Richards et al. 2008)
~1500 BC	Vanuatu	(Bentley et al. 2007)
New Kingdom period	Nile Valley, Egypt	(Buzon et al. 2007)
1000 – 1300 AD	Peru	(Knudson and Buikstra 2007)
900 – 1300 BC	Aztalan, USA	(Price et al. 2007)
Neolithic period	Germany	(Price et al. 2006b)
16^{th} century	Campeche, Mexico	(Price et al. 2006a)
750 – 1000 AD	Iceland	(Price and Gestsdóttir 2006)
Anglo – Saxon period	Britain	(Montgomery et al. 2005)
Neolithic period	Schletz, Lower Austria	(Teschler-Nicola et al. 2005)
Maya period	Tikal, Guatemala	(Wright 2005)

Tab. 2 Human migration studies based on Sr isotope ratio measurements

1.1.1. Sr isotope ratio measurements for (pre-) historic animal migration studies

The assessment of (pre-) historic animal migration by Sr isotope ratio measurements is used for the reconstruction of animal husbandry techniques, hunting strategies, ritual practices and trade routes of ancient societies and of palaeoenvironmental and climatic conditions.

Britton et al. (2011) applied a sequential sampling method (see chapter 1.5.4.) on the tooth enamel of Pleistocene reindeer and bison tooth enamel in order to get a temporally resolved record of the Sr isotopic composition. It was possible to reconstruct seasonally variable herd movements of the investigated species and to gain information about the palaeoenvironment and Neanderthal hunting strategies at the archaeological site of Jonzac in France (Britton et al. 2011). The potential of the use of intra-tooth sampling for the reconstruction of herd movements was tested by Britton et al. (2009) in modern caribou enamel in Alaska. The obtained variation in the Sr isotopic record of the animal individuals correlated with the known movements of the herd and the geological background the animals traversed (Britton et al. 2009).

Towers et al. (2010) investigated the origin of cattle remains at two excavation sites in Britain to get an insight in funeral practices and trading contacts in the Bronze Age (Towers et al. 2010). Viner et al. (2010) determined the Sr isotope ratios of 13 cattle enamel excavated from the Neolithic site Durrington Walls, Britain. The comparison with the Sr isotopic composition of local vegetation samples and the geological background of Britain allowed them to draw conclusions about their origin. The results for 11 cattle, identified as non-local animals, indicated their transport over long distances from different parts of Britain (Viner et al. 2010).

The reconstruction of animal husbandry techniques reveals information about the lifestyle of prehistoric societies. Evans et al. (2007) observed distinct differences in the Sr isotopic composition of cattle, pig and sheep tooth enamel of two Anglo-Saxon settlements in central England. As the two sites are underlined by the same geological background, the difference in Sr isotope ratios is considered to be caused by different grazing and feeding patterns (Evans et al. 2007). Bendrey et al. (2009) distinguished between domestic and free-roaming horses by the analysis of horse tooth enamel of two sites from the Iron Age in Britain. They demonstrated the movement of horses over long distances (Bendrey et al. 2009).

Hoppe and Koch (2007) reconstructed the migratory behaviour of Pleistocene mammals in Florida, USA. They attributed a change in the movement pattern over time to changing climatic conditions and vegetation structures (Hoppe and Koch 2007).

The determination of Sr isotope ratios in animal enamel was used to reconstruct herd movement patterns and herding strategies in South Africa and to give an indication about feeding grounds (Radloff et al. 2010; Smith et al. 2010). Ranging habits of horses and red deer of the late glacial period in central period were defined in order to draw conclusions about the movement of hunter-gatherer (Pellegrini et al. 2008).

1.2. Elements serving as dietary indicators

The elemental composition of mammalian bone and tooth material can point to different dietary habits and patterns. Elements relevant for this work will be discussed in the following.

The phenomenon that mammalian organisms tend to assimilate Ca in preference to Sr and Ba is known as 'biopurification'. This effect is enhanced by the increased excretion of these elements compared to Ca (Burton et al. 1999). As a result of Sr and Ba discrimination, the Sr/Ca and the Ba/Ca ratios decrease with ascending trophic position in the food chain. As a consequence, herbivores show lower Sr/Ca and Ba/Ca ratios than the plants they consume. Carnivores have lower values than their food source and than herbivores (Burton et al. 1999).

Seawater and marine species exhibit significantly lower Ba/Sr ratios than terrestrial sources. The determination of the Ba/Sr ratio could therefore be used for the reconstruction of the amount of marine consumption (Burton and Price 1990). Sr/Ca and Ba/Ca ratios have been proved to serve as adequate paleodietary indicators and tracers for studying fossil ecosystems. Studies focused on the determination of these parameters in archaeological fossils to distinguish between herbivores, carnivores and omnivores in prehistoric societies and to assess the composition of prehistoric diets (Sponheimer et al. 2005b; Sponheimer et al. 2005a; Anne Katzenberg and Harrison 1997; Velasco-Vásquez et al. 1997).

1.3. Isotope mapping – the concept of 'Isoscapes'

Variations in geographical, topographical, climatic and geological conditions in the earth's biosphere result in spatial and temporal distributions of the ratios of stable isotopes in environmental matrices. Different isotope systems with different potentials can be used for the establishment of isotope reference maps ('isoscapes') and databases for isotope based studies (Bowen 2010). The understanding of the underlying mechanistic processes, leading to characteristic isotopic pattern, is a key factor for facilitating isoscape predictability along with the spatial resolution and temporal stability of the assessed data. Isoscapes have the potential to serve as a useful tool in various scientific disciplines studying changes in the earth's biosphere such as in hydrological, ecological or anthropological systems. Applications lie in archaeological research, the analysis of climate processes and dynamics, in forensic and food authentication studies (West et al. 2010).

Isotope data are conventionally reported in absolute ratios or in δ–notation in units of per mil (Equ. 1).

Equ. 1

$$\delta_{ref} = \left(\frac{R_{samp} - R_{ref}}{R_{ref}} \right) \times 1000$$

δ_{ref} is the isotope ratio of the sample (R_{samp}) expressed in delta units (‰,per mil) relative to the isotope ratio of an international standard (R_{ref}). E.g. the standard Vienna Standard Mean Ocean Water (VSMOW) can be used for oxygen and hydrogen (West et al. 2010). In case of the carbon isotope system Pee Dee Belimnite (PDB) can serve as reference standard (Werner and Brand 2001). Specific isoscapes are discussed in the following chapters with a focus on the use in human migration studies.

1.3.1. Oxygen and hydrogen based isoscapes

The behaviour of hydrogen and oxygen isotopes in the hydrological circle results in their natural spatial isotopic distribution at the global scale. The variation in the hydrogen and oxygen isotopic ratios is caused by climatic and geographical factors including temperature, altitude, latitude and seasonally and annually variable precipitation. The hydrogen and

oxygen isotopes of water in the rainfall are shifted to lighter ones when clouds move over land masses and toward higher latitudes. As a consequence, the $^{18}O/^{16}O$ ratio of water declines with decreasing temperature, increasing altitude and distance from the coast (Kohn et al. 1998; Sponheimer and Lee-Thorp 1999). The $^{18}O/^{16}O$ ratios of skeletal tissues can either be determined in phosphate or in carbonate oxygen in hydroxyapatite. The obtained $^{18}O/^{16}O$ ratio reflects the average $^{18}O/^{16}O$ ratios of all water sources ingested by an individual (Longinelli 1984). Price et al. (2010) mapped oxygen ratios for Mesoamerica using enamel carbonate and bone phosphate from different archaeological sites and combined them with strontium isotope data (Price et al. 2010). Lachniet and Patterson (2009) mapped the $^{18}O/^{16}O$ ratios of surface waters in Guatemala and Belize to draw conclusions about precipitation and climatic changes in this region (Lachniet and Patterson 2009). Wassenaar et al. (2009) created a $\delta^{2}H$ and $\delta^{18}O$ groundwater isoscape for Mexico collecting water samples all over the country. Moreover, they developed a predictive model for the spatial isotopic patterns of hydrogen and oxygen on the basis of elevation, latitude and rainfall as main input parameters (Wassenaar et al. 2009).

1.3.2. Carbon based isoscapes

The spatial variation of $\delta^{13}C$ values depends on the different ^{13}C fractionation in plants due to differences during the process of photosynthesis. Plants can be divided in two groups using the C_3 or C_4 photosynthesis pathway. C_3 plants include wheat, barley, rice, cool season grasses and trees. Plants adapted to hot and dry climate such as tropical grasses, maize, millet and sorghum employ the more water-efficient C_4 photosynthesis. In general, $^{12}CO_2$ is preferentially assimilated to $^{13}CO_2$ during photosynthesis. The discrimination against ^{13}C is larger in C_3 than in C_4 plants. The distribution of $\delta^{13}C$ values on the global scale is related to the spatial variations in the relative abundances of C_3 and C_4 plants. The climatic conditions and the vegetation structure of a region serve as parameters for an estimation of a spatial stable carbon isotopic distribution. The $^{13}C/^{12}C$ ratio of the diet ingested by an individual is reflected in $\delta^{13}C$ of structural CO_3 in hydroxyapatite of bones and teeth (West et al. 2010).
Boeckx et al. (2006) used soil and plant samples to analyse the $\delta^{13}C$ values of the area of the city Gent in Belgium and to draw conclusions about land use and agriculture (Boeckx et al. 2006). Quillfeldt et al. (2010) determined the $^{13}C/^{12}C$ ratios of seabird feathers to track their

migration. A distinction between movement to polar regions and warmer waters was able due to the carbon stable isotope composition of the feathers (Quillfeldt et al. 2010).

1.3.3. Strontium based isoscapes

The use of isoscapes based on Sr isotope ratios, in contrast to the previously mentioned isotopic systems, has the advantage of a low temporal variability of $^{87}Sr/^{86}Sr$ ratios due to the formation time of billion years for ^{87}Sr (West et al. 2010).

The main challenge for the generation of spatial patterns of Sr isotopes by correlation of the $^{87}Sr/^{86}Sr$ ratio to a geographic coordinate is the choice of proxy materials to establish local Sr isotopic signals. One method to create $^{87}Sr/^{86}Sr$ isoscapes is the use of data about the underlying geology of a geographical area. Estimations of $^{87}Sr/^{86}Sr$ ratios can be made for specific areas on the basis of the age and lithology of bedrock (Evans et al. 2010). By the development of a geologic-based $^{87}Sr/^{86}Sr$ prediction model some factors have to be considered. Sedimentary rocks may contain multiple age and lithologic components and weathering rates differ among rock types (West et al. 2010). Moreover the $^{87}Sr/^{86}Sr$ ratios in soil, water, flora and fauna can differ significantly from the parent rock material. Therefore it is necessary to determine the biologically available Sr fraction of a specific region (Blum and Erel 1997). Different environmental matrices have been used as proxy material in several studies to produce $^{87}Sr/^{86}Sr$ isoscapes of a specific region (Tab. 3).

Evans et al. (2009) proposed the use of faunal and river samples as reliable reservoir of the biologically available Sr fraction of a region. Plants reflect the mobilised labile Sr fraction taken up by the roots from the soil and rivers those of their catchment areas (Evans et al. 2009). A $^{87}Sr/^{86}Sr$ map of the island of Skye and of Britain was created with this approach (Evans et al. 2009; Evans et al. 2010).

Bentley and Knipper (2005) analysed archaeological pig enamel to map the biologically available strontium, carbon and oxygen isotopic signatures of prehistoric southern Germany. Pigs are omnivorous, domestic animals and are considered to reflect the human dietary intake (Bentley and Knipper 2005).

Due to the immense number of different utilizations of the Sr isotopic systems in various scientific disciplines, $^{87}Sr/^{86}Sr$ isoscapes are adapted to their application on a large or small scale (West et al. 2010).

proxy material representing bioavailable Sr	$^{87}Sr/^{86}Sr$ mapped region	literature reference
fauna, river water	Isle of Skye	(Evans et al. 2010)
fauna, river water	Britain	(Evans et al. 2010)
archaeological pig enamel	southern Germany	(Bentley and Knipper 2005)
surface waters	Denmark	(Frei and Frei 2011)
archaeological bone and enamel, snail shells	mainland and islands of the Aegean region	(Nafplioti 2011)
bedrock material, water, soil, faunal samples	Maya region in Mesoamerica (Guatemala, Yucatan)	(Hoddell et al. 2004)
modern animal bone, ancient human enamel	Mesoamerica	(Price et al. 2006a; Price et al. 2010)
archaeological fauna	Midwestern United States	(Hedman et al. 2009)
stream sediments	central Japan	(Asahara et al. 2006)
archaeological human and pig enamel	Bismarck Archipelago	(Shaw et al. 2010)
recent rodent material	Western Cape in South Africa	(Radloff et al. 2010)

Tab. 3 Strategies for generating $^{87}Sr/^{86}Sr$ isoscapes

1.3.4. Global isotope databases for hydrogen and oxygen

Databases of the isotopic composition on the global scale have increasingly been installed and updated, especially by the International Atomic Energy Agency (IAEA). The Global Network for Isotopes in Precipitation (GNIP) provides global maps of δ^2H and $\delta^{18}O$ in precipitation. GNIP stations all over the world continuously record meteorological data and collect monthly precipitation samples for isotope analyses since the 1960's. The main problem is the inhomogeneous geographical coverage and temporal distribution of GNIP stations resulting in a small number of stations with a long-term record. The Global Network of Isotopes in Rivers (GNIR) and the IAEA–Terrestrial Water Isotope Network (IAEA-TWIN) represent compilations of the isotope compositions of surface waters and groundwaters (West et al. 2010).

1.3.5. Limitations, challenges and future perspectives of isoscapes

The need for time-explicit isotope maps, the high sampling density, the continuity of spatial datasets over multi-year timescales and a compromise between specificity and generality represent on the one hand limiting factors for the creation of isoscapes, but on the other hand main challenges. Effort must be taken in the expansion of global monitoring programs for the collection of isotope and meteorological data to provide global isotope maps and databases. Basic research of mechanistic processes of isotope systems is a prerequisite for the further development of predictive models for isoscapes. Those models have to work at large and fine-scale resolutions (West et al. 2010).

1.3.6. Objective of this study

The aim of this study was the establishment of a spatial $^{87}Sr/^{86}Sr$ isoscape for the geologically highly variable region of the north-western Weinviertel. Soil, water and recent fauna samples were collected and analysed due to their biologically available Sr isotopic composition. The obtained data were related to the underlying geology in order to generate a geochemical map of this region.

1.4. Diagenesis of bone and tooth matrices

The interactions between skeletal remains and its surrounding burial environment over geological and historical time periods can lead to significant alterations of the biological, chemical and physical properties of skeletal tissues. The reliability of information deduced from prehistoric bones and teeth is therefore limited by the fact that diagenetic processes can occur during deposition. The determination of the preservation state of the analysed object, the knowledge and the degree of the possible alteration, the understanding of post-mortem transformation mechanisms and the removal of diagenetic strontium may serve as key factors for the exclusion of incorrect interpretations drawn from analytical artefacts (Budd et al. 2000). The structural differences (including protein contents, crystal size and porosity) of bones and tooth dentine and enamel result in different responses to diagenetic processes. Bone and dentine show a similar matrix structure with large pores. Due to its hard and dense structure, enamel is considered to be less affected by post-burial contamination than bone and dentine (Dauphin and Williams 2004).

The complexity of diagenetic processes results from different alteration rates of chemical elements within each tissue and from site-specific contamination mechanisms. This means that each archaeological material experienced its unique diagenetic history (Price et al. 2002). Nevertheless, there are some main parameters of the burial environment that show an influence on the extent of diagenesis (Smith et al. 2007; Hedges 2002):

- pH-value
- redox potential
- humidity
- temperature
- activity of microorganisms

Diagenetic trajectories of archaeological tissues are determined by the initial taphonomy, representing the early preservation state, and the long-term soil conditions (Smith et al. 2007). In the early stages after deposition, rapid deterioration is caused by the activity of microorganisms, resulting in histological damage and collagen loss. Macroscopic damage occurs in acidic soils due to higher mineral dissolution rates, while in benign soils the skeletal remain is considered to be more affected by microbial attack (Nielsen-Marsh et al. 2007). The mutual interaction of the parameters leads to an enhancement of diagenetic processes.

Dissolution increases the porosity of the bone, while larger pores accelerate the dissolution rate. This kind of feedback mechanism is called 'catastrophic mineral dissolution' (Pike et al. 2001). The elemental diffusion and distribution in a diagenetically altered object plays an important role to assess the extent of diagenesis and to draw conclusions about the preservation state (Trueman et al. 2008).

After the stop of the living functions of an organism, the mineralization pattern of hard tissues can undergo severe transformation. The following processes of incorporation of diagenetic Sr in biological tissues can occur during deposition (Nelson et al. 1986):

- pore-filling by secondary minerals
- absorption in microcracks or onto the surfaces of original hydroxyapatite crystals
- recrystallization or remineralization of hydroxyapatite
- direct exchange with Ca or biogenic Sr in the original hydroxyapatite crystals

1.4.1. Solubility profile methods

Until now, studies on tracing prehistoric migration and dietary habits are restricted to the use of enamel and can therefore focus on a short life period only. The investigation of archaeological tooth dentine and bone material would provide information about the whole lifespan of an individual but is of limited use because of post-burial contamination. Therefore the distinction and separation between biogenic and diagenetic Sr is necessary to guarantee the integrity of the information gained from those materials. Several pre-treatment procedures have been tested, modified and used in several studies, in order to recover the biogenic Sr and to analyse the originally up taken signal (Nelson et al. 1986; Sillen and Sealy 1995; Budd et al. 2000). It should be possible to remove diagenetic Sr in secondary minerals and absorbed onto surfaces using weak acids. If Sr was incorporated into hydroxyapatite by recrystallization or exchange, the isolation of biogenic Sr might cause problems (Nelson et al. 1986; Sillen 1986).

The methods used are usually based on the different solubility behaviour of carbonate-, hydroxy- and fluorapatites. Geros and Tung (1983) exposed apatites, containing different amounts of carbonate and fluoride, to acid buffer, in order to test their chemical stability. They demonstrated that the presence of fluoride retards the dissolution of apatite in acid media, while a high carbonate content acts as a promoter. The explanation of this observed phenomenon might possibly be the effect of carbonate and fluoride on the structural

properties of apatites. Incorporation of carbonate leads to a reduction in crystallite size and to an increase in surface area and crystal strain, while the substitution of fluoride shows the opposite effect (LeGeros and Tung 1983). Fox et al. (1983) came to the conclusion that even low levels of fluorapatite significantly enhance the acid resistance (Fox et al. 1983).

Nelson et al. (1986) observed different Sr isotopic compositions in marine animal bones buried in terrestrial sediments. They used a pre-treatment procedure, including ashing of the specimens and leaching with 50:50 (v/v) acetic acid/H_2O to recover the original (marine) Sr isotopic signature (Nelson et al. 1986).

Sillen (1986) proposed a sequential leaching method, including 25 consecutive washing steps, using 0.1 M acetic acid/sodium acetate buffer, adjusted to pH 4.5 to remove diagenetic Sr (Sillen 1986). Sillen and Sealy (1995) demonstrated that the protocol used by Nelson et al. (1986) induces severe changes in the apatite structure, while Sillen's protocol does not cause analytical artefacts (Sillen and Sealy 1995).

Based on the results of this solubility profile procedure applied on fossil minerals from Ethiopia and additional spectrometry data, Sillen (1986) suggested a division of the leachates into four compartments:

- Compartment I (fractions 1 and 2) representing the most soluble compartment
- Compartment II (fractions 2-6): dissolution of a poorly crystalline, high carbonate apatite
- Compartment III (fractions 7-25): presence of biogenic mineral
- Compartment IV (residues) containing fluorapatite originating from fluoride-incorporation

Dissolution of high soluble calcareous secondary minerals (e.g. calcite) results in an increased Ca/P ratio in compartment I compared to the stable values of compartment II and III (Sillen 1986). Nelson (1981) documented a range for Ca/P ratio for molar tooth enamel between 1.48-1.67 (Nelson 1981). The Sr/Ca ratio is a valuable parameter to be observed during the solubility profile method as it reflects the trophic level of an organism (see chapter 1.2.). Enamel is developed during childhood when discrimination against Sr may not have developed fully. Therefore, studies focus on archaeological bones to get an insight in prehistoric dietary habits. The susceptibility of fossil bone material to diagenetic effects made it necessary to develop pre-treatment procedures (Sillen 1986). The elevated Sr/Ca ratios of compartment I and II are caused by higher Sr concentrations derived from the surrounding burial environment. Compartment III is characterized by stable Sr/Ca ratios and

is therefore considered to contain biogenic Sr (Sillen 1986). Schultheiss (2003) applied the leaching procedure proposed by Sillen (1986) and FT-IR measurements to diagenetically altered femur from different archaeological sites. Biogenic apatite could be identified in the same fractions (12-15) although the investigated bone material differed in age and preservation state (Schultheiss 2003).

1.4.2. Chemical imaging and spectroscopic techniques

The application of chemical imaging and spectroscopic techniques on archaeological hard tissues provides important information about the degree of diagenetic alteration and the preservation state of the analysed object. The carbonate content of apatites can be estimated by the use of infrared spectroscopy. The ratio of extinction of the carbonate band at 1415 cm^{-1} to the extinction of the phosphate band at 575 cm^{-1} is linearly related to the carbonate content of the apatite (Featherstone et al. 1984). Lebon et al. (2011) used Fourier transform IR microscopy (FTIRM) to gain information about collagen loss, carbonate uptake and mineral recrystallization by studying the histological bone structure (Lebon et al. 2011).
The utilization of X-ray diffractometry could serve as a tool to monitor alterations in powder crystallinity. Crystallinity of apatites decreases with the carbonate content and is in relation to the solubility behaviour of apatites (Kazaki et al. 1981).

1.4.3. Objective of this study

In this study the sequential leaching protocol proposed by Sillen (1986) and by Schultheiss (2003) was used and modified, concerning the centrifugation time and the extension of the extraction steps from 25 to 30 (Schultheiss 2003; Sillen 1986). The method was applied to archaeological human and animal hard tissues from the medieval excavation site Gars Thunau in Lower Austria. Additional information, including environmental sample material, the definition of a local Sr isotopic range of the excavation site and Sr isotope ratios from tooth enamel and dentine digests were taken from the master thesis of Huemer, 2008 (Huemer 2008). The applicability and effectiveness of the method of Sillen was tested and if the solubility profiles and proposed grouping in compartments could be retrieved. Moreover it was analysed if enamel, dentine and bone display different responses to pre-treatment and if a difference between human and animal species could be found.

1.5. Human and animal dentition

Mammalian dentition is heterodont, comprising four different groups of teeth including incisors, canines, premolars and molars. Incisors, canines and premolars undergo the change from milk teeth to permanent teeth, while molar teeth only occur in permanent teeth (Lippert 2000; Nickel et al. 1995). The development of teeth is under strict genetic control that determines the positions and shapes of different teeth (Thesleff and Nieminen 1996).

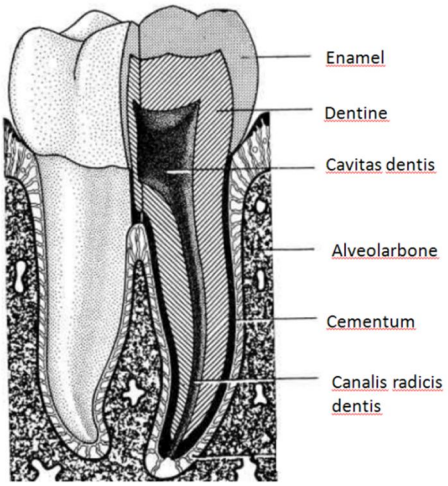

Fig. 1 Tooth anatomy

Mammalian teeth consist of the three mineralized tissues enamel, dentine and cementum (Fig. 1) (Schumacher et al. 1983). Tooth enamel is an acellular, avascular tissue which covers and protects the crown of the tooth (Lippert 2000). The mineralization of mammalian enamel is a complex process, consisting of matrix production and enamel maturation. Matrix production includes the formation of organic matter. During the following process of enamel maturation, mineral components replace continuously this organic matrix and as a result, the degree of mineralization increases to approximately 97% (Hillson 1997). While enamel represents the hardest part of the human and animal body, tooth dentine is a softer, modified bone tissue forming the core of the tooth and containing the cavum dentis with blood-vessels and nerves (Lippert 2000). The root is coated by cementum, a bone-like material which anchors the tooth via connection to the walls of the bone alveolus (Lucas et al. 2008).

Mammalian enamel tissue mineralizes during the childhood and is not remodelled and modified after formation. Hence, enamel preserves the isotope signature taken up during the childhood of an individual. Dentine, in contrast, is in contact with the human metabolism during lifetime. As a consequence of this interaction, dentine should reflect the isotopic composition of the diet recently taken up from an individual (Schweissing and Grupe 2003; Hillson 1997; Montgomery 2010).

1.5.1. Dental structure of humans

Figure 2 represents the human milk dentition (inside) and the human permanent dentition (outside).

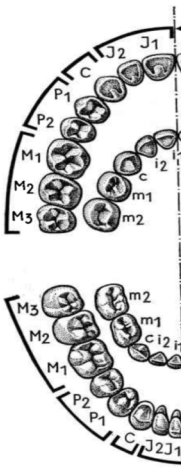

Formula of human permanent teeth:

$$\frac{1M\,1M\,1M\,1P\,1P\,1C\,1I\,1I \quad 2I\,2I\,2C\,24P\,2P\,26\,2M\,2M}{4M\,4M\,4M\,4P\,4P\,4C\,4I\,4I \quad 3I\,3I\,3C\,3P\,3P\,36\,3M\,3M} = 32 \text{ teeth}$$

1 - maxila right

2 - maxila left

3 - mandibula left

4 - mandibula right.

Fig. 2 Human dentition (Schumacher et al. 1983)

The development stages of human teeth and the change time from the milk to the permanent teeth are shown in Table 4 and 5.

tooth	first development stage of the tooth	start of enamel/dentine formation	crown developed
	months fetal	months postnatal	years postnatal
I_1	5	3 - 4	4 - 5
I_2	5.0 - 5.5	10 - 12, 3 - 4	4 - 5
C	5.5 - 6.0	4 - 5 years postnatal	6 - 7
P_1	birth, postnatal	1.5 - 2.0	5 - 6
P_2	7.5 - 8.0	2.0 - 2.5	6 - 7
M_1	3.5 - 4.0	birth	2.5 - 3.0
M_2	8.5 - 9.5 years postnatal	2.5 - 3.0	7 - 8
M_3	3.5 - 4.0	7 - 10	12 - 16

Tab. 4 Development stages of permanent human teeth (Schumacher et al. 1983)

tooth	age of eruption	age of change
I_1	6 - 9 months	6 - 8 years
I_2	8 - 12 months	8 - 9 years
C	16 – 20 months	9 - 13 years
P_1	12 – 16 months	10 - 12 years
P_2	20 - 30 months	
M_1	6 - 7 years	
M_2	13 - 15 years	
M_3	adulthood or never	

Tab. 5 Eruption time of milk teeth and change to permanent teeth (Nickel et al. 1995)

1.5.2. Dental structure of ruminants

Formula of permanent teeth: $\frac{0I\ 0C\ 3P\ 3M}{3I\ 1C\ 3P\ 3M} = 32$ teeth

Cattle dentition is shown in Figure 3 and a single molar cattle tooth in Figure 4.

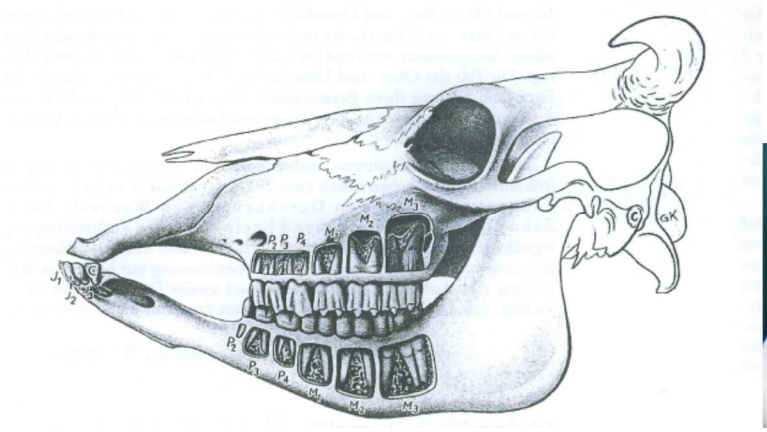

Fig. 3 Cattle dentition (Nickel et al. 1995)

Fig. 4 M_3 cattle mandibula

The development stages of the teeth and the change time from the milk to the permanent teeth of cattle are shown in Table 6.

tooth	age of eruption	age of change
I_1	before birth	14 - 25 months
I_2	before birth	17 - 33 months
I_3	2 - 6 days before birth	22 - 40 months
C	2 - 14 days before birth	32 - 42 months
P_2	14 - 21 days before birth	24 - 28 months
P_3	14 - 21 days before birth	24 - 30 months
P_4	14 - 21 days before birth	28 - 34 months
M_1	5 - 6 months	
M_2	15 - 18 months	
M_3	24 - 28 months	

Tab. 6 Dental development stages of cattle (Nickel et al. 1995)

1.5.3. Dental structure of horses

Formula of permanent teeth: $\frac{3I\ 1C\ 3P\ 3M}{3I\ 1C\ 3P\ 3M} = 40$ teeth

Horse dentition is shown in Figure 5 and a single molar horse tooth in Figure 6.

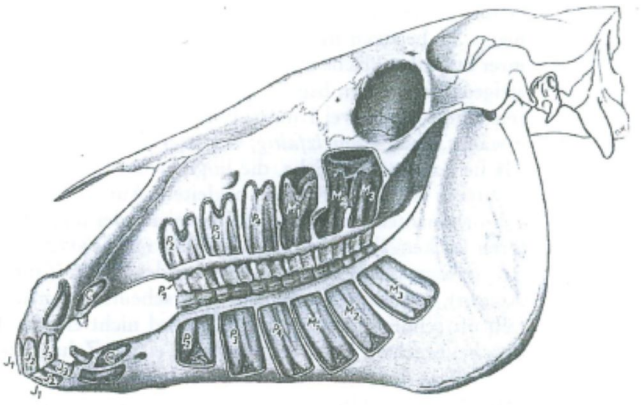

Fig. 5 Horse dentition (Nickel et al. 1995)

Fig. 6 Molar horse mandibula

The eruption time of equid teeth is known, but research concerning the timing of enamel mineralization is still ongoing. The development stages of the teeth and the change time from the milk to the permanent teeth of horses are shown in Table 8. Hoppe et al. (2004) demonstrated that enamel in equid premolars and molars continues to mineralize after eruption. They estimated the following enamel mineralization periods and the growth rates of permanent cheek equid teeth, shown in Table 7 (Hoppe et al. 2004).

tooth	start of enamel mineralization/ months	end of enamel mineralization/ months	growth rate mm/year
P_2	13	31	30
P_3	14	36	35 - 40
P_4	19	51	35 - 40
M_1	0.5	23	35 - 40
M_2	7	37	35 - 40
M_3	21	55	30

Tab. 7 Mineralization and growth time of horse permanent enamel (Hoppe et al. 2004)

tooth	age of eruption	age of change
I_1	first days before birth or after birth	2.5 – 3 years
I_2	3-4 weeks	3.5 – 4 years
I_3	5-9 months	4.5 – 5 years
C	don't break through	4 -5 years
P_2	before birth or in the first week after birth	2.5 years
P_3	before birth or in the first week after birth	2.5 years
P_4	before birth or in the first week after birth	3.5 years
M_1	6 - 9 months	
M_2	2 - 2.5 years	
M_3	3.5 – 4.5 years	

Tab. 8 Dental development stages of horses (Nickel et al. 1995)

1.5.4. The potential of animal teeth for studying ecological processes

Several studies focused on the sequential sampling of tooth enamel of animals from the top to the bottom of the crown to obtain a chronological record of the Sr isotopic composition during tooth formation. The incremental mineralization provides the potential to model the seasonal mobility of prehistoric herders and to reconstruct palaeoclimatic and palaeoenvironmental conditions. Another attempt is the assessment of animal and human movements by comparing Sr isotopic ratios of teeth that formed at different times (Balasse et al. 2002; Bendrey et al. 2009; Hoppe et al. 2004).

1.6. Bone structure and elemental turnover

Bone consists of relatively porous material containing organic matter and inorganic hydroxyapatite crystals. The mineral component gives bone its hardness and rigidity. Collagen constitutes about 90 % of the organic content of bone forming flexible and elastic fibers. The adult skeleton shows two basic bone structure components with identical molecular and cellular compositions, but with different degrees of porosity. The compact or cortical bone type is found in the walls of bone shafts and on external bone surfaces. Its structure is solid and dense. Trabecular or cancellous bone, in contrast, has a more porous, lightweight and honeycomb structure. It is found in the vertebral bodies, in the ends of long bones, in short bones and sandwiched within flat bones (White and Folkens 2005).

Trace elements show a distribution of varying degrees within a single bone, in different bone fractions and throughout the whole skeleton depending on the anatomical site. The functional and structural conditions of the observed bone material and the age and physiological factors of the organism have an impact on elemental levels. As a consequence, the trace element content is higher at epiphyseal areas of long bones than in the shaft and higher in trabecular than in cortical bones (Brätter et al. 1977; Dahl et al. 2001; Nickel et al. 1995). An explanation could be different metabolic turnover rates in compact and trabecular bone (Grupe 1988).

1.6.1. Objective of this study

Sheep hard tissues including jaw bones are analysed for their Sr isotopic composition. A two year old female sheep called 'Anja' was spiked with an intramuscular injection of an enriched solution of 40 mg ^{86}Sr corresponding to a dose of 0.66mg kg^{-1} bodyweight approximately nine months before slaughtering. Moreover, Anja was administered a ^{41}Ca spike. The work conducted in this study is part of a project in cooperation with Thomas Walczyk from the Department of Chemistry at the University of Singapore, with Anette Liesegang from the Institute of Animal Nutrition at the University of Zurich and with Tim Schulze-König from the Institute of the Laboratory of Ion Beam Physics, ETH Zurich and with Gisela Kuhn from the Institute of Biomechanics, ETH Zurich. The original aim of the project is to test if Sr can be used as a proxy for Ca turnover in living organisms in order to study osteoporosis prevention

and treatment. Denk et al. (2006) demonstrated that human bone calcium can be labelled with the isotope ^{41}Ca and that urinary ^{41}Ca excretion can be followed (Denk et al. 2006).

It is the object of this diploma thesis to investigate the incorporation of the ^{86}Sr spike into the right lower jaw bone of Anja and to find out if differences occur in the Sr turnover rate between the different sections along a bone. Moreover, the results of Anja's jaw bone are compared with the results of the jaw bone of a sheep, called 'Stronzi' with an expected uniform $^{87}Sr/^{86}Sr$ distribution.

1.7. The Celtic settlement site Roseldorf

The Celtic central settlement site Roseldorf is located about 60 km north-west from Vienna in the Weinviertel in Lower Austria (Fig. 7) and was populated in the Latène period in the fourth century BC (Holzer 2009). As written records by the Celts themselves documenting their history, culture, religion and daily life do not exist, it is of great importance to focus on archaeological sources to gain more information about the Celtic period.

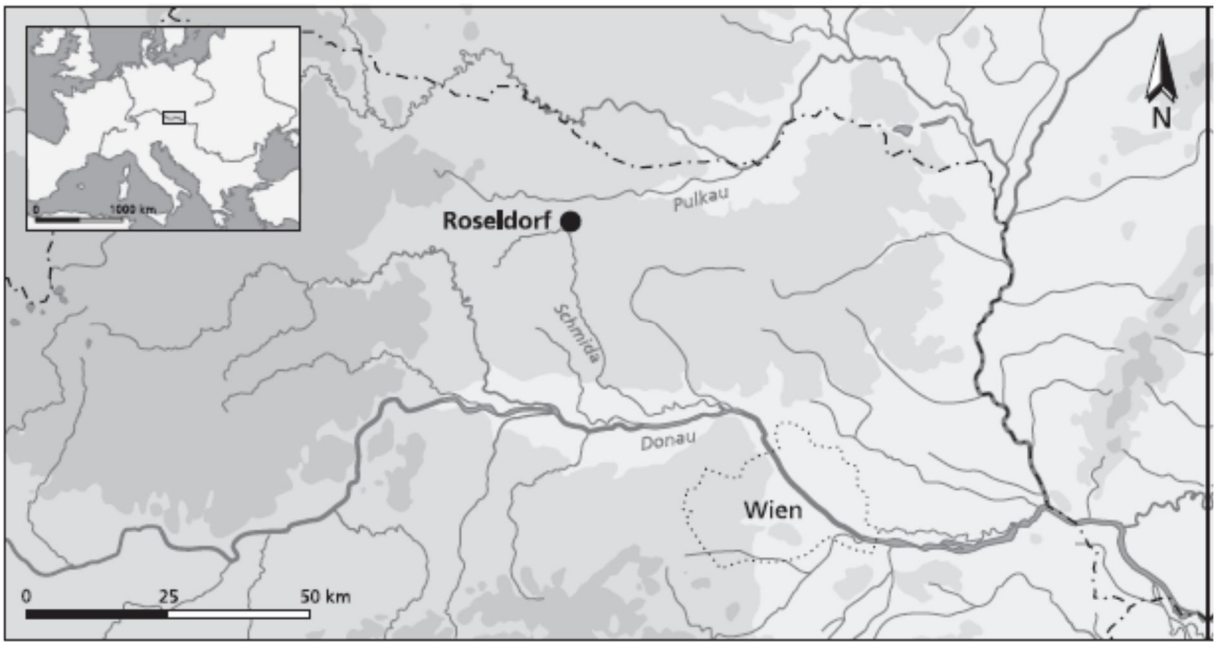

Fig. 7 The location of the Celtic settlement site Roseldorf (Holzer 2008)

Geomagnetic prospection measurements indicate a dimension of 22–40 ha of Roseldorf's Celtic settlement site on the Sandberg, 339 m above sea level. The fact, that there have not been any subsequent settlements, explains the exceptionally good preservation state of its findings. 450 pit houses, 700 settlement structures, a silo, a blacksmith's shop and two possible market places have already been identified and give evidence about Roseldorf's urban character. Its status as an important trading place in the Latène period in this area is underlined by its strategic position on the Sandberg, various numismatic findings and the fact that Roseldorf represented a minting place. The large number of about 1200 coins shows contact to the western and northern regions such as Bavaria, the Rhineland, Prague and the Pannonic-Hungarian area (Holzer 2009).

1.7.1. The ‘sanctuaries’ of Roseldorf

Particular settlement structures in Roseldorf, identified as ‘sanctuaries’ (Fig. 8), comprise outstanding findings, including metal objects such as weapons, chariots, a hors harness, jewellery and numerous different, fragmented animal and human skeletal and dental tissues (Fig. 11). Object 1 (Fig. 9) represents the biggest of these complexes (25x25m). The function of the sanctuaries challenges interpretation, as their appearance and the character and arrangement of the bone material are unique for Central Europe. Similarities including the square shape could be seen with sanctuary places of Gallian type, such as in Gournay-sur-Aronde in France (Holzer 2006). A possible reconstruction of a sanctuary is shown in Figure 10. Before deposition in the sanctuaries, metal objects of iron including swords, lances and shields were intentionally destroyed and made useless for other purposes. Concerning the bone material, both human and animal skeletal remains occur. Whole skeletons are missing and the existing bones do not allow the conclusion about a specific selection of certain skeletal parts. As the animals show butchering marks, current archaeological theory claims that human and animal sacrifices in form of ritual banquets could have taken place in Roseldorf (Holzer 2006). The exceptional finding of an iron druid crown and a deer antler for religious ceremonies could support this hypothesis (Holzer 2006; Tiefengraber et al. 2009).

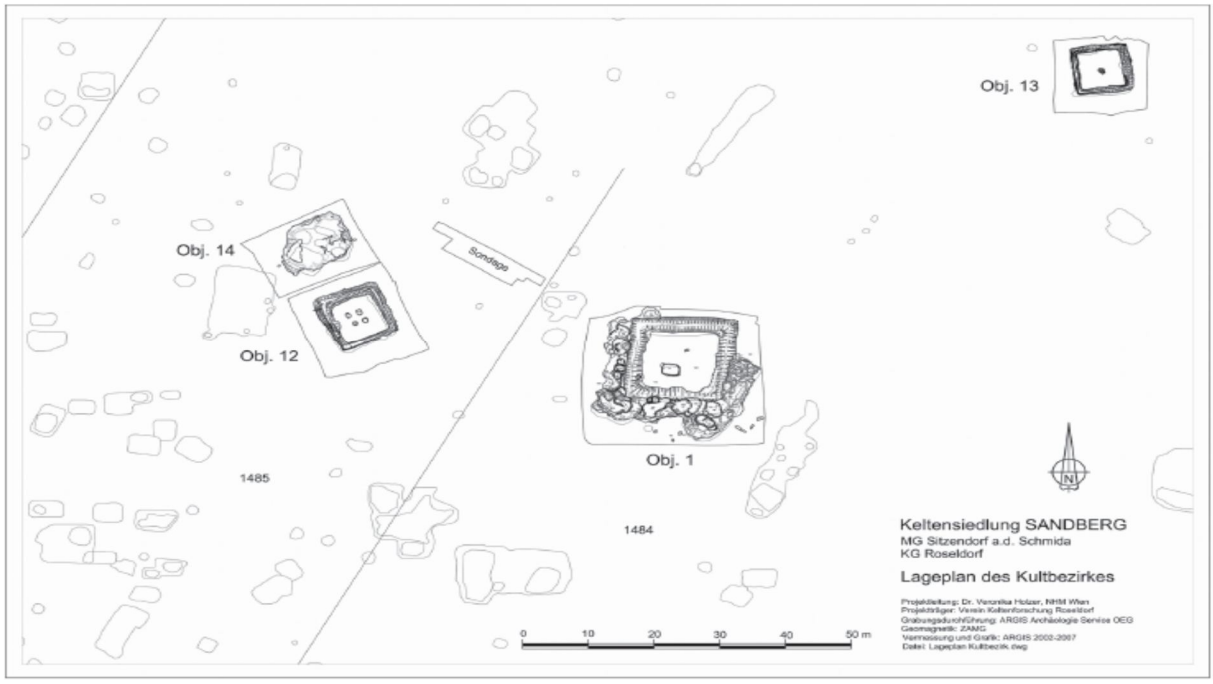

Fig. 8 The cultic area of Roseldorf (Tiefengraber et al. 2009)

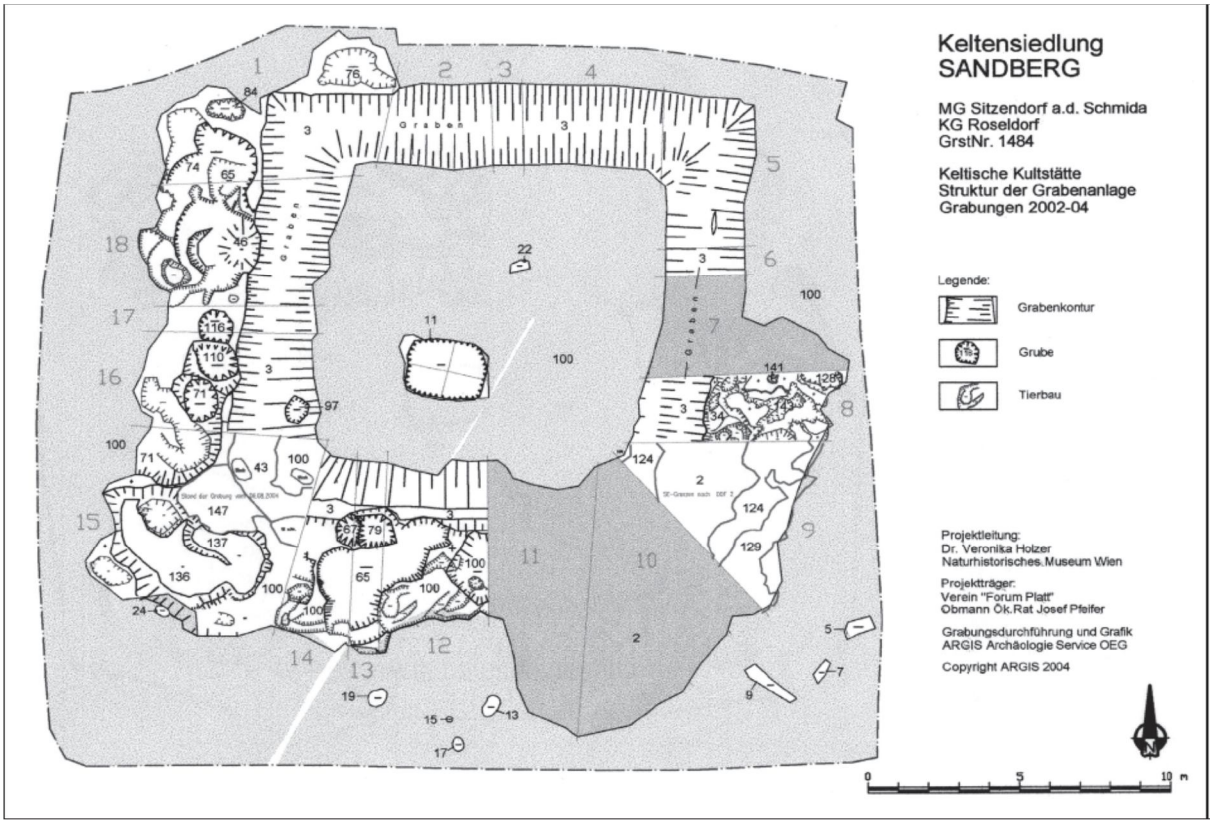

Fig. 9 The finding complex Object 1 (Holzer 2007)

Fig. 10 Possible reconstruction of a sanctuary (Holzer 2009)

Fig. 11 Fragmented human and animal remains (Holzer 2009)

1.7.2. Archaeozoological studies of Roseldorf's animal remains

Archaeozoological morphology studies of cattle and horse bone material recovered from the sanctuary Object 1 (Fig. 8 and Fig. 9) and from Roseldorf's settlement, allow a distinction between smaller Celtic and bigger Central Italian animals (Pucher and Schmitzberger 2003). A possible explanation for the appearance of Italian animals in a period long before the Roman presence in this area, could be trading contacts of the Celtic settlers in Roseldorf with tribes in the Italian region (Holzer 2009).

1.7.3. Objective of this study

The aim of this pilot study is to shed light on the Celtic period in Roseldorf with focus on the following questions:

- origin of cattle and horse remains recovered from the settlement and the sanctuaries
- Roseldorf' s trading contacts
- identification of local/non-local humans
- function of particular settlement structures identified as 'sanctuaries'
- ritual and/or burial practices of Celtic settlers in Roseldorf

Differences of the morphology between human and animal teeth made it necessary to adapt the sampling of tooth enamel for cattle and horse teeth. Due to the size and to the incrementally mineralization of animal teeth over several years, the proper selection of the sampling spot of enamel is of great importance to guarantee comparability between the species with regard to the reflected time period. With the combination of the knowledge about the morphology and the maturation stages of animal and human teeth, a proper enamel sampling method had to be developed.

First steps including the determination of Sr isotopic ratios by MC-ICP-MS of cattle, horse and human tooth enamel and dentine samples and a geographical $^{87}Sr/^{86}Sr$ mapping of Roseldorf's surroundings had to be accomplished with regard to the questions addressed. It was one objective of this work to establish a $^{87}Sr/^{86}Sr$ isoscape of the north-western part of the Weinviertel considering the underlying geology.

1.8. Strontium isotope ratio measurements by ICP-MS

The determination of strontium isotope ratios requires adequate chemical and analytical techniques. The possibility to perform analyses with a very high precision and accuracy is needed to detect subtle variations in the isotope ratios of the element strontium. Thermal Ionisation Mass Spectrometry (TIMS) and Multiple Collector-Inductively Coupled Plasma-Mass Spectrometry (MC-ICP-MS) serve as methods of choice for high precision isotope ratio measurements and (Albarède et al. 2004; Balcaen et al. 2010).

The use of TIMS offers the advantage of isotope ratio precisions down to 0.005% relative standard deviation (RSD) (Heumann et al. 1998). One major disadvantage of this method is the time-consuming measurement (Balcaen et al. 2010).

1.8.1. Inductively Coupled Plasma-Mass Spectrometry (ICP-MS)

In contrast to TIMS, ICP-MS offers high ionization efficiency and rapid analysis capabilities (Balcaen et al. 2010). The principle and main components of an ICP-MS instrument will be discussed in the following.

1.8.1.1. Sample introduction

Sample introduction strategies for the MC-ICP-MS device include solution based methods or the direct measurement of solid samples by Laser Ablation (LA). Laser ablation as sampling method offers the advantage that no severe damages are caused on the analysed object (Copeland et al. 2008).

The liquid sample introduction system is formed by a nebulizer and a spray chamber. Liquid samples are dispersed by a nebulizer into an aerosol. Different types of nebulizers are employed in ICP-MS devices including concentric and crossflow nebulizers. The parallel or rectangular gas flow breaks down the liquid stream into an aerosol. Microflow nebulizers of polymer material based on the concentric principle are favourable for applications with small sample volumes because of their lower sample uptake rate. In the spray chamber the droplets are separated due to their size to ensure a uniform droplet distribution in the plasma. Big sized droplets would lead to a longer residence time in the plasma compared to small ones resulting in a low ionisation efficiency. Common designs are the double-pass spray chamber using gravitiy and the cyclonic spray chamber operating on centrifugal force for droplet selection (Thomas 2001a).

As ICP-MS was used throughout this work, it is described shortly in the next paragraphs.

1.8.1.2. Ion generation

The ion source is composed by inductively coupled plasma. In the plasma torch, which consists of three concentric quartz tubes, argon is used as plasmagas with a flow rate of 11-17 L/min and the auxiliary gas, which is used as a cooling gas, with a flow rate of 1 L/min. A nebulizer gas with a gas flow of 1 L/min carries the sample through the plasma. A copper coil at the top end of the torch is supplied by radio frequency power of 750-1500 W. The resulting oscillation of alternating current with a frequency of 27 or 40 MHz creates an electromagnetic field. A high-voltage spark initializes the forming of the plasma by stripping off some electrons from the argon atoms. These electrons are accelerated in the magnetic field and cause collision-induced ionization of the argon atoms. As the sample droplets reach the plasma with different zones of temperature between 7500-10000 K, they are rapidly desolvated, vaporized, atomized and finally ionized (Thomas 2001b).

The created ions enter the interface region via the sampler cone with an orifice diameter of 0.8-1.2 mm and pass through the skimmer cone with an orifice of 0.4-0.8 mm. The ions are transferred through the ion optics and finally reach the mass separation device.

The pressure is constantly reduced from atmospheric pressure (1 bar) in the ion source to vacuum (10^{-7}-10^{-9} mbar) in the mass analyser via the interface (Thomas 2001c).

1.8.1.3. Mass analyser

The ions are separated due to their mass to charge (m/z) ratio in the mass analyser. ICP-instruments are equipped with different types of mass analysers. The mass analyser in the used PerkinElmer ELAN DRC e instrument is a quadrupole filter which consists of four cylindrical or hyperbolic rods. By applying direct current and alternating current with radiofrequency power on the rods, electric fields are generated along the pathway of the ions. As a consequence, only ions with a certain m/z ratio are able to reach the detector. The variation of the voltage setting allows a rapid scan over the mass range so that the ions can be detected one after the other. A double-focusing magnetic-sector mass analyser separates the ions in the used HR Nu Plasma. The design follows the Nier-Johnson geometry where an electrostatic analyser (ESA) is positioned before a magnetic analyser. The uncertainty of the kinetic energy of the ions is corrected by the ESA, before they are separated due to their m/z ratio in the magnetic analyser (Thomas 2001d).

1.8.1.4. Detector

Different detection systems can be employed in ICP-MS instruments. The separated ions are conventionally detected sequentially in commercial single-collector instruments by secondary electron multiplier (SEM). Novel developments allow the extension of the dynamic range by three orders of magnitude by using a faraday cup in addition to the SEM.

MC-ICP-MS instruments are equipped with an array of Faraday cups and are therefore able to monitor the intensities of the ion beams simultaneously (Thomas 2002a). Additionally, the central channel can use a Daily detector. As a consequence of the simultaneous detection, short term variations in signal intensity are affecting all isotopes to the same extent resulting in isotope ratio precisions down to 0.002% RSD (Heumann et al. 1998). Modern MC-ICP-MS instruments are additionally equipped with a range discrete ion counting systems to cover low concentrations or low abundant isotopes.

1.8.2. Interferences in ICP-MS on the example of Sr

Spectral interferences including isobars, multiply charged atoms and polyatomic interferences can occur when determining Sr isotope ratios using ICP-MS devices. Isobars have the same nominal mass as the analyte such as ^{87}Rb and ^{87}Sr. Prior to the measurement a matrix separation can be performed during sample preparation to overcome the problem of interferences (Thomas 2002b). In the case of strontium, a chromatography technique is applied to the samples using a Sr specific resin in order to reduce the Rb content and the matrix components (see chapter 2.3.4.). In this study tooth and bone samples consisting of hydroxyapatite with the formula $Ca_{10}(PO_4)_6(OH)_2$ are analysed by ICP-MS with argon as carrier gas. The matrix and the gas are a putative source for molecular interferences composed of the elements Ca, P, O and Ar. To overcome the problem of argon based polyatomic interferences in ICP-MS a cool or cold plasma technique can be applied. A low temperature is used to generate the plasma by decreasing the forward power (RF power) (Thomas 2002b). Krypton (Kr) can be a component of the argon (Ar) gas flow and provides an isobaric interference on mass 84 and 86. Elements in the sample can from molecular hydride, oxide and hydroxide ions (Thomas 2002b).

An alternative way to the time-consuming sample pre-treatment is the use of a collision or reaction cell to eliminate interferences. A quadrupole operated in the radio frequency-only mode serves as a collision cell and is positioned before the mass analyser quadrupole. It is

filled with a collision/reaction gas that interacts with the sample or the undesired components. Interferences are transformed to non-overlapping species or the measurant itself is converted to another ion with a non-interfered mass. Different collision/reaction gases such as He, Ar, O_2, N_2, CH_4 or NH_3 can be used (Thomas 2002c). In the case of Sr, Moens et al. (2001) showed that CH_3F can be used as a reaction gas to eliminate the Rb without prior separation procedure. While Sr reacts with CH_3F to SrF^+, the isobaric interference ^{87}Rb does not react at all. The Sr isotope ratios are then measured via SrF^+ polyatomic ions. This strategy results in a limited precision of 0.03% RSD on the $^{87}Sr/^{86}Sr$ ratio compared to a precision of 0.002% RSD of MC-ICP-MS (Moens et al. 2001, Heumann et al. 1998). The accuracy of the raw $^{87}Sr/^{86}Sr$ ratio is poor because of detector dead time losses and a mass bias of about 3.5%. The problem of the mass bias might be due to matrix dependence. The effect of mass bias is expected to be different for a pure reference standard solution and the sample (Moens et al. 2001). Drifts of mass bias were also observed for isotopic measurements of $^{44}Ca/^{40}Ca$ by the use of ICP-DRC-MS (Boulyga et al. 2007).

Phenomenon of 'mass bias' causes a deviation of the measured ratio from the 'true' ratio represented by a certified value. Ions of lighter masses are discriminated against ions of heavier masses resulting in a shift to higher isotopic values of $^{87}Sr/^{86}Sr$. Space charge effects are believed to be the main source of mass bias in ICP-MS instruments (Niu and Houk 1996).

The effect of mass fractionation can either be corrected externally using a Certified Reference Material (CRM) with known isotopic composition or internally using a constant isotope ratio of the same element or of a dopant element (Albarède et al. 2004). If the isotope system does not possess a naturally invariant isotope ratio, the sample can be spiked with an isotope pair of known isotope composition of another element. This approach of internal correction requires similar mass bias behaviours and ionisation potentials of the used isotope pairs. This method has been used for Pb (using Tl) (Weiss et al. 2004; White et al. 2000), for Fe (using Cu)(Anbar et al. 2000) and for Cu and Zn (Maréchal et al. 1999). In the case of the Sr isotopic system the presumably invariant $^{86}Sr/^{88}Sr$ ratio is commonly used to correct internally for mass fractionation of the measured $^{87}Sr/^{86}Sr$ ratio (Cavazzini 2005).

Different mathematical models including the Exponential Law, the Linear Law, the Power Law and the Russel equation exist to correct for mass bias (Albarède et al. 2004). The mathematical corrections used in this work to overcome the problem of mass bias are described in chapter 2.4.3.

2. Materials and Methods

The preparative laboratory work was performed in the laboratories (including clean rooms of class 10 000 and 100 000) of the Division of Analytical Chemistry at the University of Natural Resources and Life Sciences, Vienna and in the laboratories of the Centre of Earth Sciences at the University of Vienna, Vienna. The drilling of archaeological animal teeth was carried out at the Museum of Natural History, 1st Department of Zoology, Vienna. Archaeological human tooth samples were drilled in the laboratories of the Centre of Earth Sciences at the University of Vienna, Vienna.

2.1. Reagents and Materials

All laboratory equipment, consisting of synthetic polymers, was cleaned in a clean room class 10 000 including three washing steps with varying concentrations of HNO_3 before usage.

De-mineralized water (F+L GmbH, Vienna, Austria) was doubly-subboiled by means of a purification system (MLS DuoPur, MLS, Leutkirch im Allgau, Germany). Nitric acid (65%) (Merck KGaA, Darmstadt, Germany) underwent two purification steps in a subboiling distillation quartz apparatus (MLS DuoPur, MLS, Leutkirch im Allgau, Germany) before usage.

Double sub-boiled H_2O, double sub-boiled HNO_3 (65%) and H_2O_2 (31%) (p.a. grade, MERCK KGaA, Darmstadt, Germany) were taken for sample digestions, preparation of standard solutions and dilutions.

Indium was used as internal normalization standard for liquid concentration measurements by means of the ICP-QMS ELAN DRC e (PerkinElmer, Waltham, Massachusetts, USA). A 110 ng g^{-1} indium standard stock solution was prepared out of a 1000 mg L^{-1} Indium ICP Standard (CertiPur, MERCK KGaA, Darmstadt, Germany).

An ICP Multi Element Standard Solution VI (CertiPur, suprapure, MERCK KGaA, Darmstadt, Germany) was taken for quantitative analysis by external calibration at the ICP-QMS ELAN. For the diagenesis study phosphorus standards were made out of a 1000 mg L^{-1} Phosphorus ICP Standard (Sigma-Aldrich, Nr. 207357) and used for calibration (see chapter 2.4.1).

The certified standard reference material NIST SRM 987 $SrCO_3$ (National Institute for Standards and Technology, Gaithersburg, USA) with the certified value $^{87}Sr/^{86}Sr = 0.71034 \pm 0.00026$ was used to verify the accuracy of strontium isotope ratio measurements accomplished by MC-ICP-SFMS (Nu Plasma (Nu Instruments Ltd., Wrexham, UK)).

2.2. Sample material

2.2.1. Tooth material for the diagenesis study

Archaeological tooth and bone samples from the medieval excavation site Gars Thunau (Lower Austria) for the investigation of diagenetic effects on human and animal skeletal and dental tissues were provided by the Department of Anthropology of the Natural History Museum, Vienna. The sample material is listed in Table 9 and in Table 10.

sample code	inventory number NHM	grave number	sex	age	species	sample type	quantity [mg]
A	GT 24958	7	male	40-60	human	tooth dentine	64.2
B	GT 23877	-	-	-	sheep 1	tooth dentine	83.2
C	GT 25123	146	male	25-35	human	tooth dentine	59.1
D	GT 17477	-	-	-	cattle 3	tooth dentine	33.4
E	GT 24986	32	indiff.	30-40	human	tooth dentine	62.0
F	GT 25096	126	female	35-45	human	tooth dentine	45.7
G	GT 10961	-	-	-	sheep 2	jaw bone	44.4
H	GT 17268	-	-	-	cattle 1	tooth dentine	38.8
I	GT 23877	-	-	-	sheep 1	jaw bone	98.2
J	GT 29124	-	-	-	horse 1	tooth dentine	43.5
K	GT 25146	167	male	40-50	human	tooth dentine	129.1
L	GT 10961	-	-	-	sheep 2	tooth dentine	26.4
M	GT 24958	7	male	40-60	human	tooth enamel	17.5
N	GT 24986	32	indiff.	30-40	human	tooth enamel	35.8

Tab.9 Sample list of archaeological tissues from Gars Thunau used for sequential leaching

inventory number NHM	grave number	sex	age	species	sample type	quantity [mg]
GT 23877	-	-	-	sheep 1	jaw bone	53.3
GT 10961	-	-	-	sheep 2	jaw bone	16.0
GT 25096	126	female	35-45	human	tooth dentine	16.7
GT 25096	126	female	35-45	human	tooth enamel	8.8

Tab. 10 Samples from Gars Thunau used for digestion

2.2.2. Recent sheep hard tissues for the investigation of Sr turnover

A recent right lower jaw bone from a non-migrated sheep called ‘Stronzi’ and a recent right lower jaw bone from a spiked sheep called ‘Anja’ were analysed. The sheep Anja was spiked with an enriched solution of ^{86}Sr by an intramuscular injection of a solution of strontium chloride approximately nine months before slaughtering (procedure and project partners see chapter 1.6.1).

Drilling positions on the bones are listed in Table 11, 12 and shown in Figure 12, 13.

right lower jaw bone			
inside		**outside**	
sample code	**quantity [mg]**	**sample code**	**quantity [mg]**
1A	4.5	1B	10.9
2A	9.9	2B	7.7
3A	3.4	3B	6.8
4A	4.7	4B	4.2
5A	8.7	5B	1.0
6A	7.6	6B	6.3
7A	9.3	7B	11.5
8A	3.6		

Tab. 11 Sample list of the right lower jaw bone of the sheep ‘Stronzi’

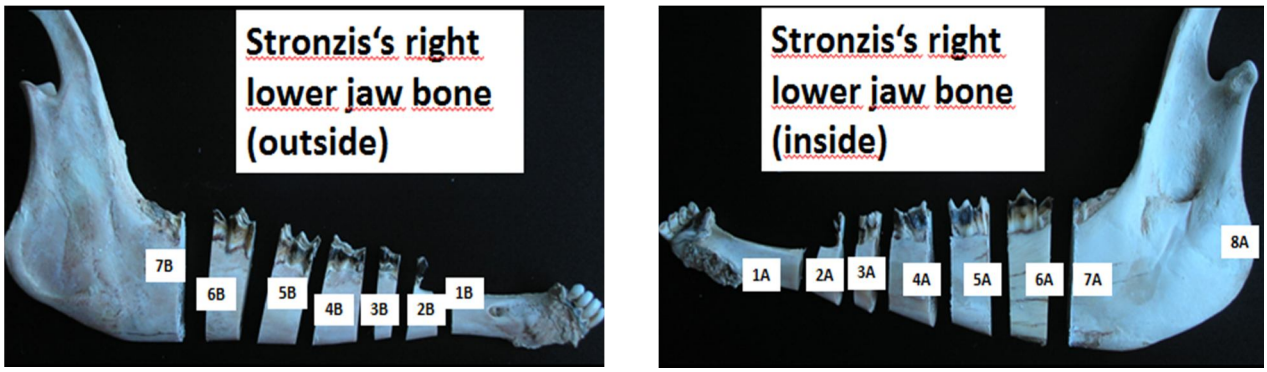

Fig. 12 Drilling positions of the right lower jaw bone of ‘Stronzi’

right lower jaw bone			
inside		outside	
sample code	quantity [mg]	sample code	quantity [mg]
0A	32.6	0B	27.7
1A	14.3	1B	37.0
2A	33.6	2B	28.4
3A	19.8	3B	13.8
4A	12.3	4B	5.6
5A	12.1	5B	20.5
6A	22.8	6B	12.6
7A	10.6	7B	10.3
8A	13.1	8B	21.0

Tab. 12 Sample list of the right lower jaw bone of Anja

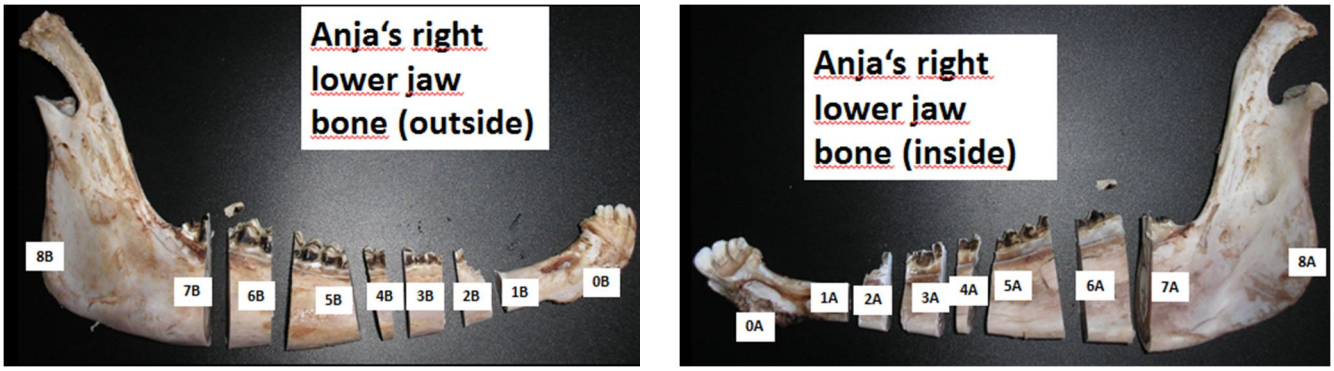

Fig. 13 Drilling positions of the right lower jaw bone of Anja

2.2.3. Sample material from Roseldorf

2.2.3.1. Archaeological tooth material

Archaeological animal and human tooth samples (Table 13 and 14) from the Celtic settlement site Roseldorf were provided by the 1st Department of Zoology and the Department of Anthropology of the Natural History Museum, Vienna.

inventory number NHM	animal type	find spot	possible origin[1]	tooth	quantity [mg]
R5-1-15-43-4489	cattle	Object 1	Italian	M3/Mandibula	13.8
R4-1-5-53-4328	cattle	Object 1	Italian	M3/Mandibula	13.0
R3-1-16-70-1934	cattle	Object 1	Italian	M3/Mandibula	19.6
R3-1-12-60-1745	cattle	Object 1	Italian	M3/Mandibula	14.2
R4-1-15-117-3735	cattle	Object 1	Celtic	M3/Mandibula	17.5
R4-1-15-131-4285	cattle	Object 1	Celtic	M3/Mandibula	15.5
R2-1-14-54-607	cattle	Object 1	Celtic	M3/Mandibula	25.1
R3-1-1-43-2953	cattle	Object 1	Celtic	M3/Mandibula	22.0
R2-1-4-37-365	cattle	Object 1	Celtic	M3/Mandibula	16.7
R2-1-12-2-858	cattle	Object 1	Celtic	M3/Mandibula	25.9
R3-1-16-107-2548	cattle	Object 1	Celtic	Molar/Mandibula	28.5
R3-1-15-103-2260	cattle	Object 1	Celtic	Molar/Mandibula	12.1
R3-1-15-103-2788	cattle	Object 1	Celtic	Molar/Mandibula	13.0
R6-1-11-59-5614	cattle	Object 1	Celtic	Molar/Mandibula	12.1
R1-50-112	cattle	Settlement	Celtic	M3/Mandibula	12.3
R1-168-102	cattle	Settlement	Celtic	M3/Mandibula	13.0
R1-28-13	cattle	Settlement	Italian	M2/Mandibula	22.3
R1-140-89	cattle	Settlement	Italian	M2/Mandibula	24.0
R6-1-10-217-5490	horse	Object 1	Celtic	M1-2/Mandibula	19.9
R2-1-12-2-454	horse	Object 1	Celtic	M1-2/Mandibula	20.0
R6-1-10-217-5495	horse	Object 1	Celtic	M1-2/Mandibula	17.7
R2-1-18-2-941	horse	Object 1	Celtic	M1-2/Mandibula	7.0
R3-1-1-2-2027	horse	Object 1	Celtic	M1-2/Mandibula	7.3
R3-1-1-43-2702	horse	Object 1	Celtic	M1-2/Maxilla	14.6
R2-1-4-2-945	horse	Object 1	Celtic	M1-2/Maxilla	11.6
R4-1-15-135-4366	horse	Object 1	Celtic	M1-2/Maxilla	7.8
R3-1-16-43-2268	horse	Object 1	Celtic	M1-2/Maxilla	13.0
R2-1-4-37-951	horse	Object 1	Celtic	M1-2/Maxilla	20.5
R1-0.Nr	horse	Settlement	Celtic	Premolar/Maxilla	14.0
R1-227-209	horse	Settlement	Celtic	Premolar/Maxilla	14.4

Tab. 13 Sample list of animal tooth enamel excavated in Roseldorf

[1] Based on archaeozoologic studies of the occurring bone material

inventory number NHM	sample ID	find spot	age	tooth material	quantity [mg]
R7-14-3-3-51	R7-14-3-3-51_E	Object 14	adult	enamel	12.4
R7-14-3-3-51	R7-14-3-3-51_D	Object 14	adult	dentine	13.9
SENr. 48; 14/3798	Obj.14-1	Object 14	adult	enamel	12.2
SENr. 48; 14/3798	Obj.14-2	Object 14	adult	enamel	78.7
SENr. 2; 30-1031	Object 30/I_1	Object 30/I	child	enamel/Maxilla	18.1
SENr. 2; 30-1031	Object 30/I_2	Object 30/I	child	enamel/Maxilla	16.9
SENr. 2; 30-1031	Object 30/I_3	Object 30/I	child	enamel/Maxilla	58.4

Tab. 14 Sample list of human tooth material excavated in Roseldorf

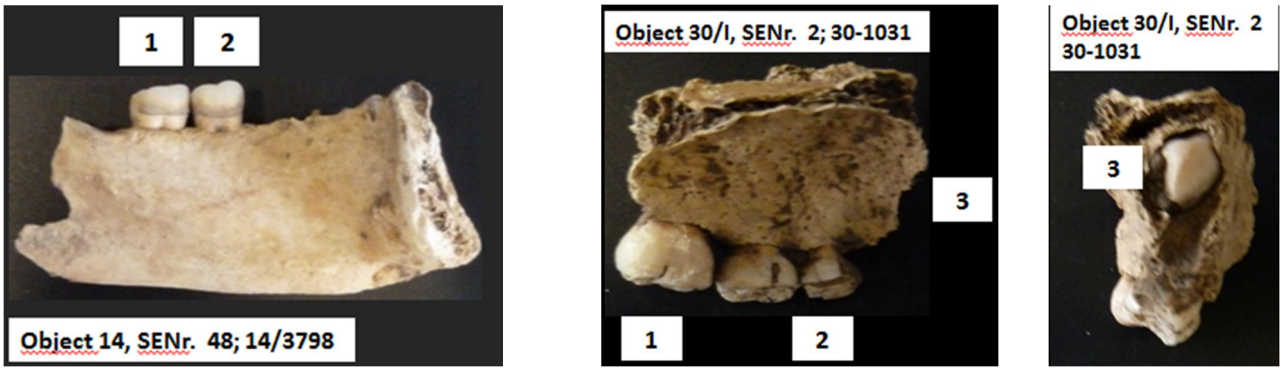

Fig.15 Drilled teeth of human individuals excavated in Roseldorf

2.2.3.2. Environmental samples

Environmental samples including soil, water and recent fauna such as cereals and grapes were derived from the settlement site itself from the Sandberg and from Roseldorf's surroundings in the north-western Weinviertel in Lower Austria. The sampling spots are shown in Figure 16 and the corresponding GPS-data and names of the locations are given in Table 15, 16 and 17.

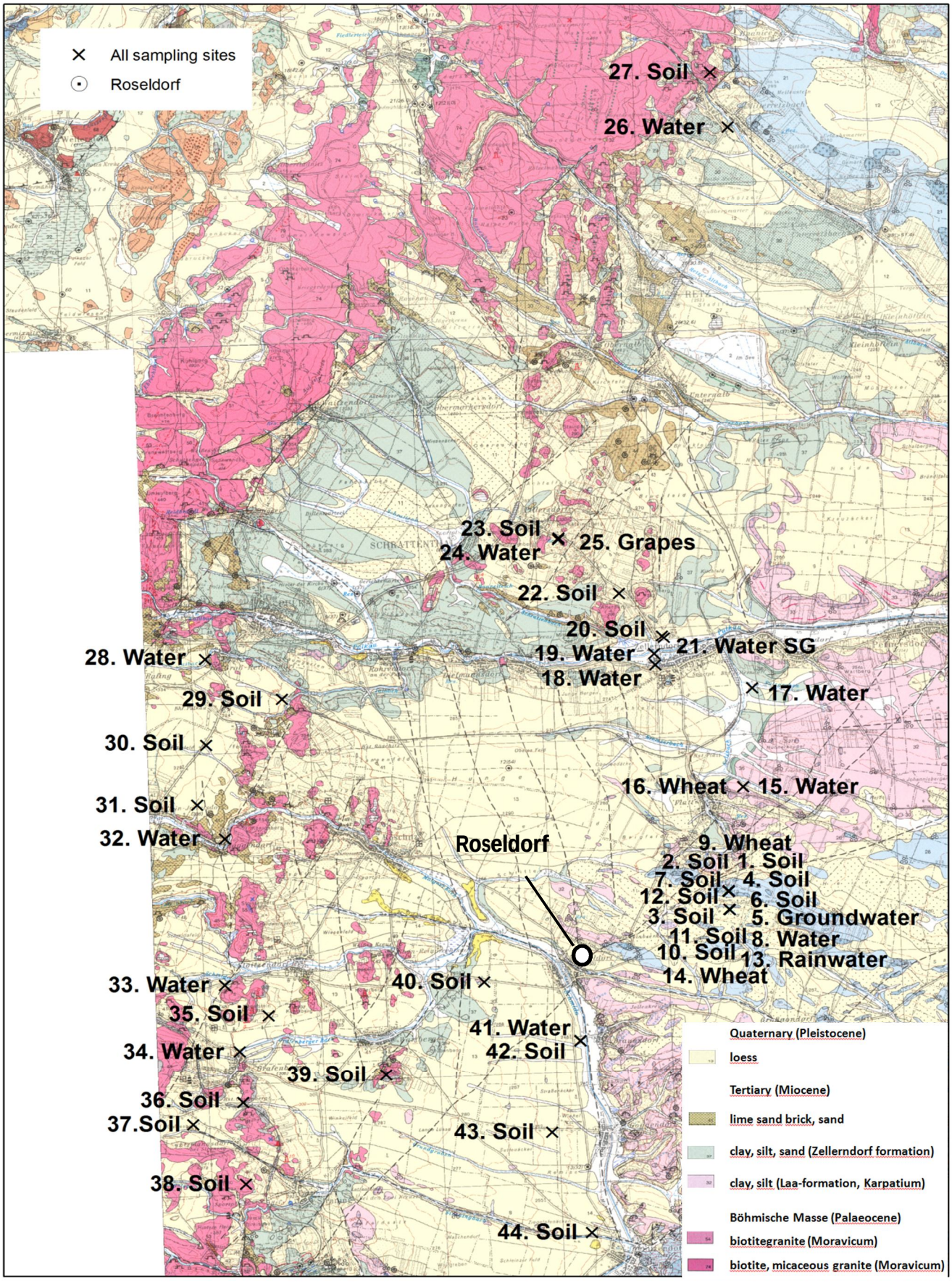

Fig. 16 Sample locations of environmental material

sample code	sample number	location name	x coordinate	y coordinate	quantity [g]
RD_1	1	Sandberg	15.967800	48.658580	20.466
RD_2	2	Sandberg	15.967800	48.658580	22.423
RD_3	3	Sandberg	15.967800	48.658580	20.049
RD_4	4	Sandberg	15.967800	48.658580	22.184
RD_5	6	Sandberg	15.967800	48.658580	21.582
RD_6	7	Sandberg	15.967800	48.658580	20.758
RD_7	10	Sandberg	15.967790	48.655560	21.9
RD_8	11	Sandberg	15.967790	48.655560	21.199
RD_9	12	Sandberg	15.967790	48.655560	21.491
RD_10	20	gotic church	15.954340	48.700540	21.253
RD_11	22	Zellerndorf	15.944720	48.707660	19.23
RD_12	23	Zellerndorf	15.931000	48.717000	21.52
RD_13	27	Heiliger Stein	15.970280	48.792020	21.295
RD_14	29	Großreipersdorf	15.865170	48.692060	20.798
RD_15	30	Großreipersdorf	15.847091	48.685010	22.916
RD_16	31	Großreipersdorf	15.844516	48.675320	21.035
RD_17	35	Grafenberg	15.859530	48.640610	22.453
RD_18	36	Grafenberg	15.852940	48.626600	22.603
RD_19	37	Grafenberg	15.841080	48.623230	22.547
RD_20	38	Sauberg	15.852910	48.613310	21.127
RD_21	39	Kirchberg	15.886420	48.630410	21.742
RD_22	40	Roseldorf	15.910060	48.645050	19.846
RD_23	42	Schmida	15.931930	48.634980	21.538
RD_24	43	Goggendorf	15.924710	48.620210	21.908
RD_25	44	Goggendorf	15.933150	48.603710	19.767

Tab 15 Sample list of soil material sampled at the site in Roseldorf and in surrounding areas

sample code	sample number	sample type	location name	x coordinate	y coordinate
RD_G1	9	cereals	Sandberg	15.967810	48.658490
RD_G2	14	cereals	Sandberg	15.967880	48.655530
RD_G3	16	cereals	Sulzbach	15.972090	48.675530
RD_T1	25	grape	Zellerndorf	15.931000	48.717000
RD_T1	25	leaf of grape	Zellerndorf	15.931000	48.717000
RD_T1	25	branche of grape	Zellerndorf	15.931000	48.717000

Tab. 16 Sample list of recent fauna sampled at the site in Roseldorf and in surrounding areas

sample code	sample number	location name	X Coord.	Y Coord.
RD_W_1	5	Sandberg	15.967800	48.658580
RD_W_2	8	Sandberg	15.967800	48.658580
RD_W_3	13	Sandberg	15.967800	48.655560
RD_W_4	15	Sulzbach	48.675530	15.972090
RD_W_5	17	Sulzgraben	15.974920	48.691540
RD_W_6	18	Zellerndorf	15.952550	48.695810
RD_W_7	19	Pulkau	15.952360	48.697570
RD_W_8	21	gotische Kirche	15.954760	48.700220
RD_W_9	24	Zellerndorf	15.930890	48.716760
RD_W_10	26	Mitterretzbach	15.973890	48.783030
RD_W_11	28	Thallerbach	15.847520	48.698910
RD_W_12	32	Maignerbach	15.850782	48.669708
RD_W_13	33	Schmida	15.849560	48.645830
RD_W_14	34	Grafenbergerbach	15.852480	48.634920
RD_W_15	41	Schmida	15.932020	48.634980

Tab.17 Sample list of water sampled at the site in Roseldorf and in surrounding areas

2.3. Sample preparation

2.3.1. Diagenesis study and sequential leaching procedure

The surface of the archaeological tooth and bone samples was cleaned with double sub-boiled 1% HNO_3 (w/w) and with Isopropanol. An electrical dental driller (Moto Tool, 10000-30000) was used to obtain the sample material in powdered form.

A sequential leaching procedure was subsequently applied to animal jaw bones and tooth dentine and to human tooth enamel and dentine samples which were obtained from a previous investigation (Huemer 2008) from the medieval excavation site Gars Thunau in Lower Austria.

A 0.1 mol L^{-1} acetic acid/sodium acetate buffer with a pH of 4.5 was prepared using suprapure chemicals (Merk KgaA, Darmstadt, Germany). About 0.05 g of the drilled samples was dissolved in 1 mL of buffer and sonicated in an ultrasonic bath (Transsonic T80, Elma Hans Schmidbauer GmbH & Co. KG, Singen, Germany) for 1 min. The separation of the solution from the powder was performed by centrifugation (Mikro 200R, Hettich Zentrifugen, Tullingen, Germany) for 1 min at 15000 rpm and a temperature of 30°C. The supernatant solution was decanted and the procedure was repeated several times resulting in 30 consecutive leachates for dentine and bone material and in 20 leachates for enamel samples. After multielemental analysis the solutions were pooled to 11 fractions shown in Table 18.

pooled leaching fraction	leachates
1	1, 2
2	3, 4, 5
3	6, 7, 8
4	9, 10, 11
5	12, 13 ,14
6	15, 16, 17
7	18, 19, 20
8	21, 22
9	23, 24
10	25, 26, 27
11	28, 29, 30

Tab. 18 Pooled leaching fractions

The residues were washed with sub-boiled H_2O and dried for 48 h at 60°C after leachate 20 before the sequential leaching procedure was continued. 0.5 mL double sub-boiled HNO_3 (65%) was added to every fraction and a Sr/matrix separation (see chapter 2.3.4.) was performed. The residual powder was washed with double sub-boiled H_2O and dried at 60°C to constant weight. The residues were digested in 2 mL double sub-boiled HNO_3 (65%) and 1 mL H_2O_2 (31%) on a heating plate at 150°C for 4 hours. The digested samples were diluted with double sub-boiled 8 mol L^{-1} HNO_3.to a final approximate weight of 10 g.

2.3.2. The investigation of Sr turnover in sheep hard tissues

The jaw bone of the sheep Anja (see chapter 1.6.1.) was cleaned in boiled water and vacuum packed by Tim Schulze-König at the ETH Zurich. On the surface of the jaw bone of the sheep Stronzi was adherent meat and muscle tissues were removed with a knife. The two jaw bones were dried using a freeze drier (Alpha 1-2 LD, Christ Gefriertrocknungs GmbH, Osterode am Harz, Germany) and cut into slices. Systematic sampling of bone material over the two jaw bones was performed with an electrical dental driller. 2 mL double sub-boiled HNO_3 (65%) and 1 mL H_2O_2 (31%) were added to the powdered samples. The samples were digested on a heating plate at 150°C for 4 hours. After that double sub-boiled 8 mol L^{-1} HNO_3 was added to a final approximate weight of 10 g.

2.3.3. Roseldorf

2.3.3.1. Soil samples

Preparation of soil was performed at the Department of Forest- and Soil Sciences, University of Natural Resources and Life Sciences, Vienna. The extraction protocol was done according to DIN V 19730. The soil samples were dried for 48 hours at 40 °C and sieved (ISO 595, 2 mm). Soil extraction was done in duplicates. Approximately two times 20 g dried and sieved soil material were taken from each sample and 50 mL of 1 mol L^{-1} NH_4NO_3 solution were added. The samples were shaken in 100 mL PE vials for 2h at 20 rpm at room temperature with an overhead shaker (GFL Gesellschaft fuer Labortechnik GmbH, Burgwedel, Germany) and then filtered (Munktell, Falun, Sweden, grade 14/N, d=150 mm, 80 g/m²). The first drops were discarded and the rest was collected and acidified with 0.5 mL double sub-boiled HNO_3 (65%).

2.3.3.2. Water samples

The water samples were acidified with 1 mL of double sub-boiled HNO_3 (65%) for stability. The samples were filtered with pre-cleaned 5 mL syringes (Injekt, B. Braun Melsungen AG, Melsungen, Germany) and 0.45 µm filters (Minisart RC 25, Sartorius AG, Göttingen, Germany). An aliquot of the filtered water samples was acidified with double sub-boiled HNO_3 (65%) and separated with a Sr specific resin. 10 mL of acidified samples were taken for multielemental analysis. Water samples were diluted 1:100 in double sub-boiled 8 mol L^{-1} HNO_3 and used for multielemental analysis.

2.3.3.3. Cereals and Grapes

Cereals and grapes were dried in a freeze drier (Alpha 1-2 LD, Christ Gefriertrocknungs GmbH, Osterode am Harz, Germany) for 120 h and powdered using a ball mill. About 0.25 g of the samples were transferred into Teflon digestion vessels and 3 mL double sub-boiled HNO_3 (65%) and 1 mL H_2O_2 (31%) were added. The samples were digested using a microwave (MLS 1200mega, MLS GmbH-Microwave Laborsysteme, Leutkirch im Allgäu, Germany) with the time and temperature program given in Table 6 and Table 7. Microwave programs were chosen according to the sample matrix. Each run included a blank with the reagents. The Teflon vessels were cleaned between each sample digestion using 3 mL double sub-boiled HNO_3 (65%) and the same program.

step	time [min]	power [W]	press	temp. 1	temp. 2
1	2	250	0	0	0
2	2	0	0	0	0
3	6	250	0	0	0
4	5	400	0	0	0
5	5	600	0	0	0
Vent	15				

Tab. 19 Microwave program for cereals

step	time [min]	power [W]	press	temp. 1	temp. 2
1	3	250	0	0	0
2	2	0	0	0	0
3	5	250	0	0	0
4	5	500	0	0	0
5	2	0	0	0	0
6	2	500	0	0	0
Vent	15				

Tab. 20 Microwave program for grapes

Digested samples were filled up with double sub-boiled H_2O to a weight of about 10 g. The digested samples with residual precipitate were filtered with pre-cleaned 5 mL syringes (Injekt, B. Braun Melsungen AG, Melsungen, Germany) and 0.45 µm filters (Minisart RC 25, Sartorius AG, Göttingen, Germany). 2 mL of the samples were used to separate the Sr from undesired components. The samples were stored at room temperature.

2.3.3.4. Tooth samples

The archaeological animal and human teeth were prepared by removing the cementum with an electrical dental driller. They were cleaned mechanically with double sub-boiled 1% HNO_3 (w/w) and then with Isopropanol as it was not possible to use an ultrasonic bath due to their size. Sampling of tooth enamel in powdered form was performed with an electrical dental driller. 2 mL double sub-boiled HNO_3 (65%) and 1 mL H_2O_2 (31%) were added to the sample. The samples were digested on a heating plate at 150°C for 4 hours. A blank was undertaken the same procedure. The digested samples were filled up with double sub-boiled 8 mol L^{-1} HNO_3 to a weight of about 10 g.

2.3.4. Sr/matrix separation

A Sr specific resin (EIChrom Industries, Inc., Darien, IL, USA) with a particle size of 100 µm – 150 µm was used to separate Sr from Rb and other matrix components in order to minimize disturbing influences of possible interferences. It is a cation exchange resin which consists of a crown ether (bis-t-butyl-cis-dicyclohexano-18-crown-6) absorbed on an inert substrate. By the variation of the pH value using different concentrations of nitric acid a separation of Sr and Rb can be obtained. Sr is retained by the resin at a low pH, whilst Rb can be eliminated by several washing steps. At neutral pH Sr can be eluted with water (EIChrom 2007).

For the separation procedure, 10 µm filters (Separtis GmbH, Grenzach-Wyhlen, Germany) were put in 3 mL columns and resin was added to result in a final column bed of about 1 mL. The resin was washed 4 times with 0.5 mL double sub-boiled H_2O and slowly conditioned 6 times with 0.5mL 6 mol L^{-1} HNO_3. 2 mL of the sample was applied slowly to the resin. 0.5mL 8 mol L^{-1} HNO_3 was added for 10 times to get rid of the undesired components. The strontium was eluted 4 times with 0.5mL double sub-boiled water. A blank including the used reagents 6 mol L^{-1} HNO_3 8 mol L^{-1} HNO_3 and double sub-boiled H_2O was run in order to monitor impurities of the resin and reagents.

Used columns were first washed with HQ water, then stored for 1 day in 10 % HNO_3 (w/w) and for another day in 1 % HNO_3 (w/w). The 10 µm filters were cleaned in an ultrasonic bath (Transsonic T80, Elma Hans Schmidbauer GmbH & Co. KG, Singen, Germany) and stored in 5 % HNO_3 (w/w). The powdered Sr resin was conditioned in 1 % HNO_3 (w/w) overnight and was stored in the refrigerator at -8°C.

2.4. Instrumentation

2.4.1. The ICP-QMS instrument (ICP-QMS ELAN DRC e)

Multielement analysis and Rb/Sr screening of blanks and samples was performed using the ICP-quadrupole MS instrument ELAN DRC-e (PerkinElmer, Waltham, Massachusetts, USA). The ELAN DRC-e instrument used in the VIRIS laboratory is equipped with a PerkinElmer autosampler AS 93 Plus (PerkinElmer, Ontario, Canada). A cyclonic spray chamber (CPI International, Amsterdam, Netherlands) in combination with either a PFA nebulizer (PFA ST nebulizer, Amsterdam, Netherlands) or a glass concentric MicroMist nebulizer (PerkinElmer, Ontario, Canada) form the sample introduction system. The ELAN DRC-e contains an additional quadrupole as a 'dynamic reaction cell' (DRC). The DRC offers the possibility to remove interferences by interaction of the sample or the undesired components with a collision gas (e.g. He, Ar, O_2, N_2, CH_4 or NH_3). The DRC mode was not used within this work. The mass analyser is a quadrupole. A dual-stage discrete dynode detector is used to detect ions either in pulse counting mode (0–2 000 000 cps) or in analogue mode (> 50 000 cps) depending on the amount of ions reaching the detector. Furthermore, the dual detector

mode enables the measurement over a wide concentration range without overcharging the detector by switching automatically between the two detection modes.

The optimization of the instrument was performed daily including the nebulizer gas flow, the x/y torch position and autolens calibration.

Typical operating conditions of the ICP-QMS ELAN DRC-e are shown in Table 21.

nebulizer type	concentric
spray chamber design	cyclonic
sample cone material	nickel
skimmer cone material	nickel
nebulizer gas flow [L min^{-1}]	~1
plasma gas flow [L min^{-1}]	15
auxiliary gas flow [L min^{-1}]	0.6
RF power [W]	1250
pump velocity during analyses [rpm]	20
number of sweeps	8
number of readings	1
number of replicates	4
scan mode	peak hopping
detection mode	dual
analog stage voltage [V]	-1937
pulse stage voltage [V]	1200

Tab. 21 ELAN DRC-e parameters

A 10 ng g^{-1} indium solution was used as internal normalization standard. The measurements were controlled by an in house prepared reference solution including a set of trace elements with known concentrations.

An external nine-point calibration was performed using a subset of calibration standards prepared from a stock solution ICP Multi Element Standard Solution VI (CertiPur, suprapure, MERCK KGaA, Darmstadt, Germany) including the elements Li, Be, B, Na, Mg, Al, V, Cr, Mn, Fe, Co, Ni, Cu, Zn, Ga, As, Se, Rb, Sr, Mo, Ag, Cd, In, Te, Ba, Tl, Pb, Bi, U.

The nominal concentrations of the standards are 0.05 ng g^{-1}, 0.1 ng g^{-1}, 0.5 ng g^{-1}, 1 ng g^{-1}, 5 ng g^{-1}, 10 ng g^{-1}, 25 ng g^{-1}, 50 ng g^{-1} and 100 ng g^{-1}.

Additionally, a five point calibration was done with calibration standards including the elements sodium, calcium, magnesium and strontium. The standards were prepared using 1000 mg L^{-1} Na, Ca, Mg and Sr ICP Standards (CertiPur, MERCK KGaA, Darmstadt, Germany). The concentrations of the elements in ng g^{-1} are listed in Table 22.

	Na	Mg	Ca	Sr
Std. I	25	50	50	0.5
Std.II	50	100	100	1
Std. III	100	200	200	10
Std. IV	200	300	500	50
Std. V	300	400	1000	100

Tab. 22 Element concentrations in ng g^{-1} in standard solutions

For the diagenesis study seven phosphorus standards with the concentrations of 0.05 µg g^{-1}, 0.10 µg g^{-1}, 0.25 µg g^{-1}, 0.50 µg g^{-1}, 1 µg g^{-1}, 2.5 µg g^{-1} and 5.0 µg g^{-1}were made out of a 1000 mg L^{-1} Phosphorus ICP Standard (Sigma-Aldrich, Nr. 207357) and used for calibration.

2.4.2. The multiple collector sector field instrument (MC-ICP-SFMS Nu Plasma)

The MC-ICP-SFMS Nu Plasma instrument (Nu Instruments Ltd., Wrexham, UK) was used for strontium isotope ratio measurements. The MC-ICP-SFMS is equipped with an ESI SC 4 (Elemental Scientific, Inc., Omaha, USA) autosampler and a membrane desolvating system (DSN 100, Nu Instruments Ltd, North Wales, UK). The latter is used for drying the aerosols before entering the plasma for ionization. A double focusing magnetic sector field forms the mass analyzer by combination of an electrostatic field and a magnet following the Nier-Johnson geometry. The detector unit is a multiple collector and consists of 12 Faraday cups and three ion-counting (IC) units (NuInstruments 2007).

Typical operating conditions of the MC-ICP-SFMS Nu Plasma for routine Sr isotope ratio measurements are shown in Table 23.

nebulizer type	PFA
sample cone material	nickel
skimmer cone material	nickel
plasma gas flow [L min-1]	13
auxiliary gas flow [L min-1]	1.2
RF power [W]	1300
nebulizer back pressure [psi]	~ 30
axial m/z	86
mass resolution m/Δm	300
sample uptake rate [µL min-1]	~ 140
DSN 100 hot gas flow [L min-1]	~ 0.3
DSN 100 membrane gas flow [L min-1]	~ 3
DSN 100 membrane temperature [°C]	~ 115
spray chamber temperature [°C]	~ 115
measurements per block	10
number of blocks	6
dwell time [s]	5

Tab. 23 NuPlasma instrument settings for Sr isotope ratio measurements

The NuPlasma instrument was tuned daily by adjusting operating parameters including the torch position, lens settings, gas flows and peak shapes in order to achieve maximum sensitivity and stability for Sr. During Sr isotope ratio measurements the signal intensity of ^{88}Sr should be above 2V to obtain maximum precision and not above 8V to avoid detector overload. Prior to measurements at the NuPlasma Rb/Sr screenings at the ELAN DRC-e are performed, so that samples and standard solutions are diluted to final concentrations of Sr resulting in a beam intensity of 3-8V of ^{88} Sr.

Mass 86 was measured at the axial detector. A mass separation of 0.5 is required for Sr, so that every second Faraday cup was used for detection. The Faraday collector block and the measured masses with the corresponding isotopes are listed in Table 24.

cup	mass	isotope	interference
H6			
H5			
H4	88	^{88}Sr	
H3			
H2	87	^{87}Sr	^{87}Rb
H1			
Ax	86	^{86}Sr	^{86}Kr
L1			
L2	85		^{85}Rb
L3	84	^{84}Sr	^{84}Kr
L4	83		^{83}Kr
L5	82		^{82}Kr

Tab. 24 Faraday collector block setup

2.4.3. Data processing

2.4.3.1. Blank correction

A blank (1% HNO_3 (w/w)) and a solution of ~20 ng g^{-1} of the CRM NIST SRM 987 in 1% HNO_3 (w/w) are measured every fifth sample. Blank correction was done with the method 'On-peak-zeros' provided by the NuPlasma software. The blank defines the background signal for each cup and is subtracted from all measured voltages.

2.4.3.2. Mass bias and correction laws

Mass bias and correction techniques are explained in chapter 1.8.3.

In this work the $^{86}Sr/^{88}Sr$ is used to calculate the fractionation factor for Sr (Equ. 2) according to the exponential law (Albarède et al. 2004). The intensity of the signal at mass 87 needs to be corrected for the isobaric interference of ^{87}Rb. The contribution of ^{87}Rb to the intensity of the ion beam is calculated with the non-interfered ^{85}Rb applying the same mass fractionation (Equ. 3) and then subtracted from the measured intensity at mass 87 (Equ. 4). The $^{87}Sr/^{86}Sr$ ratio is then corrected for mass bias using the fractionation factor (Equ. 5).

Equ. 2

$$f = \frac{\ln\left[\left(\frac{^{86}Sr}{^{88}Sr}\right)_{ref} \Big/ \left(\frac{^{86}Sr}{^{88}Sr}\right)_{meas}\right]}{\ln\left(\frac{m_{86}}{m_{88}}\right)}$$

Equ. 3

$$^{87}Rb_{meas} = \frac{\left(\frac{^{87}Rb}{^{85}Rb}\right)_{true} x\, ^{85}Rb_{meas}}{\left(\frac{m_{87}}{m_{85}}\right)^{f}}$$

Equ. 4

$$^{87}Sr = ^{87}\text{Intensity} - ^{87}Rb_{meas}$$

Equ. 5

$$\left(\frac{^{87}Sr}{^{86}Sr}\right)_{corr} = \left(\frac{^{87}Sr}{^{86}Sr}\right)_{meas} x \left(\frac{m_{87}}{m_{86}}\right)^{f}$$

Equ. 6

$$\left(\frac{^{86}Sr}{^{88}Sr}\right)_{corr} = \left(\frac{^{86}Sr}{^{88}Sr}\right)_{obs} x \left(\frac{m_{86}}{m_{88}}\right)^{f}$$

A sample-standard bracketing method was applied to correct for mass bias for the measurement of Anja's right lower jaw bone, which is enriched in ^{86}Sr. Every sample was bracketed by two measurements of the certified reference material NIST SRM987. The average value of the mass fractionation factors of the standard runs serves as fractionation factor for the sample. After elimination of the ^{87}Rb interference (Equ. 4), the corrected $^{87}Sr/^{86}Sr$ (Equ. 5) and $^{86}Sr/^{88}Sr$ (Equ. 6) were calculated.

3. Results and Discussion

3.1. Diagenesis study of tooth and bone matrices

All data of elemental and isotope ratios of leached human and animal tooth and bone samples are given in the Appendix 7.2.1. An overview about the elemental ratios Ca/P and Sr/Ca and the $^{87}Sr/^{86}Sr$ ratios will be given in chapter 3.1.3. The results of some selected examples of leached samples including different hard tissues of human individuals and of different animal species will be discussed in the following. The rest of the results are illustrated in Figures in the Appendix 7.2.1.

The increased elemental ratios after leaching fraction 20 might be due to the drying process and will be discussed in chapter 3.1.3.

The $^{87}Sr/^{86}Sr$ ratios of leached human and animal material will be set in relation to the local Sr isotope signature of the excavation site Gars Thunau which was established in the master thesis of Huemer, 2008. The local Sr isotope signal ranges between 0.7133 and 0.7210 (Huemer 2008).

3.1.1. Human tooth dentine and enamel

Results for the leached dentine and enamel of the human individual with the inventory number GT 24958 are illustrated in Figure 17, 18, 19 and 20.

For the human dentine sample a decrease in the Ca/P ratios can be observed for the dissolution steps 1-3. The initial Ca/P ratio is 2.48, in the leachates 4-20 a stable value of 1.85 ±0.02 is approached which is in accordance with the Ca/P range of 1.48–2.21 in modern human tooth samples (Nelson 1981; Woodward 1962)

The Sr*1000/Ca ratios show a decline in the leaching fractions 1-7 with an initial value of 2.59 before a stable value of 0.91 ±0.12 is reached in the following leachates. This ratio can be compared with values of biogenic hydroxyapatite in modern mammalian teeth of 0.47 – 1.50 (Sponheimer et al. 2005b).

The $^{87}Sr/^{86}Sr$ ratio of the first pooled leaching fraction corresponds to the value of the total digest of the dentine. The first five fractions show decreasing $^{87}Sr/^{86}Sr$ ratios, the following fractions 6-11 exhibit a stable Sr isotope value and converge towards the value of 0.7157 of

the digest of the leached dentine. This result is in agreement with the local range of the excavation site Gars Thunau.

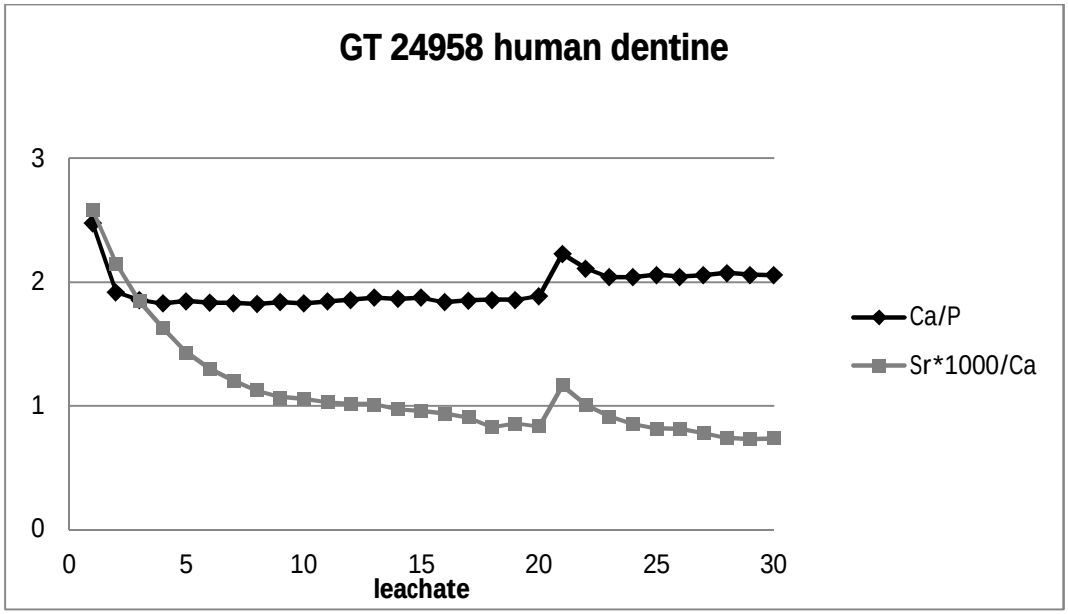

Fig. 17 Elemental ratios of leachates of human dentine GT 24958

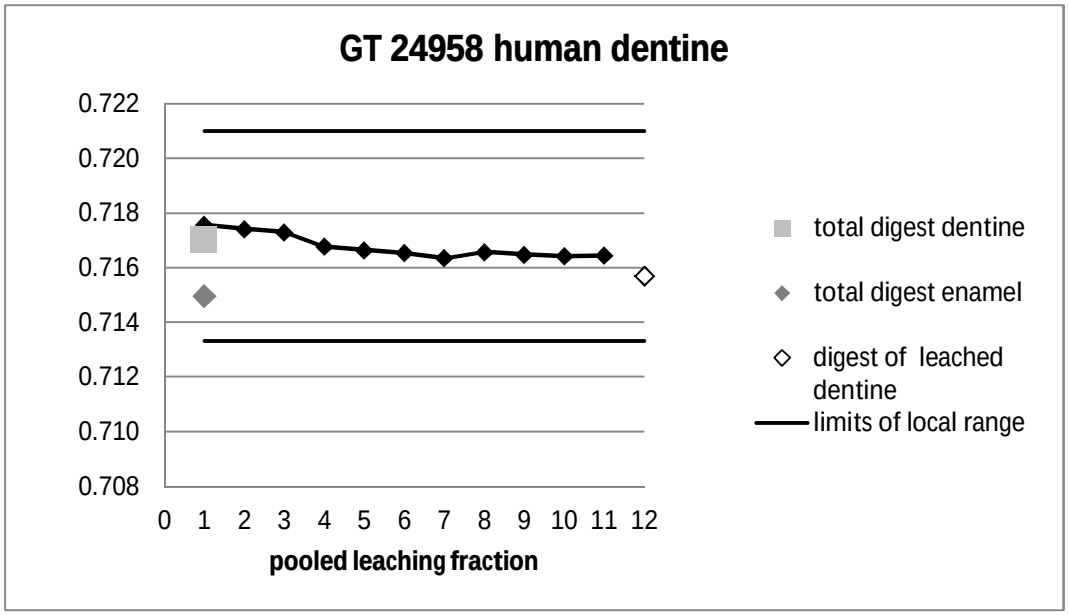

Fig. 18 $^{87}Sr/^{86}Sr$ ratios of pooled leaching fractions of human dentine GT 24958

The Ca/P ratios of leached human enamel decrease in the first three dissolution steps and show after the third fraction a stable Ca/P value of 2.00 ±0.03. Biogenic hydroxyapatite

displays Ca/P ratios between 1.48–2.21 (Woodward 1962; Nelson 1981). The initial value of the Ca/P ratio of 4.22 is higher than the corresponding value of the first fraction of the leached dentine with 2.48.

The Sr*1000/Ca ratio of enamel shows a value of 0.63 for the first leachate and a stable value of 0.43 ±0.04 for the consecutive leachates. These values are in the range of 0.47–1.50 reported in literature (Sponheimer et al. 2005b).

The $^{87}Sr/^{86}Sr$ ratios of the leaching fractions range between 0.7157 and 0.7161 with a mean value of 0.7158 ±0.0002 and thus, can be seen to be stable. The Sr isotope ratios of the fractions are between the values of the total digest of dentine and enamel.

The leached human enamel with the inventory number GT 24986 has an initial Ca/P ratio of 2.58 before reaching a stable value of 2.02 ±0.02 for the consecutive leachates. The stable ratio is comparable with the result obtained for human enamel GT 2958, while the Ca/P value of the first leachate is lower. The Sr*1000/Ca ratio exhibits a stable value of 0.33 ±0.05 for all the leachates.

Schultheiss (2003) observed relatively high Ca/P ratios for the first fraction of modern femur. The elevated Ca/P ratio of the first leaching fraction of the two enamel samples may be caused by residues of soft tissues on the surface of the tooth that had not been successfully removed (Schultheiss 2003). This might also be the reason for the elevated Sr*1000/Ca of human enamel GT 24958 compared stable values of enamel GT 24986.

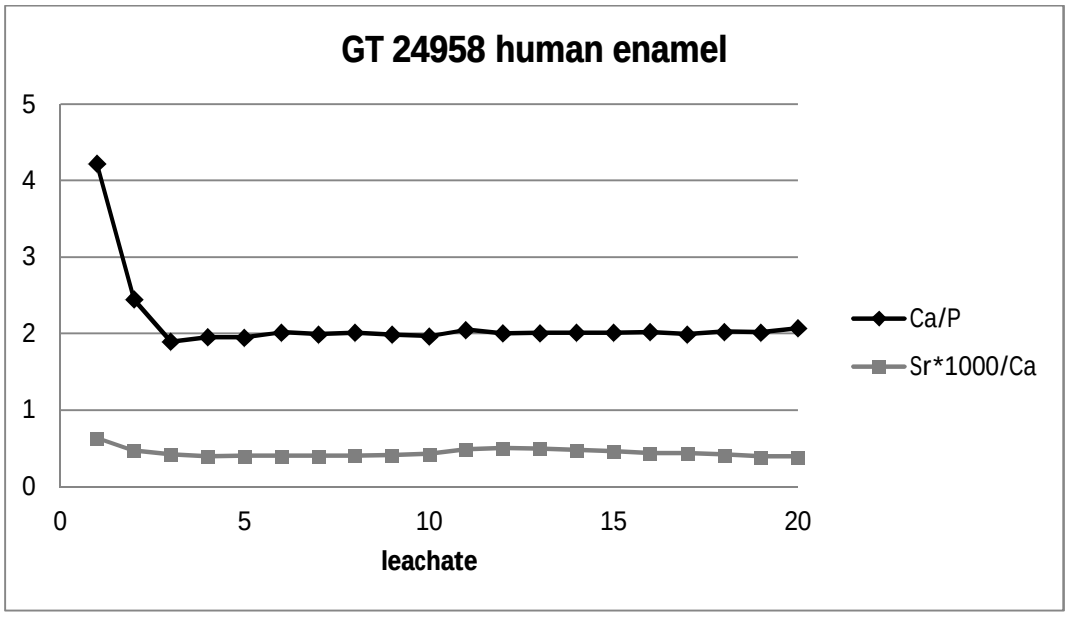

Fig. 19 Elemental ratios of leachates of human enamel GT 24958

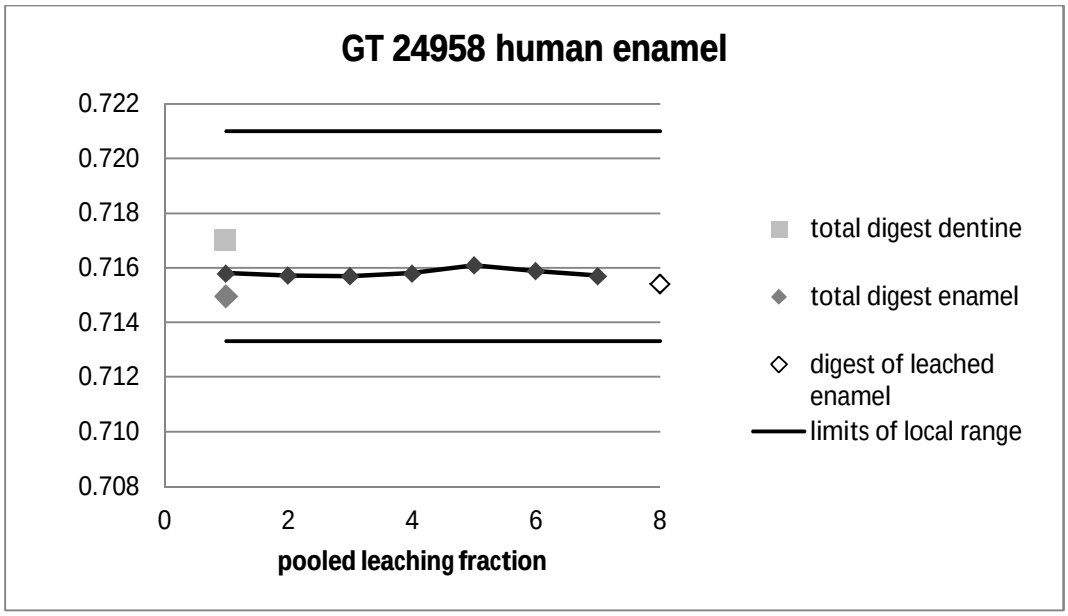

Fig. 20 $^{87}Sr/^{86}Sr$ ratios of pooled leaching fractions of human enamel GT 24958

The results for the human individual with the inventory number GT 25096 are illustrated in Figure 21 and 22. The elemental ratios Ca/P and Sr*1000/Ca of this human dentine sample show similar patterns as the human individual GT 24958 with decreasing ratios in the first leachates. In the subsequent leachates a stable value of 2.08 ±0.04 for Ca/P and of 0.31 ±0.05 for Sr*1000/Ca is reached which are in accordance with the values of biogenic hydroxyapatite (Sponheimer et al. 2005b; Nelson 1981; Woodward 1962).

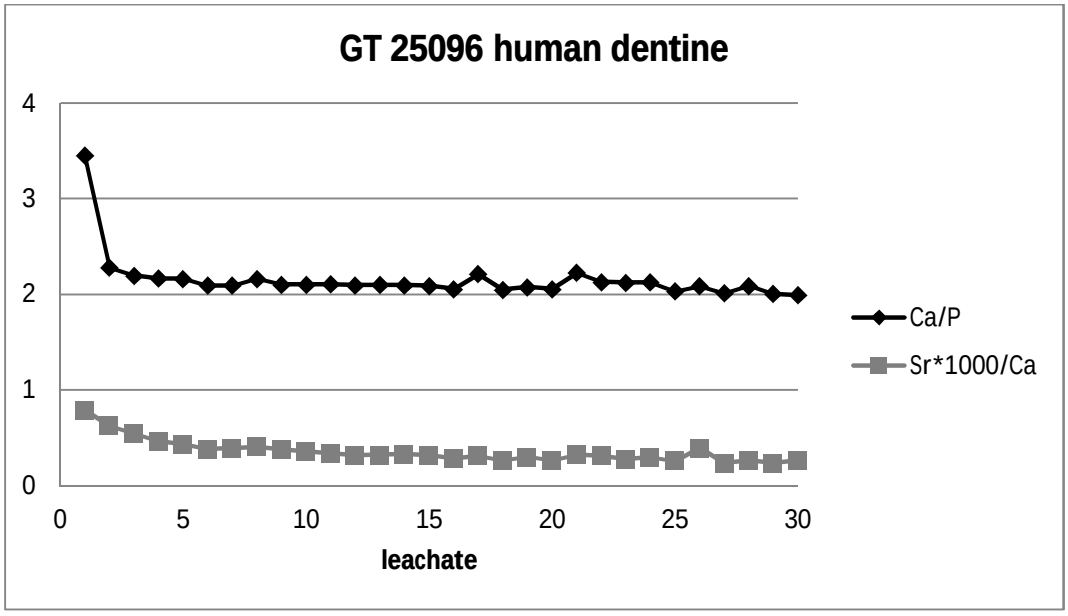

Fig. 21 Elemental ratios of leachates of human dentine GT 25096

The Sr isotope ratio of the total digest is in agreement with the local range of Gars Thunau. The $^{87}Sr/^{86}Sr$ ratios of the pooled leaching fractions decline and go below the local Sr isotope signature of the excavation site. They converge towards the Sr isotope value of the total digest of the corresponding enamel sample. An increase in Sr isotope values between leachate 6 and 7 and between leachate 9 and 10 is observed illustrated in Figure 22. The digest of the leached dentine displays a Sr isotope ratio of 0.7121 which is relatively higher than the values of leachates 4-6. This result is in accordance with the observations made by and Sillen (1986) and Schultheiss (2003) that the residual powder of the sequential leaching procedure contains recrystallized, diagenetic (fluoride-) apatite (Sillen 1986; Schultheiss 2003).

It can be suggested that the total digest of dentine displays a local Sr isotopic signature due to diagenetic alteration of the tissue. This could indicate that this human individual did not live at the excavation site in the lifespan reflected in enamel and dentine.

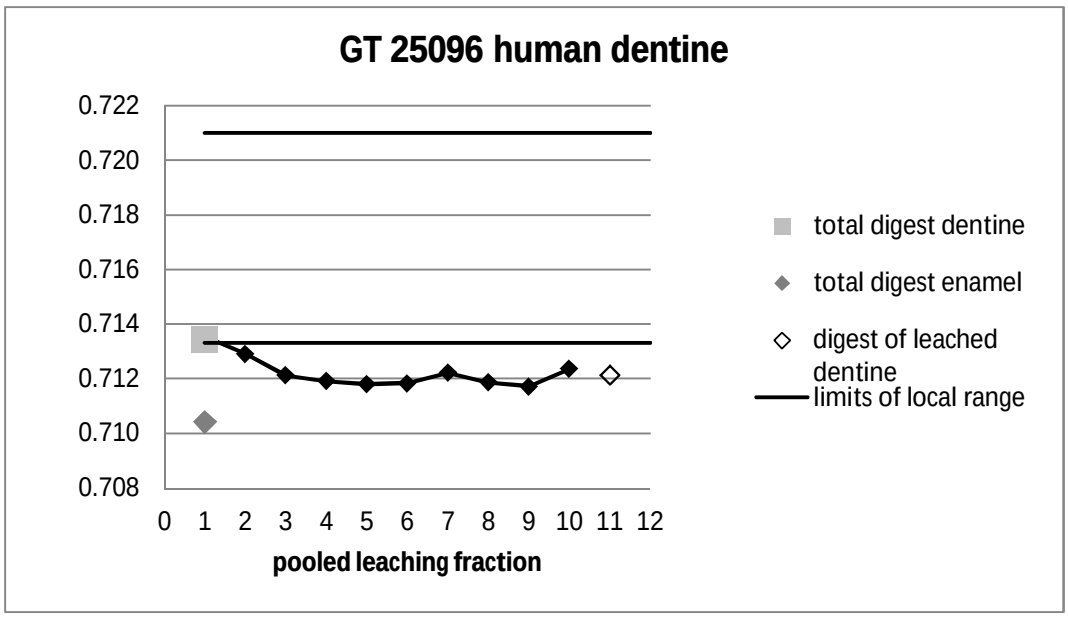

Fig. 22 $^{87}Sr/^{86}Sr$ ratios of pooled leaching fractions of human dentine GT 25096

The human dentine samples with the inventory number GT 24986, GT 25123 and GT 25146 show similar patterns in their elemental ratios Ca/P and Sr/Ca as the human dentine samples discussed. The Sr isotope ratios decline from fractions 1-6, an increase in values is observed between fractions 6-8.

3.1.2. Animal tooth dentine and bone

Elemental and isotopic ratios of hard tissues of the sheep with the inventory number GT 23877 are illustrated in Figures 23, 24, 25 and 26.

Tooth dentine shows an initial Ca/P value of 9.58. Seven dissolution steps are required to reach a stable Ca/P value of 2.11 ± 0.05. The jaw bone exhibits for the Ca/P ratio with 45 a higher value for the first leachate than the dentine The Ca/P ratios for these tissues are continuously decreasing from leachate 1 to leachate 20. The reached Ca/P ratios in fraction 20 of the dentine and the jaw bone can be compared to the value range of 1.48–2.21 reported in literature (Nelson 1981; Woodward 1962).

No significant difference occurred in the profiles and values of the Sr/Ca ratio for the dentine and jaw bone. The Sr*1000/Ca ratios of the leached jaw bone and dentine decrease continuously from leachate 1 to leachate 30. Dentine shows a decline from the value 2.42 to 1.45 and jaw bone from 2.49 to 1.56 converging towards the Sr*1000/Ca ratio of 1.05 of biogenic hydroxyapatite (Burton et al. 1999).

The $^{87}Sr/^{86}Sr$ ratio of the first pooled leaching fraction of sheep dentine corresponds to the value of the total digest of the dentine. The Sr isotope ratios of the following leaching fractions decline until fraction 7. An increase from fraction 7 with a value of 0.7119 to fraction 8 with a value of 0.7139 is observed. After fraction 8 the $^{87}Sr/^{86}Sr$ ratios decrease again towards a value of 0.7125 for the digest of the leached dentine. These results are in accordance with the pattern obtained for human dentine GT 25096.

The observed $^{87}Sr/^{86}Sr$ ratios for the fractions 4-7 and 10-12 are not consistent with the local range and thus, point to a non-local origin of this sheep. The total digest of the corresponding enamel also indicates that it was not autochthonous. The Sr isotopic profile of the jaw bone sample shows a decreasing tendency, but in contrast to the dentine it is in agreement with the local range. This could indicate that it was not possible to remove all diagenetic strontium and to recover the original Sr isotope signature. Due to the structure of bones compared to dentine (see chapter 1.4) bone material is considered to be more affected by diagenetic alteration (Dauphin and Williams 2004).

In Table 25 the results of the leached tissues of the two analyzed sheep are compared. The Ca/P and Sr*1000/Ca ratios of the dentine and jaw bone of the sheep 2 with the inventory number GT10961 show similar trends as sheep 1. The initial Ca/P ratios of dentine and jaw bone of sheep 1 are higher than the values of sheep 2 for the same tissues. An explanation

could be the different preservation state of the remains of the two sheep (see chapter 1.4.). The reached values in fraction 20 are comparable between the two sheep and in conjunction with literature values (Burton et al. 1999; Woodward 1962; Nelson 1981). The Sr isotope ratios decrease continuously in the jaw bone samples of the two sheep while in both dentine samples an increase in the $^{87}Sr/^{86}Sr$ ratios could be observed between leaching fraction 7 and 8.

sample material	Ca/P (fraction1)	Ca/P (fraction 20)	Sr*1000/Ca (fraction 1)	Sr*1000/Ca (fraction 20)
sheep 1 dentine	9.58	2.17	2.42	1.45
sheep 2 dentine	4.09	1.86	2.47	0.90
sheep 1 jaw bone	42.85	2.19	2.49	1.56
sheep 2 jaw bone	8.31	2.05	3.31	1.20

Tab. 25 Elemental ratios Ca/P and Sr/Ca of sheep hard tissues

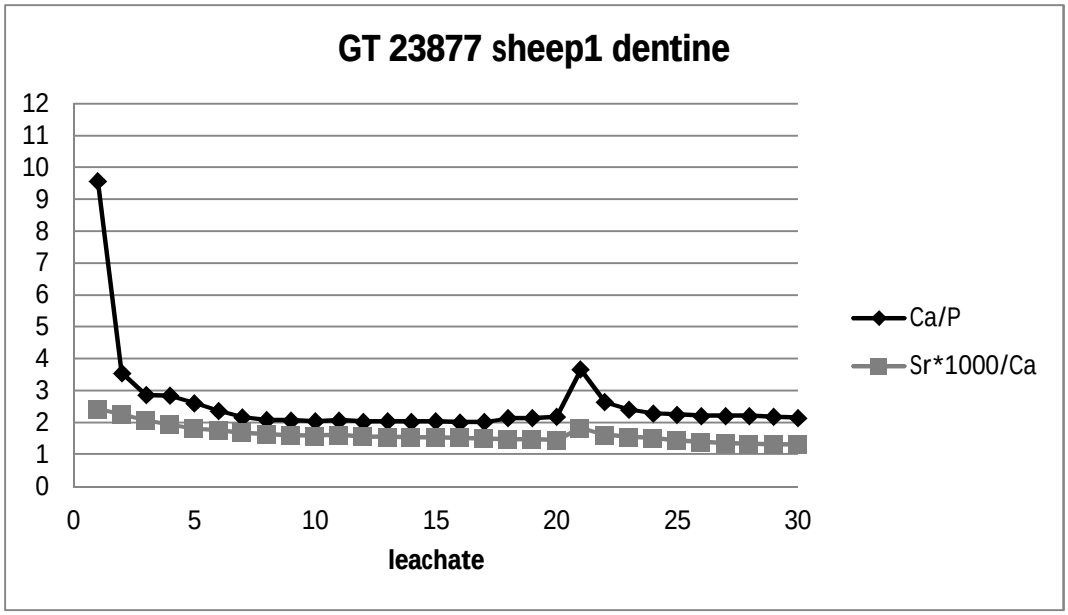

Fig. 23 Elemental ratios of leachates of sheep dentine

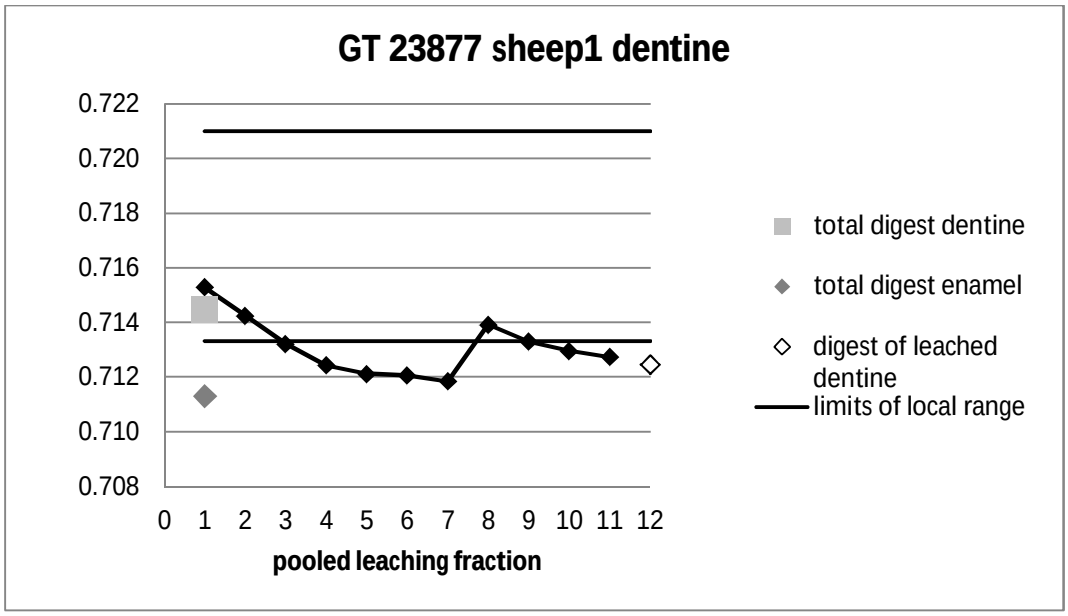

Fig. 24 $^{87}Sr/^{86}Sr$ ratios of pooled leaching fractions of sheep dentine

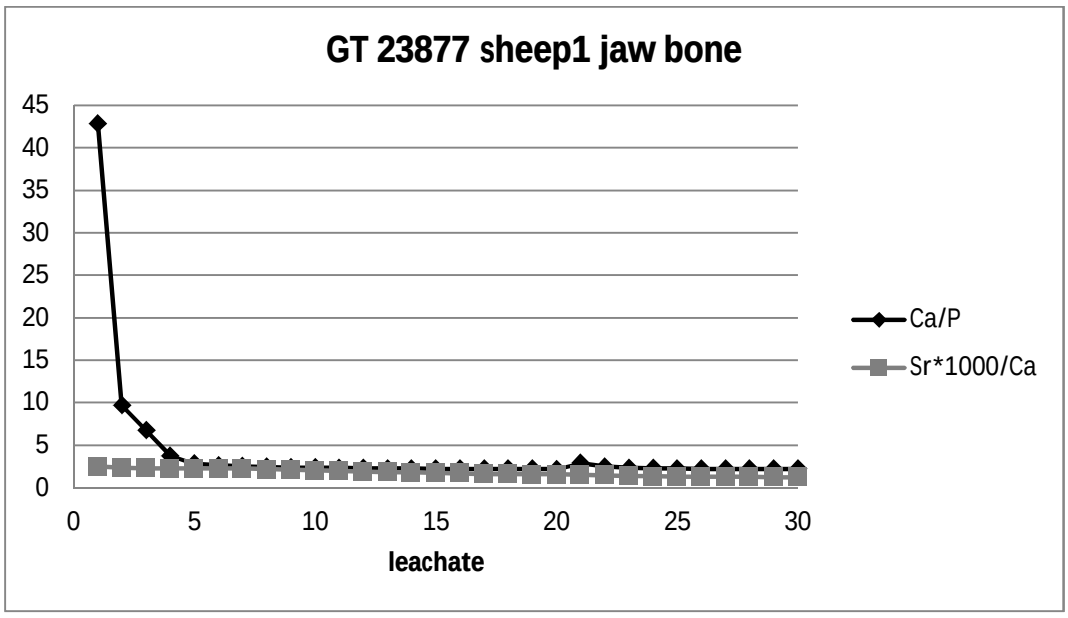

Fig. 25 Elemental ratios of leachates of sheep jaw bone

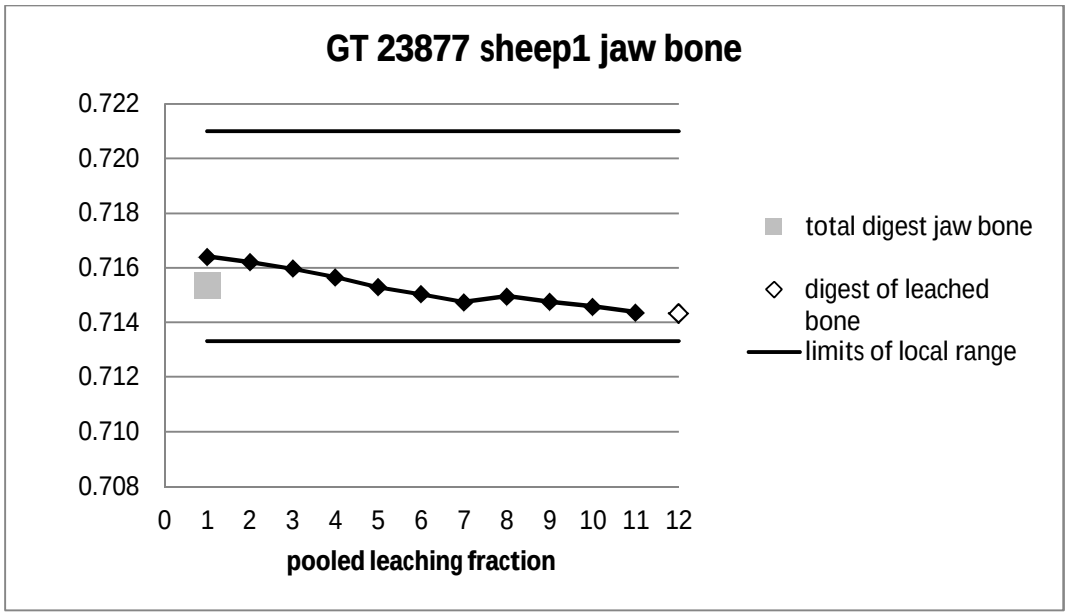

Fig. 26 $^{87}Sr/^{86}Sr$ ratios of pooled leaching fractions of sheep jaw bone

Results for horse and cattle dentine are illustrated in Figures 27, 28, 29 and 30.

The elemental patterns of the leachates of human dentine are retrieved in horse and cattle dentine. A decay of Ca/P and Sr/Ca ratios is observed for the first leachates before a stable value is exhibited for the consecutive leachates.

The $^{87}Sr/^{86}Sr$ ratio of the total digests of horse hard tissues are with values of 0.7138 for dentine and 0.7128 for enamel near the lower limit 0.7133 of the local range. As a consequence, it is difficult to draw conclusions about the autochthonous character of the horse. The values for the pooled leaching fractions of horse dentine decrease and converge towards the $^{87}Sr/^{86}Sr$ ratio of the enamel. After leaching fraction 7 the Sr isotope value shows a distinct decline from 0.7130 to 0.7117 for fraction 8. After fraction 8 the values increase again towards the $^{87}Sr/^{86}Sr$ ratio of 0.7128 of the digest of the leached dentine.

The Sr isotope ratios of cattle dentine show a decreasing trend in fractions 1-7 before they start to increase again in the last fractions. The obtained $^{87}Sr/^{86}Sr$ ratios maintain in agreement with the local range.

The observed increase in the Sr isotope ratios of the leached dentine of cattle and horse after fraction 7 corresponds to the results obtained for human and sheep dentine.

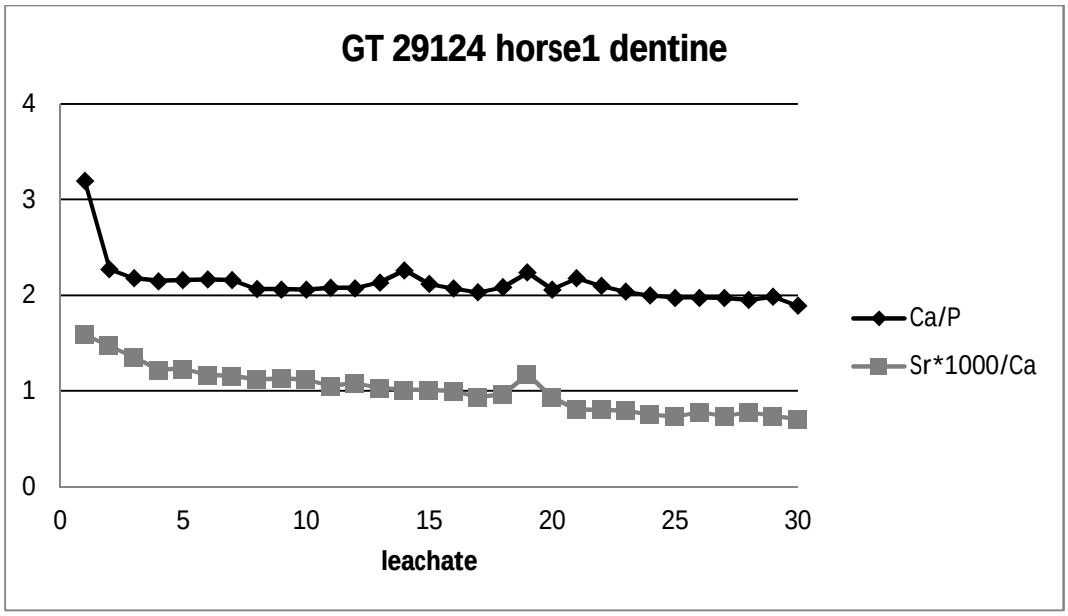

Fig. 27 Elemental ratios of leachates of horse dentine

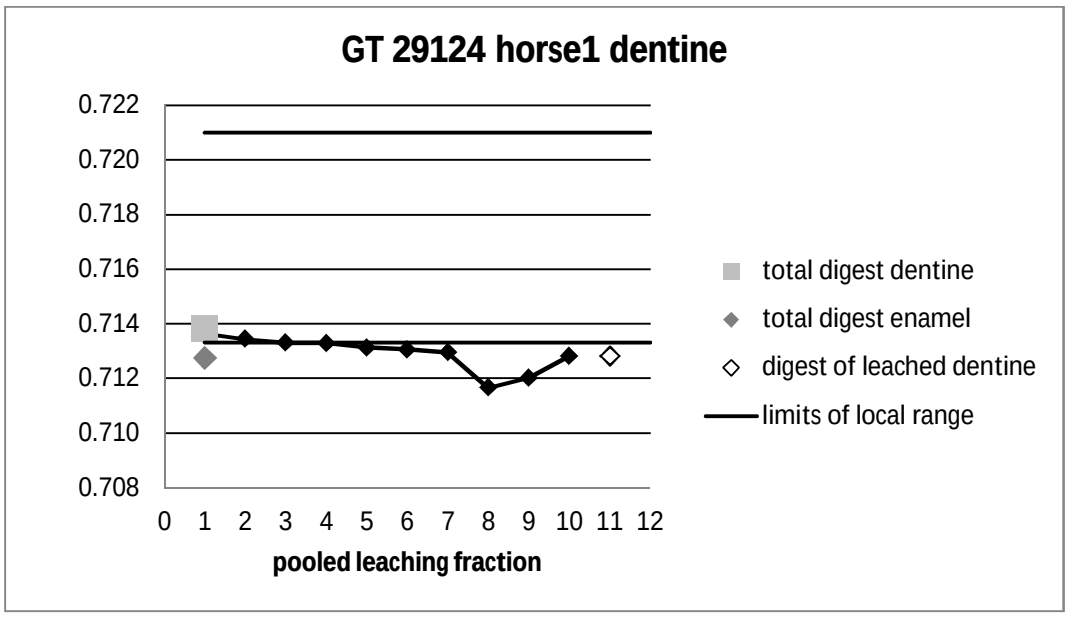

Fig. 28 $^{87}Sr/^{86}Sr$ ratios of pooled leaching fractions of horse dentine

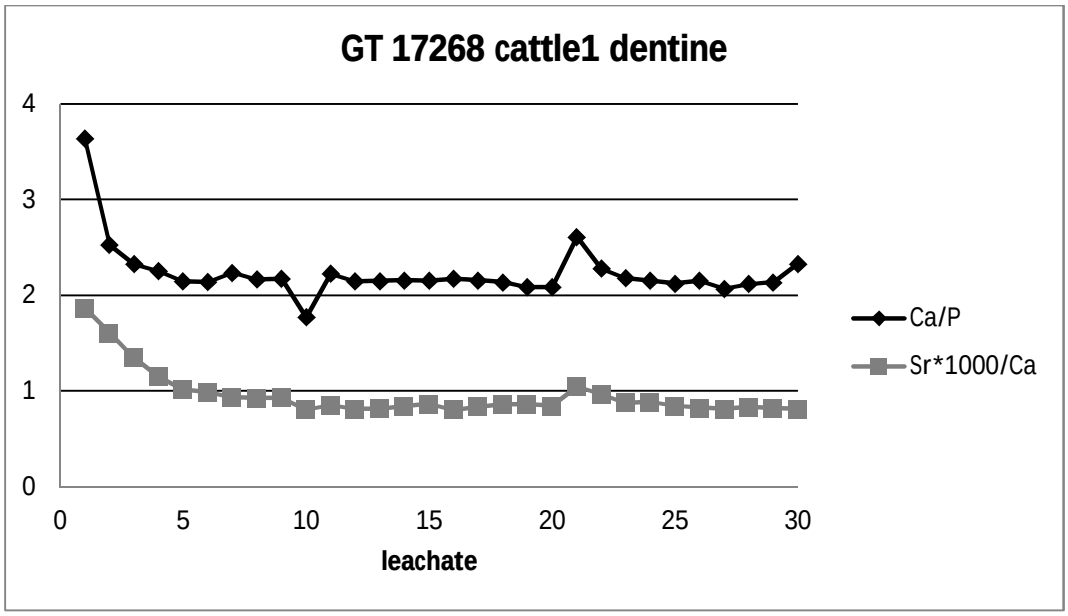

Fig. 29 Elemental ratios of leachates of cattle dentine

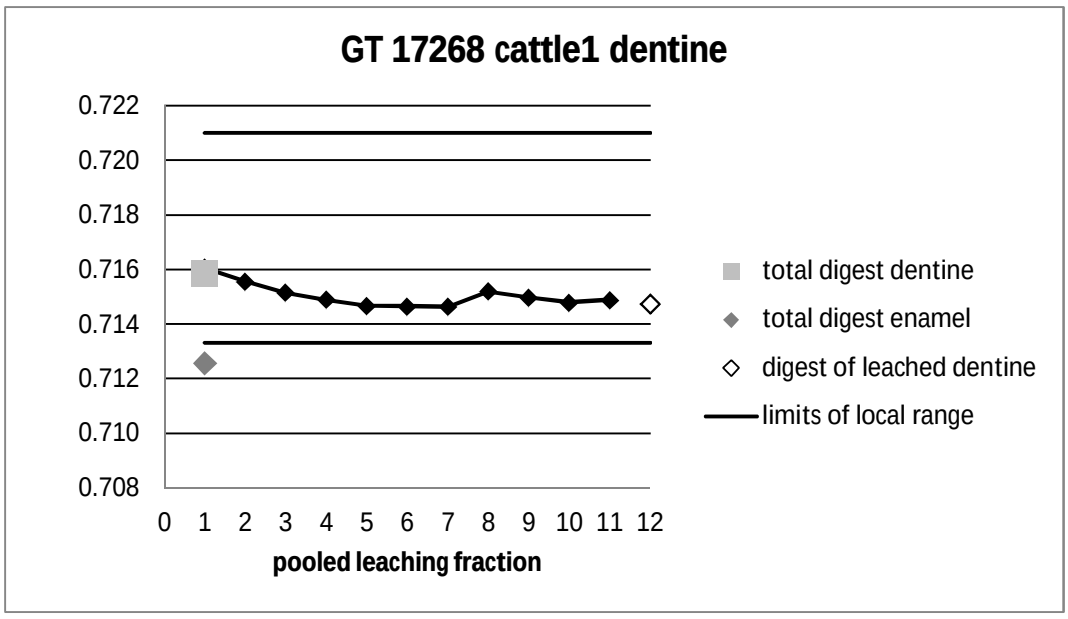

Fig. 30 $^{87}Sr/^{86}Sr$ ratios of pooled leaching fractions of cattle dentine

3.1.3. General observations

After leachate fraction 20 increasing values could be observed for elemental ratios for dental and skeletal tissues. In the following fractions the ratios converge towards the stable value of the leachates before number 20. After 20 consecutive leaching steps the residues were dried for 48h before the leaching was continued. Leaching fractions 21, 22 and 23 show a higher concentration of Sr than the leachates of 10-20. Therefore, the drying procedure of the sample may have an influence on the solubility behavior of Sr and as a consequence on the results.

The elemental ratios Ca/P and Sr*1000/Ca are listed in Table 26, 27, 28 and 29 and the $^{87}Sr/^{86}Sr$ ratios in Table 30. Human and animal hard tissues show similar characteristics concerning their elemental pattern of Ca/P and Sr/Ca. A decrease of the Ca/P value in the first two leachates is observed before the ratio stabilizes after wash two. An exception is the jaw bone of sheep 1 GT 23877 needing five dissolution steps to reach a stable value. The Ca/P pattern is in accordance with the observations made by Sillen (1986) in fossil specimen. The elevated Ca/P ratios of the initial leachates could be explained with the dissolution of secondary (especially calcareous) minerals within the tooth and bone structure. Thus, fraction 1 and 2 are considered to represent the most soluble mineral (Sillen 1986). The Sr/Ca ratios decline from leachate 1 to leachate 6 or 10 depending on the investigated tissue before approaching a stable value. Sillen (1986) obtained in the first 6 washes high Sr/Ca values indicating the existence of soluble diagenetic mineral (Sillen 1986). The measurements of Ca/P and Sr/Ca ratios in the total digest and the digest of the leached material have not been carried out so far in this study. The $^{87}Sr/^{86}Sr$ ratios in leached human and animal tooth dentine show an increase of values after leaching fraction 7 and in the leached digest of the material. This is in conjunction with observations made by Sillen (1986) and Schultheiss (2003) proposing the presence of recrystallized apatite in the residues (Sillen 1986; Schultheiss 2003).

Due to the observed patterns in the elemental and isotopic ratios the leached fractions can be grouped into the following compartments corresponding to the results found by Sillen (1986):

- Compartment I including the leached fractions 1-2 is characterized by elevated Ca/P and Sr/Ca ratios indicating the presence of highly soluble minerals.

- Compartment II comprises leached fractions 2-6 (10) depending on the analyzed sample. It is characterized by stable Ca/P values and elevated Sr/Ca ratios. Thus, it can be assumed that those fractions still contain diagenetic Sr.
- Compartment III exhibits stable Ca/P and Sr/Ca ratios in the fractions 10–20. It can be suggested that those fractions consist of biogenic Sr.
- Compartment IV comprises fractions 20-30. The fluctuation of Ca/P and Sr/Ca ratios indicate the possible presence of diagenetic Sr.
- Compartment V is the digest of the leached residue containing diagenetic material expressed by elevated Sr isotope ratios.

The characteristics of compartment I-III and compartment V are in accordance with the results by Sillen (1986) and Schultheiss (2003). As far as compartment IV is concerned, the leaching fractions 20-30 are characterized by elevated Ca/P and Sr/Ca ratios compared to leachates 10-20. Especially from fraction 20-22 an increase in the values is observed. Animal and human dentine samples show an increase in the Sr isotope ratios in pooled leaching fractions 8 and 9 corresponding to the leachates 21, 22 and 23, 24. These results could be explained by the drying process of the residues after leaching step 20. But there is also the possibility of the presence of diagenetic Sr in the last washes.

	GT 24958	**GT 24958**	**GT 24986**	**GT 24986**	**GT 25123**	**GT 25096**	**GT 25146**
	human dentine	**human enamel**	**human dentine**	**human enamel**	**human dentine**	**human dentine**	**human dentine**
fraction	**Ca/P**	**Ca/P**	**Ca/P**	**Ca/P**	**Ca/P**	**Ca/P**	**Ca/P**
1	2.48	4.22	2.74	2.57	2.50	3.46	2.97
2	1.92	2.45	2.24	1.98	2.16	2.28	2.22
3-20	1.85 ±0.02	2.00 ±0.03	2.12 ±0.01	2.02 ±0.02	2.04 ±0.01	2.08 ±0.04	2.11 ±0.03
21	2.23		2.39		2.19	2.23	2.94
22	2.11		2.19		2.15	2.13	2.40
23	2.04		2.18		2.04	2.12	2.31
24	2.04		2.15		2.08	2.13	2.26
25	2.06		2.18		2.08	2.03	2.23
26	2.04		2.12		2.07	2.08	2.15
27	2.06		2.12		2.10	2.01	2.15
28	2.07		2.12		2.07	2.09	2.12
29	2.06		2.14		2.06	2.01	2.11
30	2.06		2.15		2.11	1.99	2.14

Tab. 26 The Ca/P ratios of leached human hard tissues

	GT 23877	GT 10961	GT 10961	GT 17268	GT 17477	GT 29124
	sheep 1 dentine	sheep 2 dentine	sheep 2 jaw bone	cattle 1 dentine	cattle 3 dentine	horse 1 dentine
fraction	Ca/P	Ca/P	Ca/P	Ca/P	Ca/P	Ca/P
1	9.58	4.09	8.31	3.64	2.84	3.20
2	3.55	2.44	2.70	2.53	2.28	2.27
3-20	2.11 ±0.05	1.95 ±0.06	2.15 ±0.11	2.16 ±0.05	2.12 ±0.04	2.08 ±0.09
21	3.66	2.34	2.25	2.61	2.41	2.18
22	2.64	2.16	2.19	2.28	2.21	2.10
23	2.41	2.07	2.16	2.18	2.20	2.04
24	2.29	2.18	2.07	2.15	2.10	2.00
25	2.24	1.93	2.09	2.12	2.11	1.98
26	2.21	1.97	2.03	2.15	2.12	1.98
27	2.20	1.88	2.02	2.07	2.08	1.97
28	2.20	1.93	2.05	2.12	2.29	1.95
29	2.18	2.41	2.24	2.14	2.05	1.99
30	2.15	1.78	1.92	2.33	2.50	1.89

Tab. 27 The Ca/P ratios of leached animal hard tissues

	GT 24958	GT 24958	GT 24986	GT 24986	GT 25123	GT 25096	GT 25146
	human dentine	human enamel	human dentine	human enamel	human dentine	human dentine	human dentine
fraction	Sr*1000/Ca	Sr*1000/Ca	Sr*1000/Ca	Sr*1000/Ca	Sr*1000/Ca	Sr*1000/Ca	Sr*1000/Ca
1	2.59	0.63	2.31		1.15	0.79	1.34
2	2.15		1.82		0.97	0.63	1.09
3	1.85		1.53		0.84	0.54	0.95
4	1.63		1.27		0.72	0.46	0.84
5	1.43		1.18		0.67	0.43	0.80
6	1.30		1.07		0.62		0.77
7	1.20		1.02		0.59		
8	1.12		1.01		0.56		
biogenic	0.93 ±0.07	0.43 ±0.04	0.85 ±0.02	0.33 ±0.05	0.46 ±0.04	0.33 ±0.04	0.73 ±0.02
21	1.17		1.12		0.56	0.32	1.06
22	1.01		1.11		0.48	0.31	0.94
23	0.91		0.91		0.45	0.27	0.84
24	0.85		0.91		0.45	0.29	0.85
25	0.82		0.93		0.43	0.26	0.81
26	0.81		0.89		0.42	0.40	0.79
27	0.78		0.85		0.42	0.23	0.75
28	0.74		0.88		0.40	0.26	0.75
29	0.73		0.87		0.39	0.23	0.69
30	0.74		0.82		0.40	0.26	0.67

Tab. 28 The Sr*1000/Ca ratios of leached human hard tissues

	GT 23877	GT 10961	GT 10961	GT 17268	GT 17477	GT 29124
	Sheep 1 dentine	Sheep 2 dentine	sheep 2 jaw bone	cattle 1 dentine	cattle 3 dentine	horse 1 dentine
fraction	Sr*1000/Ca	Sr*1000/Ca	Sr*1000/Ca	Sr*1000/Ca	Sr*1000/Ca	Sr*1000/Ca
1	2.42	2.47	3.31	1.87	2.25	1.59
2	2.26	1.97	2.63	1.61	1.92	1.47
3	2.07	1.67	2.27	1.35	1.75	1.35
4	1.93	1.36	2.06	1.15	1.66	1.22
5	1.80	1.32	1.74	1.01	1.67	1.23
6	1.74	1.20	1.43	0.98		1.16
7	1.67		1.48	0.93		1.15
8	1.63		1.79	0.92		1.12
9			1.66	0.93		1.13
10			1.41			1.12
biogenic	1.53 ±0.05	1.10 ±0.05	1.23 ±0.05	0.83 ±0.02	1.53 ±0.05	1.00 ±0.05
21	1.83	1.36	1.14	1.04	1.52	0.81
22	1.61	1.17	1.06	0.96	1.45	0.80
23	1.55	1.14	1.10	0.87	1.43	0.79
24	1.51	1.34	1.10	0.88	1.46	0.75
25	1.43	1.07	1.09	0.84	1.38	0.73
26	1.39	1.01	1.09	0.82	1.35	0.78
27	1.34	0.95	1.08	0.81	1.34	0.74
28	1.32	1.02	1.04	0.83	1.38	0.78
29	1.31	0.89	1.02	0.82	1.35	0.73
30	1.30	1.02	1.02	0.81	1.35	0.70

Tab. 29 The Sr*1000/Ca ratios of leached animal hard tissues

inventory number	sample	$^{87}Sr/^{86}Sr$ (total digest)	$^{87}Sr/^{86}Sr$ (fraction 1)	$^{87}Sr/^{86}Sr$ (fraction 11)	$^{87}Sr/^{86}Sr$ (leached digest)
GT 24958	human dentine	0.7170	0.7176	0.7165	0.7157
GT 24958	human enamel	0.7150	0.7158	0.7157	0.7154
GT 24986	human dentine	0.7169	0.7180	0.7167	0.7165
GT 24986	human enamel	0.7108	0.7123	0.7125	0.7106
GT 25123	human dentine	0.7153	0.7164	0.7145	0.7146
GT 25096	human dentine	0.7100	0.7136	0.7124	0.7147
GT 25146	human dentine	0.7143	0.7155	0.7147	0.7141
GT 23877	sheep 1 dentine	0.7145	0.7153	0.7127	0.7125
GT 23877	sheep 1 jaw bone	0.7154	0.7164	0.7144	0.7143
GT 10961	sheep 2 dentine	0.7165	0.7161	0.7152	0.7150
GT 10961	sheep 2 jaw bone	0.7155	0.7164	0.7144	0.7147
GT 17268	cattle 1 dentine	0.7159	0.7161	0.7149	0.7147
GT 17477	cattle 3 dentine	0.7151	0.7153	0.7152	0.7151
GT 29124	horse 1 dentine	0.7138	0.7137	0.7128	0.7128

Tab. 30 The $^{87}Sr/^{86}Sr$ ratios of leached human and animal samples

3.2. Investigation of Sr turnover in sheep hard tissues

3.2.1. Jaw bone of the sheep 'Stronzi'

Results for the right lower jaw bone of the sheep Stronzi are shown in the Appendix 7.2.2. The spatial variation of the Sr isotope values over the bone is illustrated in Figure 31. The $^{87}Sr/^{86}Sr$ ratios for the inside and outside of the jaw bone range between 0.7085 and 0.7090. The mean value of the $^{87}Sr/^{86}Sr$ ratios is 0.7087 ±0.0001. Significant differences in the Sr isotope values between the sampling positions couldn't be observed.

In the work for a Bachelor thesis of David Gölles which is still in preparation the Sr sources that have an influence on the Sr isotope composition of bone material of Stronzi were investigated. The analysed samples included soil on which the sheep grazed and the ingested water and hay (Gölles in prep.) The average values of the $^{87}Sr/^{86}Sr$ ratios of the analysed hay, water and soil extracts are shown in Table 31.

sample material	average value $^{87}Sr/^{86}Sr$	standard deviation	n
hay	0.7086	0.0004	3
water	0.7077	0.00003	3
soil extract	0.7089	0.0003	4

Tab 31 The Sr isotope ratios of hay, water and soil (Gölles in prep.)

The water and food sources did not change during the life of the sheep Stronzi grazing on the same soil based on what is known from talking to the farmer (Gölles in prep.). The $^{87}Sr/^{86}Sr$ ratios of the hay and soil are retrieved in the right lower jaw bone of Stronzi with a mean value of 0.7087. This result indicates that no natural fractionation of the Sr isotope composition occurred in the food chain and in the metabolism of the sheep before incorporation of the Sr into the jaw bone. The water samples are with an average value of 0.7077 lower than the Sr isotope ratio of the jaw bone.

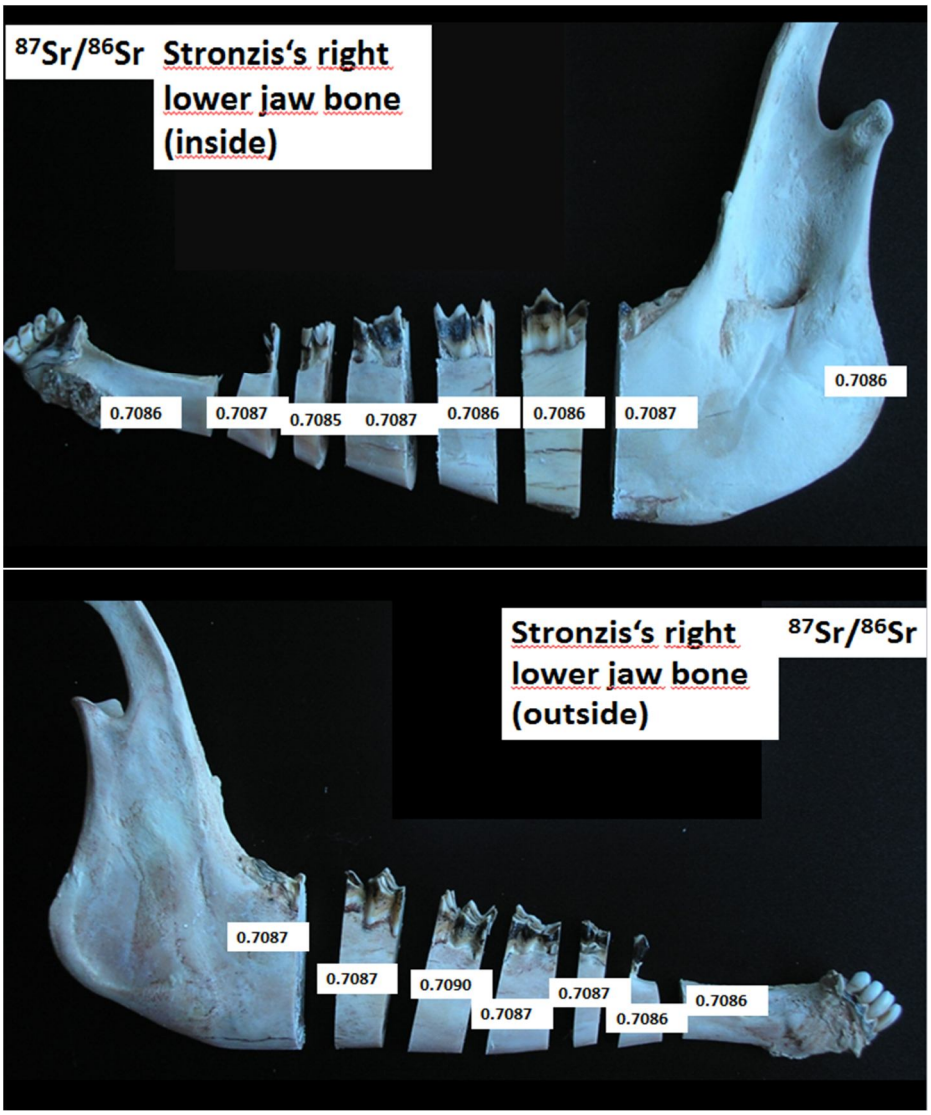

Fig. 31 Distribution of $^{87}Sr/^{86}Sr$ ratios on Stronzi's right lower jaw bone

3.2.2. Jaw bone of the ^{86}Sr spiked sheep 'Anja'

The results of the jaw bone of the sheep Anja are shown in the Appendix 7.2.2. The distribution of $^{86}Sr/^{88}Sr$ and $^{87}Sr/^{86}Sr$ ratios is illustrated in Figure 32 and 33.

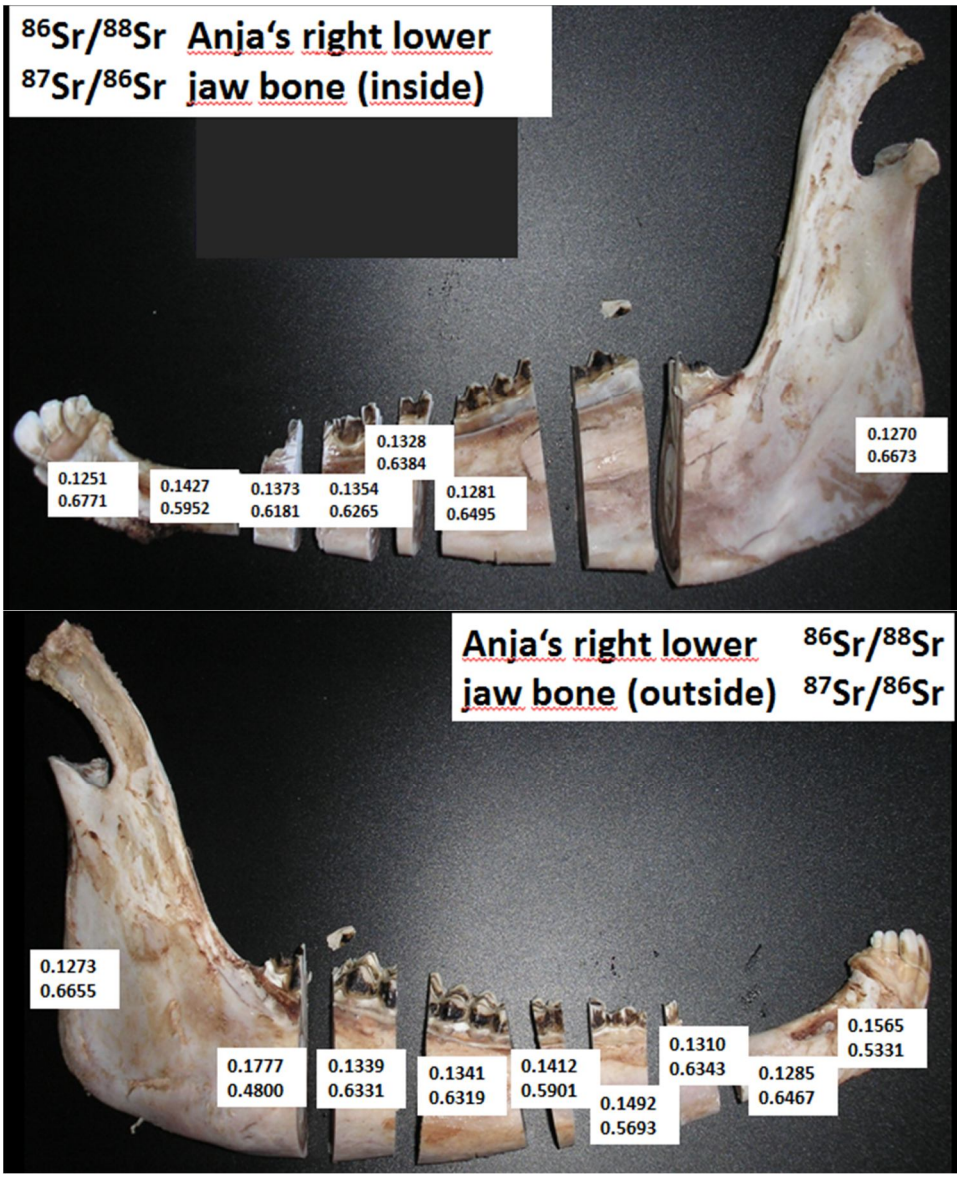

Fig. 32 Distribution of $^{86}Sr/^{88}Sr$ and $^{87}Sr/^{86}Sr$ ratios Anja's right lower jaw bone

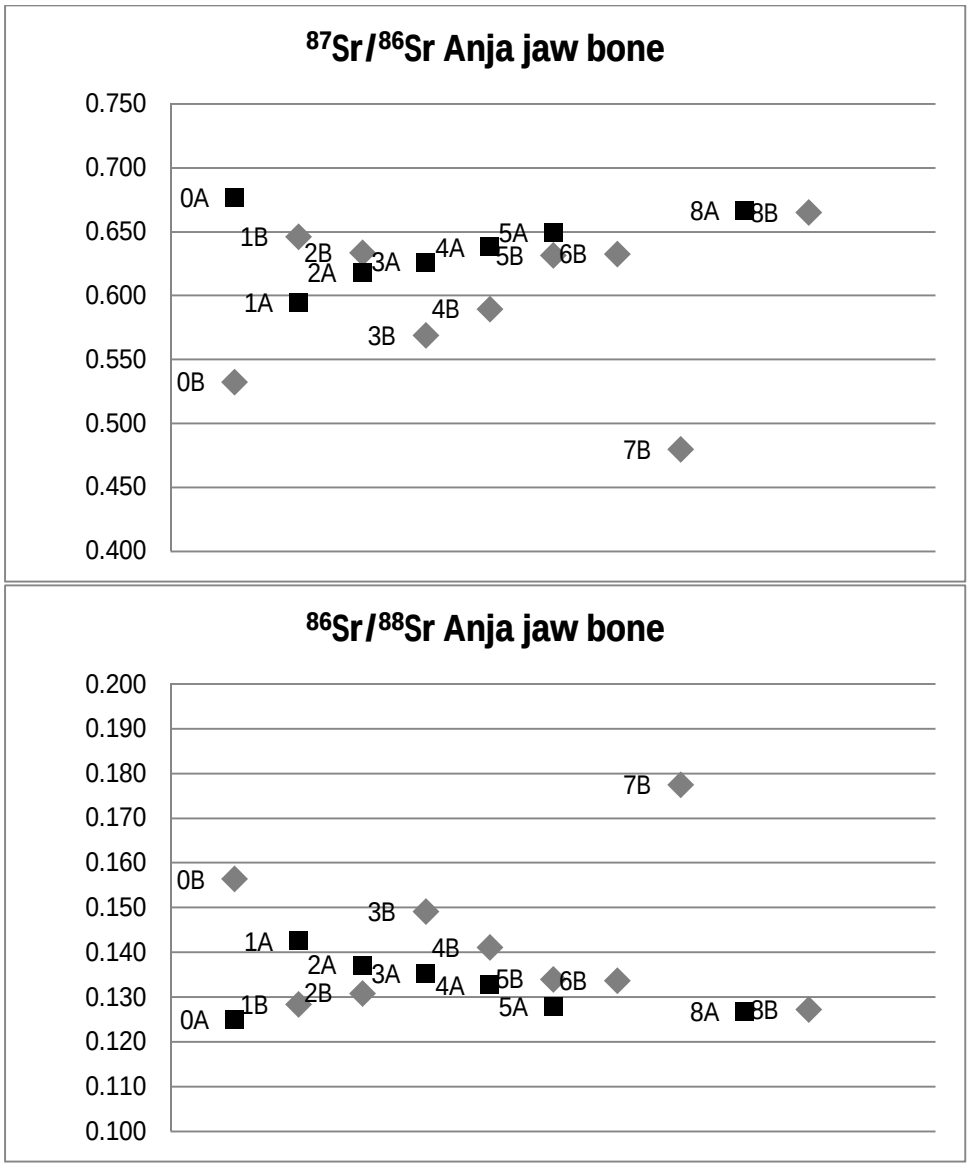

Fig. 33 $^{87}Sr/^{86}Sr$ and $^{86}Sr/^{88}Sr$ ratios of Anja's jaw bone

The ^{86}Sr spike was retrieved in the right lower jaw bone of the sheep Anja expressed by Sr isotope ratios significantly different from the naturally possible Sr isotopic values (provided by the IUPAC). The obtained $^{86}Sr/^{88}Sr$ and $^{87}Sr/^{86}Sr$ ratios range from 0.1251 to 0.1777 and from 0.4800 to 0.6771 implying that the whole jaw bone underwent metabolic turnover between injection of the ^{86}Sr spike and the date of Anja's death.

The obtained $^{86}Sr/^{88}Sr$ and $^{87}Sr/^{86}Sr$ ratios differ significantly between different sampling positions and the inner and outer side of the jaw bone. The outside of the jaw bone exhibits higher $^{86}Sr/^{88}Sr$ ratios on sampling spots OB, 3B, 4B and 5B and lower values on1B and 2B than the inside. Sample 8 do not differ significantly in their Sr isotope composition between

the inner and outer side of the jaw bone. The biggest disagreement in the $^{86}Sr/^{88}Sr$ ratios was observed for the sampling positions 0, 1 and 3. A comparison between the positions 6 and 7 is not possible because Sr isotope ratios were only obtained for the outside.

The jaw bone samples 0B, 3B and 7B on the outside exhibit the highest $^{86}Sr/^{88}Sr$ ratios and thus, show the greatest influence of ^{86}Sr spiking. Sampling position 7B displays the highest value of all the observed $^{86}Sr/^{88}Sr$ ratios. It is at the back part on the outside of the bone beneath the third molar tooth. The sample 0B was taken at the front part on the outside of the jaw bone where the teeth are anchored in the bone. Sampling positions 0B and 7B represent parts of the jaw bone that are under high tension. Higher $^{86}Sr/^{88}Sr$ ratios and the major ^{86}Sr spike incorporation in these components of the bone point to a fast Sr turnover rate.

The $^{86}Sr/^{88}Sr$ ratios of the metatarsus of Anja ranged from 0.1239 to 0.1342 (Strobl 2010). For the right lower jaw bone of Anja a greater variation of Sr isotope values was observed ranging from 0.1251 to 0.1777. The jaw bone shows on some sampling positions especially on 0B, 3B and 7B a greater impact of the ^{86}Sr spike than the sampled bone material of the metatarsus. These results indicate differences in the Sr turnover rates in the jaw bone and the metatarsus which might be caused by differences in the physical tension of the two bones.

The dentine of the third molar tooth of the sheep Anja was analysed. It was not possible to sample tooth enamel without contamination of dentine material. The dentine sample shows a $^{86}Sr/^{88}Sr$ ratio of 0.1471 and a $^{87}Sr/^{86}Sr$ ratio of 0.5772. The Sr isotope composition demonstrates the retrieval of the ^{86}Sr in the dentine material of the molar tooth. The $^{86}Sr/^{88}Sr$ ratio of dentine is in the range of Sr isotope values obtained for the right lower jaw bone. The $^{86}Sr/^{88}Sr$ ratio is higher than those of the jaw bone samples except sampling positions 0B and 7B on the outside of the bone. These results indicate that no distinct difference in the Sr turnover rates between bone and dentine material occurred.

3.3. The Celtic excavation site Roseldorf

3.3.1. Sr isotope mapping

Background samples were derived from different locations in the north-western part of the Weinviertel in Lower Austria in order to generate a $^{87}Sr/^{86}Sr$ isoscape of this region (see chapter 2.2.3.2.). Sampling locations were chosen considering the geological background and possible grasslands for cattle and horses recovered from the Celtic settlement site Roseldorf. The main sample sets collected for this study included soil and water samples and recent cereals and grapes.

3.3.1.1. The establishment of a Sr based isoscape

The Weinviertel in Lower Austria is a geologically highly diverse region. It is part of systems from different geologic ages and geologic formations (Tab. 32). The underlying geology of this region mainly consists of loess, clay, silt, sand, biotite and granite.

rock type	**geological system**	**geologic age**
loess	Pleistocene (Quatenary)	2.6 Mio - 9600 years BC
clay, silt, sand	Miocene (Tertiary)	23.0 Mio - 5.3 Mio years BC
biotite, granite	Palaeocene; Böhmische Masse	65.5 Mio - 55.8 Mio years BC

Tab. 32 The geological background of the Weinviertel

The analysed environmental materials of the investigated region in the Weinviertel display a significant variation of $^{87}Sr/^{86}Sr$ ratios ranging between 0.7099 and 0.7154 illustrated in Figure 34. The obtained Sr isotope ratios of the background samples were related via GPS data of their sampling location to the underlying geology. An $^{87}Sr/^{86}Sr$ ratio isoscape was generated using geological maps from Geologische Bundesanstalt/Geological Survey of Austria, Fachabteilung ADV & GIS/Department of Computing Services and Geographic Information Systems. The maps were incorporated into ARCGIS via Image Service http://gisgba.geologie.ac.at/ArcGIS/services. The spatial variation of $^{87}Sr/^{86}Sr$ ratios of the sampled region in the Weinviertel is shown in Figure 35.

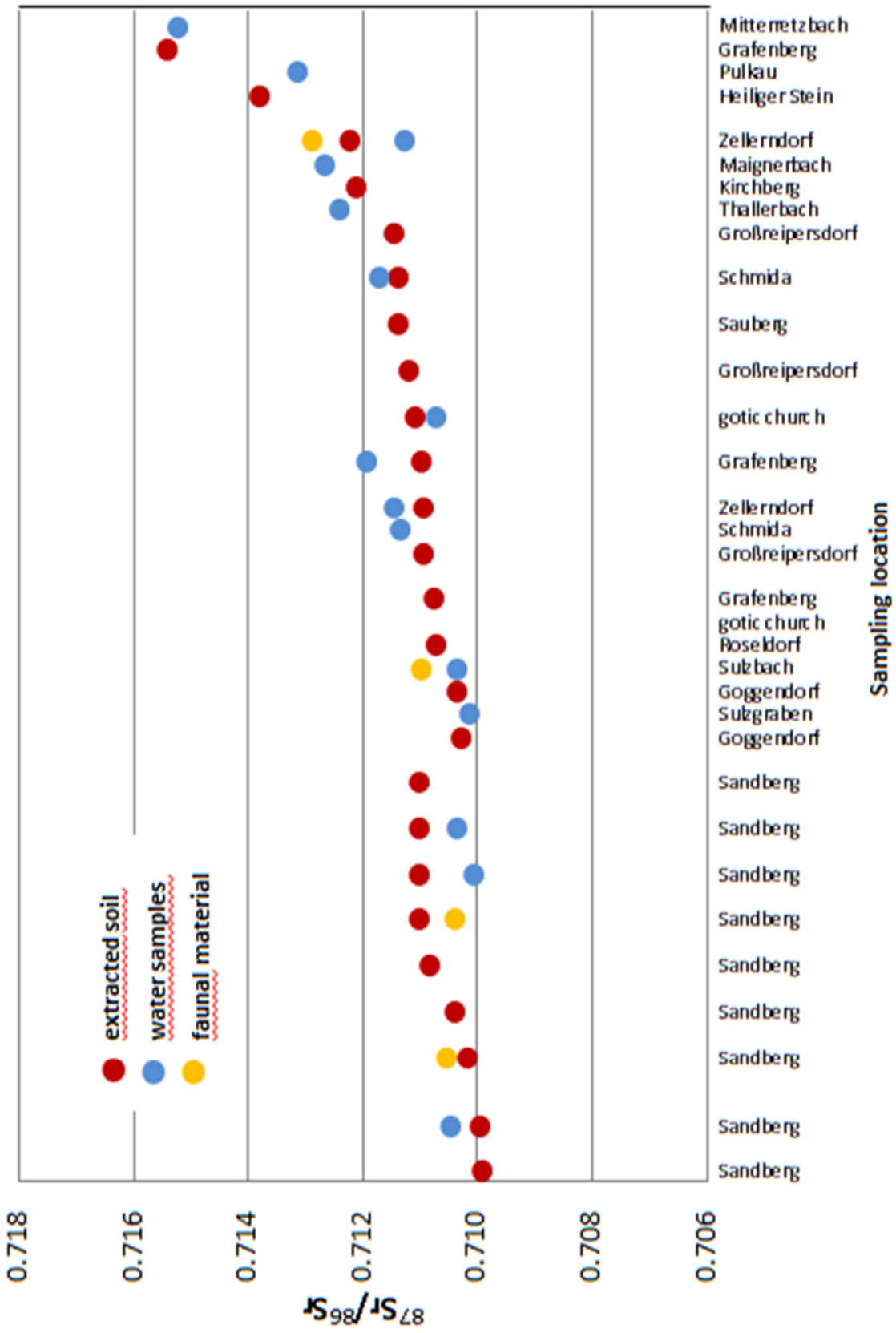

Fig. 37 $^{87}Sr/^{86}Sr$ ratios of environmental material

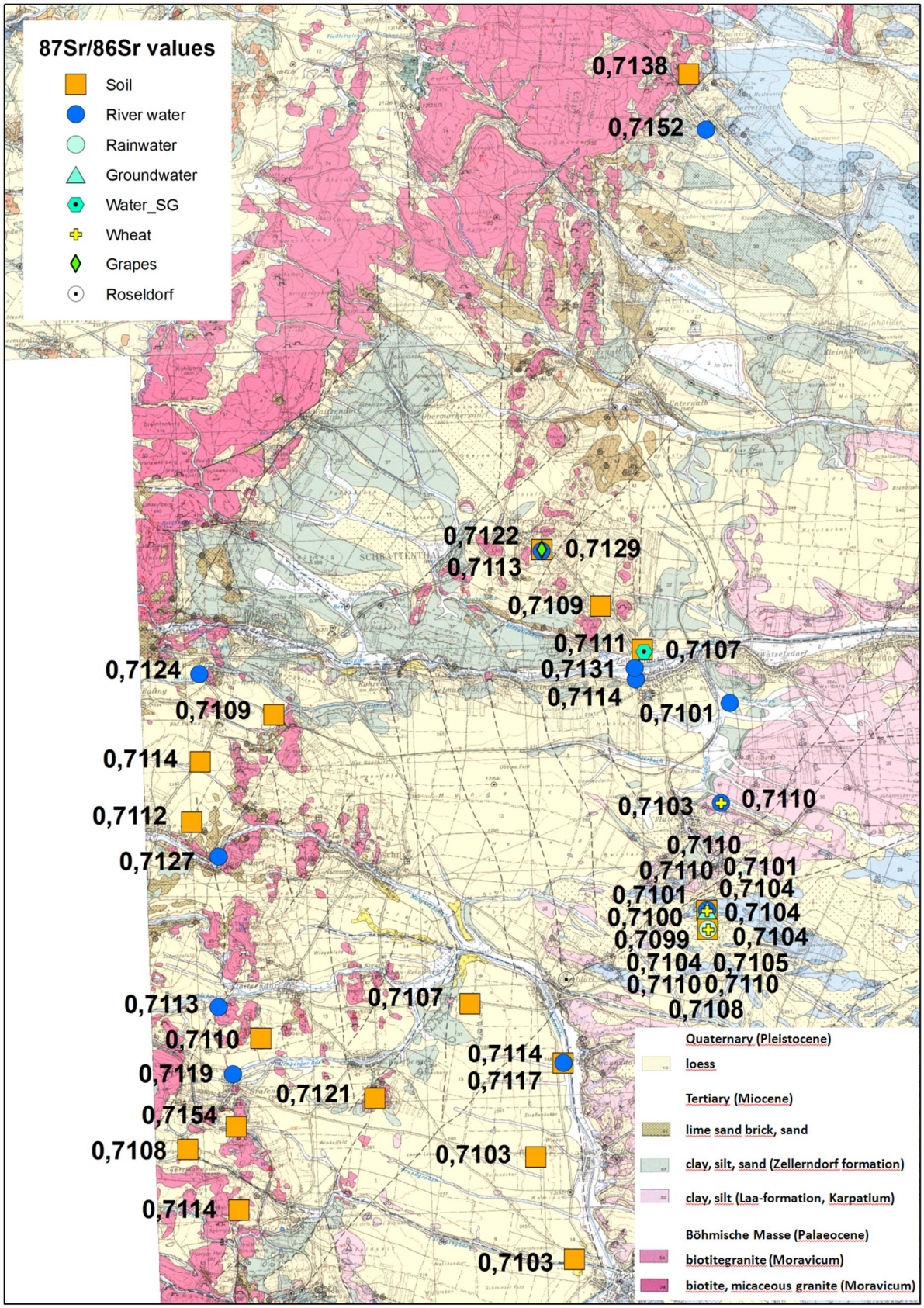

Fig. 35 Spatial variation of $^{87}Sr/^{86}Sr$ ratios of environmental material

3.3.1.2. Sr isotope packages

Evans et al. (2009) proposed to group the Sr isotope data into 'isotope packages' (Evans et al. 2009). Taking into account the geological background of the sampling locations, three $^{87}Sr/^{86}Sr$ ratio ranges were defined for the north-western part of the Weinviertel (Tab. 33). The spatial distribution of the Sr isotope packages in the Weinviertel is illustrated in Figure 36. In Table 33 the Sr isotope packages are related to the main lithological components of the Weinviertel.

$^{87}Sr/^{86}Sr$ range	**rock type**	**geological system**
0.7099 – 0.7115	loess, clay, slit, sand	Pleistocene, Miocene
0.7117 – 0.7135 0.7138 – 0.7154	biotitegranite, biotite, micaceous granite	Palaeocene, Böhmische Masse (Moravicum)

Tab. 33 $^{87}Sr/^{86}Sr$ ranges related to the geological background

The analysed environmental materials exhibit higher $^{87}Sr/^{86}Sr$ ratios than 0.7099. Due to the geological background of the sampled region it can be considered that no lower Sr isotope ratios can be expected for this part of the Weinviertel. Therefore the $^{87}Sr/^{86}Sr$ ratio of 0.7099 was defined as lower Sr isotope limit for this region. No significant differences in the results between loess, clay, silt and sand occurred. 'Böhmische Masse' forms the oldest geological system in the sampled region and contains higher amounts of radiogenic Sr than the other geological substrates. The age of the rocks is reflected in the results and in Sr isotope ratios between 0.7117–0.7154. Such high Sr isotope values can be expected for the northern regions around Roseldorf and in particular for the southern part of the Czech Republic. The highest $^{87}Sr/^{86}Sr$ values were observed with 0.7137 for the sacral place of 'Heiliger Stein' and with 0.7152 for Mitterretzbach near the border to the Czech Republic. Rivers with source in old rock formations exhibit higher $^{87}Sr/^{86}Sr$ ratios than those with source in younger formations. An interesting example is the river Pulkau. The water sample shows with 0.7131 a higher Sr isotope ratio than the surrounding environmental material taken at the same sampling location. The high value of the water derived from the Pulkau can be related to the geological formation Böhmische Masse at its source and not to the loess background at its sampling location.

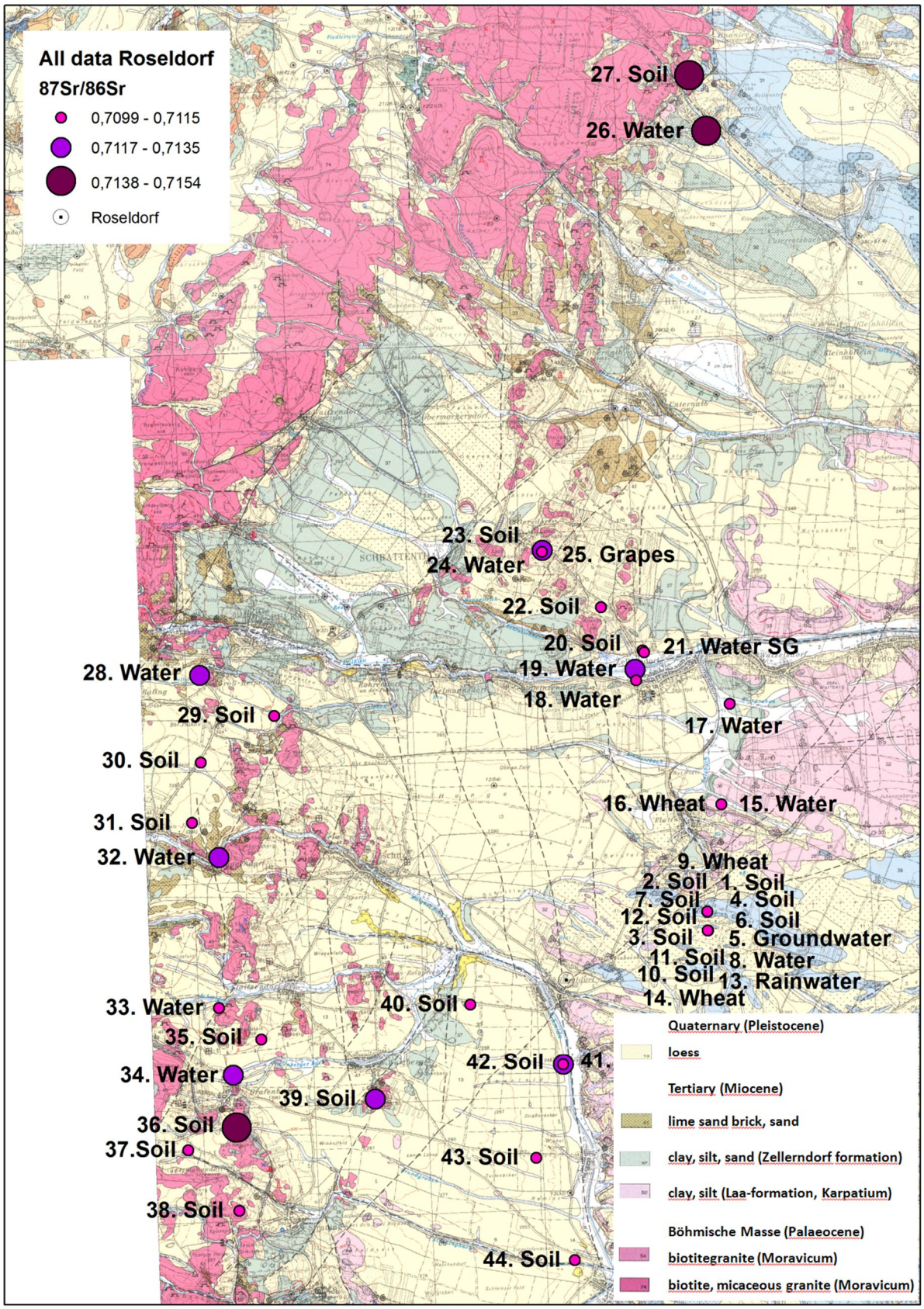

Fig. 36 Spatial distribution of Sr isotope packages

3.3.2. The local range of the Celtic settlement site Roseldorf

The local Sr isotopic range of the Celtic settlement site Roseldorf on the Sandberg was established by the $^{87}Sr/^{86}Sr$ ratios of the extracted soil samples, the rainwater and recent cereals directly derived from the archaeological site Roseldorf (Fig. 37). The $^{87}Sr/^{86}Sr$ values ± 2 σ (standard deviations) of those analyzed environmental materials lead to a definition of the local Sr isotopic range of the Sandberg between 0.7097 and 0.7112 (Fig. 37). The underlying geology of the Sandberg consists of loess and sand. Thus, the observed $^{87}Sr/^{86}Sr$ ratios for the excavation site Roseldorf can be associated to the first isotope package including values between 0.7099 and 0.7115.

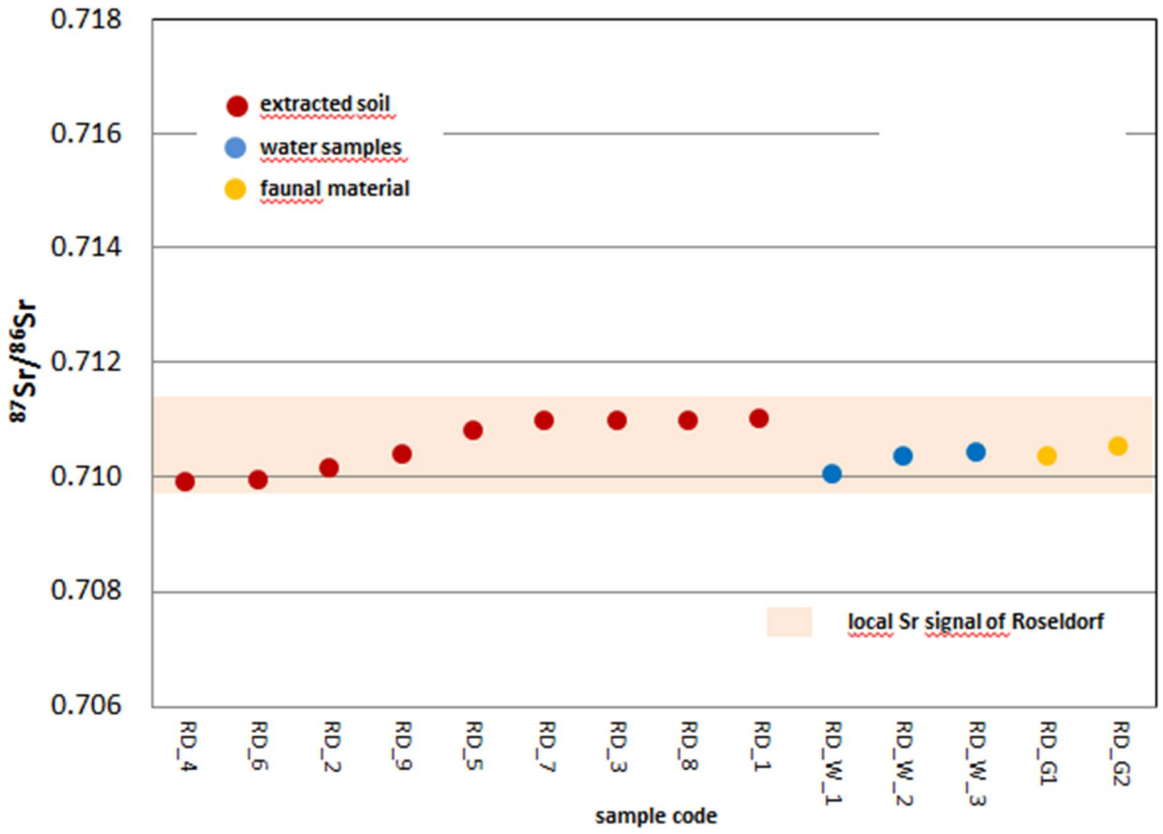

Fig. 37 Definition of the local Sr isotope range of the Celtic excavation site Roseldorf

In Figure 38 the local Sr isotope range of the Celtic site is shown in relation to the $^{87}Sr/^{86}Sr$ ratios of environmental samples of the different sampling locations in the Weinviertel.

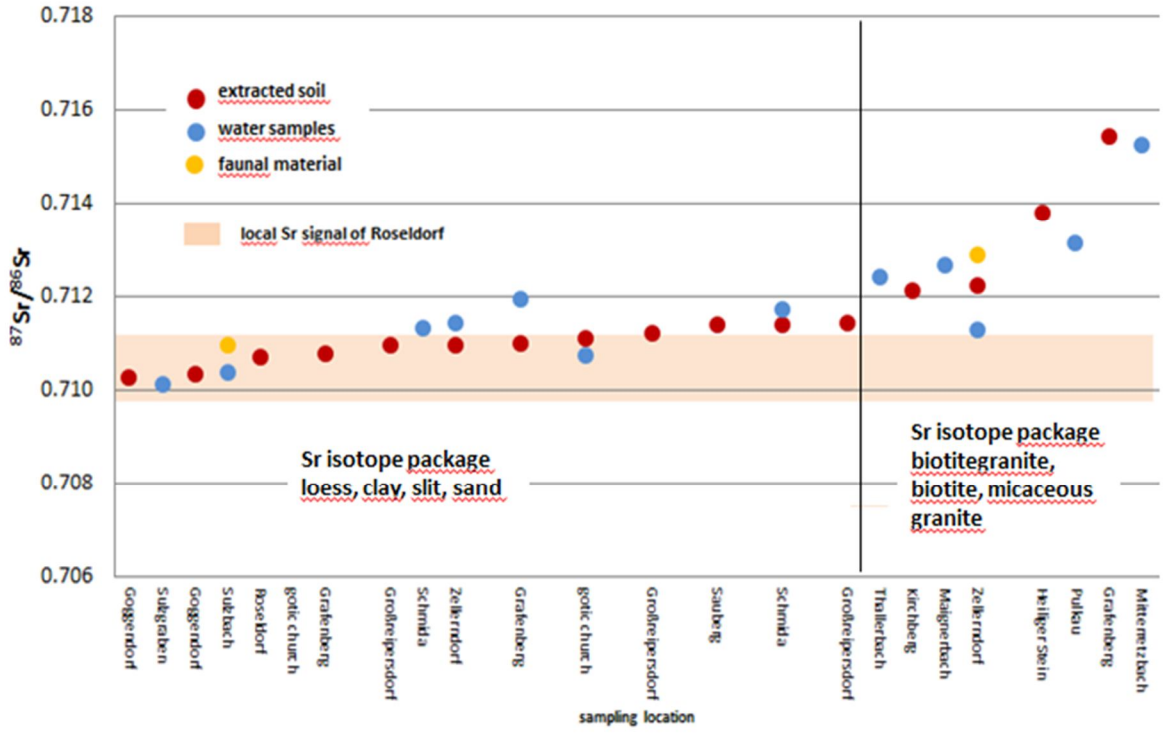

Fig. 38 $^{87}Sr/^{86}Sr$ ratios of Roseldorf's surroundings

Environmental samples derived from the geological background formed by loess, sand, silt and clay exhibit $^{87}Sr/^{86}Sr$ ratios that are in the local Sr isotope range of the Celtic excavation site Roseldorf (see Figure 38). As a consequence, no clear distinction between animals browsing on the Sandberg or on one of the locations shown in Table 34 is possible. The Sr isotope values of the locations presented in Table 35 can be attributed to the geological system Böhmische Masse formed by the geological substrate biotitegranite, biotite and micaceous granite.

location name	sample type	rock type
Goggendorf	soil	loess
Sulzgraben	water	clay, silt, sand
Sulzbach	water, cereal	clay, silt
Roseldorf	soil	loess
Gotic church	soil, water	loess
Grafenberg	soil, water	loess
Großreipersdorf	soil	loess
Schmida	soil,water	loess
Zellerndorf	soil,water	loess, clay, silt, sand

Tab. 34 Locations belonging to the first Sr isotope package

location name	sample type	geological system
Thallerbach	water	Böhmische Masse
Kirchberg	soil	Böhmische Masse
Maignerbach	water	Böhmische Masse
Zellerndorf	soil, water	Böhmische Masse
Heiliger Stein	soil	Böhmische Masse
Pulkau	water	Böhmische Masse
Grafenberg	soil	Böhmische Masse
Mitterretzbach	water	Böhmische Masse

Tab. 35 Locations belonging to the second isotope package

3.3.3. Human and animal tooth samples of the Celtic excavation site Roseldorf

3.3.3.1. Human individuals of the Celtic site Roseldorf

The $^{87}Sr/^{86}Sr$ ratios of the investigated dental materials of three human individuals, recovered from Object 14 and Object 30/I, are listed in the Appendix 7.2.3. and shown in Figure 39. The results are underlined by the local Sr isotope signature of the Celtic settlement site on the Sandberg in order to be able to draw conclusions about local and non-local human individuals at Roseldorf.

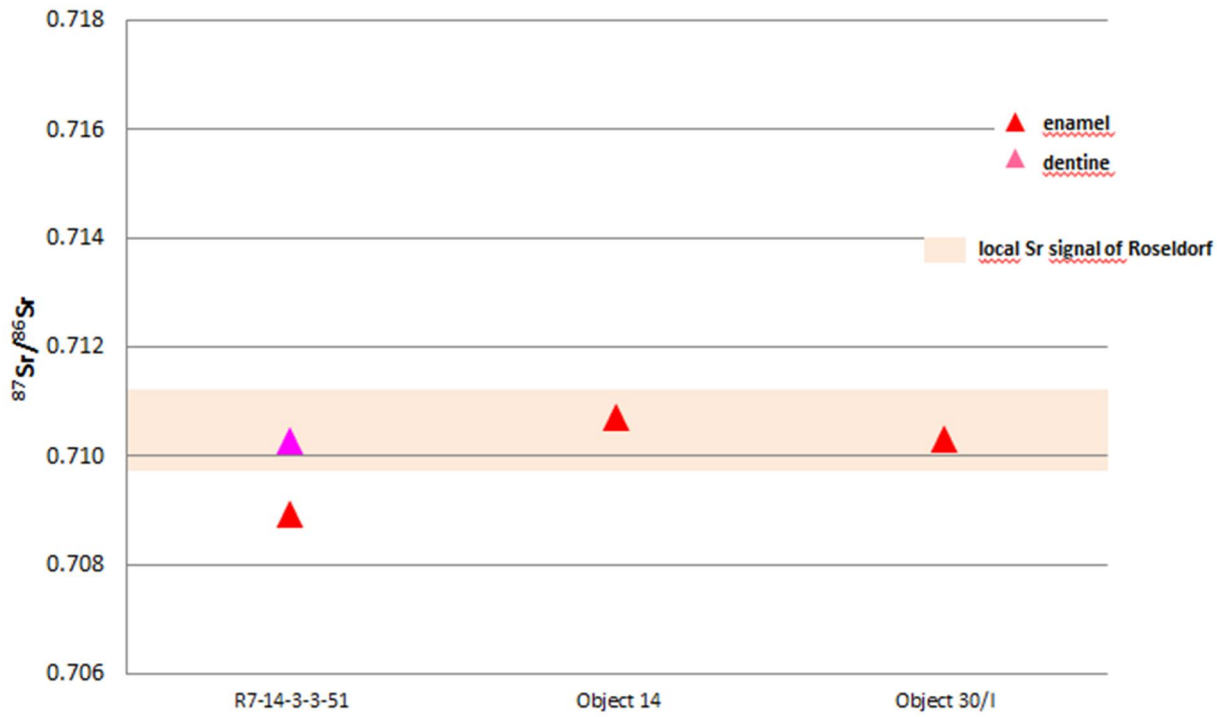

Fig. 39 $^{87}Sr/^{86}Sr$ ratios of Roseldorf's human tooth samples

Tooth samples of the two human individuals, recovered from Object 14 and Object 30/I, include enamel. It was not possible to sample dentine material without causing damage because the teeth were anchored in the jaw bone. The tooth enamel samples show $^{87}Sr/^{86}Sr$ ratios of 0.7107 and 0.7103. These results are in agreement with the local Sr isotope range of the Sandberg. Therefore, the adult and the child seem to be from the settlement site Roseldorf.

Tooth enamel and dentine was analysed from the adult human individual with the inventory number R7-14-3-3-51, recovered from Object 14. The $^{87}Sr/^{86}Sr$ value of 0.7103 of the tooth dentine of the human individual corresponds to the local Sr isotope signature of the Celtic excavation site Roseldorf. The corresponding tooth enamel displays an $^{87}Sr/^{86}Sr$ ratio of 0.7089 which is under the defined local range represented by a $^{87}Sr/^{86}Sr$ ratio of 0.7097. A significant difference between the obtained enamel and dentine Sr isotope values occurs, resulting in a local signal for dentine and in a non-local signal for enamel. This could indicate a residence change of this human individual between childhood and later stages in life. As the analysed tooth dentine shows the Sr isotopic composition of the surrounding burial environment, the possible diagenetic alteration of the soft dentine material has to be taken in account for the interpretation. Diagenetic Sr would hide the original Sr isotope signal. Therefore it would be necessary to determine the preservation state of this tooth using chemical imaging techniques and to apply a pre-treatment procedure on the dentine to unmask the original Sr isotope signature. Due to the fact that the investigated tooth enamel shows a non-local $^{87}Sr/^{86}Sr$ ratio, it can be considered that this human individual did not live at the Celtic settlement site Roseldorf during childhood. Moreover the enamel Sr isotope signal of 0.7089 is under the defined Sr isotope limit of 0.7099 for the mapped region and therefore this adult does not seem to come from this part of the Weinviertel.

3.3.3.2. Cattle and horses of the Celtic site Roseldorf

Cattle and horse tooth enamel samples were analysed for their Sr isotopic composition to be able to draw conclusions about the possible origin of the animals. The obtained $^{87}Sr/^{86}Sr$ ratios of Roseldorf's animal tooth enamel are listed in Appendix 7.2.3. and illustrated in Figure 40. The results are underlined by the local Sr signal of Celtic excavation site (Fig. 40). A summary about the local character of the investigated animals and their attribution to a certain specific geologic background is given in Table 36.

inventory number	animal type/origin	$^{87}Sr/^{86}Sr$	possible origin	geological background
R3-1-16-107-2548	cattle object 1/Celtic	0.7094	non-local	?
R3-1-15-103-2260	cattle object 1/Celtic	0.7094	non-local	?
R1-50-112	cattle settlement/Celtic	0.7094	non-local	?
R4-1-15-117-3735	cattle object 1/Celtic	0.7100	local	loess, silt, clay, sand
R5-1-15-43-4489	cattle object 1/Italian	0.7101	local	loess, silt, clay, sand
R1-28-13	cattle settlement/Italian	0.7103	local	loess, silt, clay, sand
R6-1-11-59-5614	cattle object 1/Celtic	0.7103	local	loess, silt, clay, sand
R2-1-4-37-365	cattle object 1/Celtic	0.7103	local	loess, silt, clay, sand
R4-1-15-131-4285	cattle object 1/Celtic	0.7105	local	loess, silt, clay, sand
R3-1-15-103-2788	cattle object 1/Celtic	0.7106	local	loess, silt, clay, sand
R3-1-1-43-2953	cattle object 1/Celtic	0.7106	local	loess, silt, clay, sand
R3-1-16-70-1934	cattle object 1/Italian	0.7109	local	loess, silt, clay, sand
R3-1-12-60-1745	cattle object 1/Italian	0.7109	local	loess, silt, clay, sand
R4-1-5-53-4328	cattle object 1/Italian	0.7110	local	loess, silt, clay, sand
R1-140-89	cattle settlement/Italian	0.7111	local	loess, silt, clay, sand
R1-168-102	cattle settlement/Celtic	0.7114	non-local	Böhmische Masse
R2-1-12-2-858	cattle object 1/Celtic	0.7118	non-local	Böhmische Masse
R2-1-14-54-607	cattle object 1/Celtic	0.7124	non-local	Böhmische Masse
R1-227-209	horse settlement/Celtic	0.7091	non-local	?
R1-0.Nr	horse settlement/Celtic	0.7092	non-local	?
R3-1-1-43-2702	horse object 1/Celtic	0.7094	non-local	?
R3-1-1-2-2027	horse object 1/Celtic	0.7099	local	loess, silt, clay, sand
R4-1-15-135-4366	horse object 1/Celtic	0.7099	local	loess, silt, clay, sand
R3-1-16-43-2268	horse object 1/Celtic	0.7101	local	loess, silt, clay, sand
R2-1-18-2-941	horse object 1/Celtic	0.7101	local	loess, silt, clay, sand
R6-1-10-217-5495	horse object 1/Celtic	0.7113	non-local	Böhmische Masse
R2-1-4-2-945	horse object 1/Celtic	0.7122	non-local	Böhmische Masse
R6-1-10-217-5490	horse object 1/Celtic	0.7156	non-local	Böhmische Masse
R2-1-4-37-951	horse object 1/Celtic	0.7166	non-local	Böhmische Masse
R2-1-12-2-454	horse object 1/Celtic	0.7166	non-local	Böhmische Masse

Tab.36 Cattle and horses excavated at Roseldorf related to the geological background

53% of the analysed animals, among them 67% cattle and 33% horses, exhibit Sr isotope signatures belonging to the first isotope package of 0.7099–0.7115. This means that it is likely that those animals derived their food and water from a region where loess, slit, sand and/or clay formed the geological background system. They could possibly be from the Sandberg itself or they could have browsed in loess regions nearby.

Archaeozoological studies differentiated between Celtic and Italian cattle due to morphological characteristics of the occurring bone material. The six cattle, identified as

Italian cattle, display $^{87}Sr/^{86}Sr$ ratios in the local range of the Sandberg and seem to be of local origin (Fig. 40).

Skeletal and dental remains of cattle and horses were recovered from the settlement and the sanctuary 'Object 1' of the Celtic site Roseldorf. The composition of the faunal assemblages of the finding places showed distinct differences. The settlement contained a relatively low proportion of 16 per cent cattle bones compared to other Celtic settlement sites in the Latène period. Object 1, in contrast comprises the huge amount of 55 per cent cattle remains. Horse bones contributed with two per cent in the settlement to the recovered animal remains compared to 11 per cent in Object 1 (Holzer 2009). The finding place of the animals has to be taken into account for interpretation of their intended use. One explanation could be a rearrangement of bigger animal remains from the settlement in the Object 1 and the use of Object 1 as a garbage disposal. Archaeological theory claims that the animals recovered from there were used for ritual practices (Holzer 2009).

Six of thirty investigated animals were found at the settlement. The Sr isotope signal of one Italian cattle from the settlement with the inventory number R1-28-13 is in the local range of the archaeological site. The five other animals (two horses and three Celtic cattle) found in the settlement show non-local $^{87}Sr/^{86}Sr$ ratios. Sixteen of the investigated animals showing local $^{87}Sr/^{86}Sr$ ratios were found in Object 1.

The $^{87}Sr/^{86}Sr$ ratios of thirteen animals are not in agreement with the local signal of the Sandberg and don't correspond to the first isotope package. Combining environmental data with animal tooth enamel data (Fig. 41), there is the ability to constrain the possible origin of the animals by relating a certain animal to specific grasslands in Roseldorf's surroundings.

Fig. 40 $^{87}Sr/^{86}Sr$ ratios of Roseldorf's cattle and horse tooth enamel samples

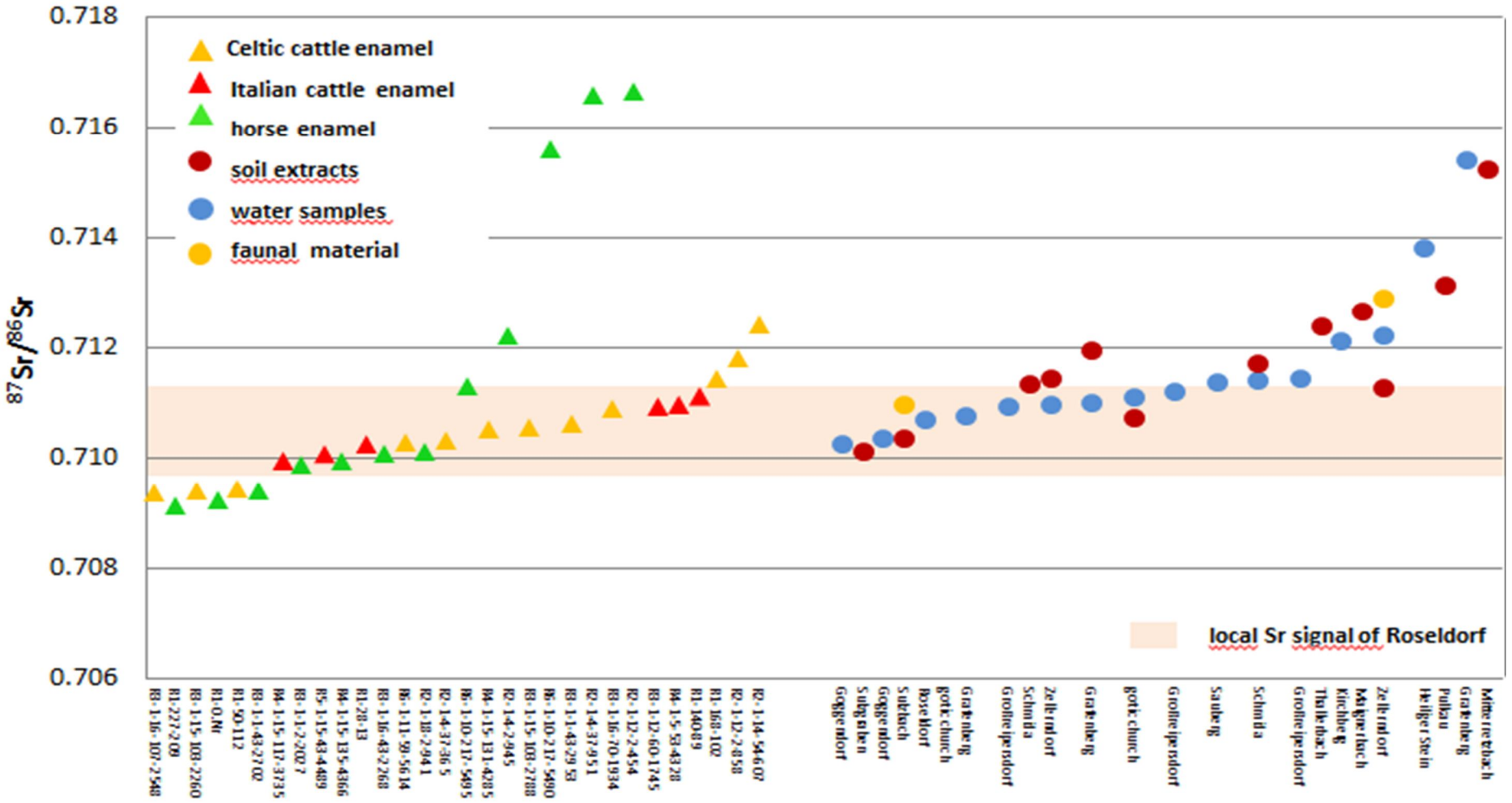

Fig. 41 $^{87}Sr/^{86}Sr$ ratios of Roseldorf's cattle and horse tooth enamel samples and environmental material

The obtained $^{87}Sr/^{86}Sr$ ratios of three cattle and three horse (Table 37) tooth enamel samples are lower than those found in the environmental samples of the settlement site itself (0.7097-0.7112) and of Roseldorf's surroundings. Those animals could not be related to any location of the mapped region. Taking into account the geological background of the north-western Weinviertel, those cattle and horses do not seem to come from there. As the animals were recovered from the settlement and Object 1, no correlation between the finding place and their origin could be drawn for interpretation of their intended use. Among the non-autochthonous cattle and horses are no Italian ones.

inventory number	animal type	finding place	$^{87}Sr/^{86}Sr$
R3-1-16-107-2548	Celtic cattle	Object 1	0.7094
R3-1-15-103-2260	Celtic cattle	Object 1	0.7094
R1-50-112	Celtic cattle	Settlement	0.7094
R1-227-209	Celtic horse	Settlement	0.7091
R1-0.Nr	Celtic horse	Settlement	0.7092
R3-1-1-43-2702	Celtic horse	Object 1	0.7094

Tab. 37 Non-autochthonous cattle and horses

The Sr isotope ratios of two cattle and one horse recovered from Object 1 (Tab. 38) correspond to the second Sr isotope package and the geologic formation Böhmische Masse.

inventory number	animal type	finding place	$^{87}Sr/^{86}Sr$
R2-1-12-2-858	Celtic cattle	Object 1	0.7118
R2-1-14-54-607	Celtic cattle	Object 1	0.7124
R2-1-4-2-945	Celtic horse	Object 1	0.7122

Tab. 38 Cattle and horse corresponding to the second Sr isotope package

Three horses with the highest $^{87}Sr/^{86}Sr$ ratios are shown in Table 39. The values correspond to the Sr isotope signatures of the environmental material of the locations given in Table 38 and shown in Figure 42. Possible origins could be Grafenberg in the south-west of Roseldorf and Mitterretzbach or 'Heiliger Stein' in the north of Roseldorf near the border to the Czech Republic. The three sampling sites have the same geological background of biotite and granite and belong to the geological system Böhmische Masse.

inventory number	animal type	finding place	$^{87}Sr/^{86}Sr$
R6-1-10-217-5490	Celtic horse	Object 1	0.7156
R2-1-4-37-951	Celtic horse	Object 1	0.7166
R2-1-12-2-454	Celtic horse	Object 1	0.7166
sample number	**sample type**	**location name**	
36	soil	Grafenberg	0.7154
26	water	Mitterretzbach	0.7152
27	soil	Heiliger Stein	0.7138

Tab. 39 Horses with the highest $^{87}Sr/^{86}Sr$ ratios and their possible place of origin

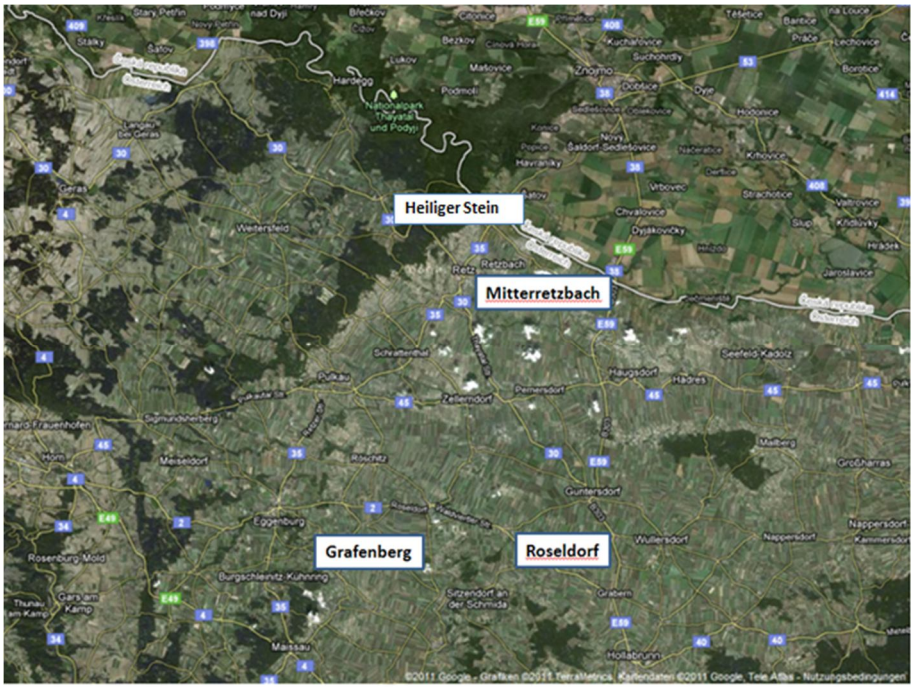

Fig. 42 Places of the possible origin of horses with the highest $^{87}Sr/^{86}Sr$ ratios (Google maps)

In Mitterretzbach archaeological findings give evidence of a continuous settlement from the Middle Neolithicum (about 4800 BC) until nowadays. Settlement structures including a pit house and a house for weaving are dated due to ceramic findings in the Latène period from 450 BC until the time of Christ's birth (Lauermann 2001). In Grafenberg remains from the Celtic period are not known, so far. It seems possible that contacts between the Celtic site Roseldorf and its neighbour Celtic settlement Mitterretzbach existed and that that an exchange of horses took place.

3.3.4. Multielemental analysis

The results from the multielemental measurements are listed in the Appendix 7.2.4. The limit of detection (LoD) was calculated for each element by three times the standard deviation of the concentration measurements of at least three independent method blanks. The method blanks include the whole sample preparation procedure and the measurement itself. The values below the LoD were sorted out and marked with <LoD. Minima, maxima and the average value of elements in soil, water and animal and human tooth samples are given in Table 40, 41 and 42.

soil samples	Sr [µg g^{-1}]	Rb [ng g^{-1}]	Al [µg g^{-1}]	Fe [µg g^{-1}]	Zn [ng g^{-1}]	Mg [µg g^{-1}]	Ba [µg g^{-1}]	U [ng g^{-1}]	As [ng g^{-1}]	Pb [ng g^{-1}]
Minima	10.89	54.97	6.08	1.92	0.12	140.69	3.34	0.19	1.52	0.06
Maxima	60.58	441.53	154.52	9.13	0.92	507.98	16.20	83.77	4.23	4.56
average	30.78	220.15	96.43	5.65	0.46	199.37	8.47	31.76	2.84	1.62

Tab. 40 Elemental concentrations in soil material

water samples	Sr [µg g^{-1}]	Rb [ng g^{-1}]	Al [µg g^{-1}]	Fe [µg g^{-1}]	Zn [ng g^{-1}]	Mg [µg g^{-1}]	Ba [µg g^{-1}]	U [ng g^{-1}]	As [ng g^{-1}]	Pb [ng g^{-1}]
Minima	0.01	0.34	0.01	0.21	1.41	0.27	0.01	0.19	0.40	0.15
Maxima	5.54	192.35	6.64	7.80	124.30	332.24	1.53	83.77	131.83	29.63
average	2.64	26.88	0.92	3.77	52.59	130.25	0.47	31.76	19.67	8.06

Tab. 41 Elemental concentrations in water samples

	Sr [µg g^{-1}]	Rb [ng g^{-1}]	Al [µg g^{-1}]	Fe [µg g^{-1}]	Zn [µg g^{-1}]
Minima	11.20	18.20	5.20	129.20	7.60
Maxima	132.70	813.30	406.10	530.60	121.90
average value	60.93	190.92	52.27	291.30	23.14
	Mg [µg g^{-1}]	**Ba [µg g^{-1}]**	**U [ng g^{-1}]**	**As [ng g^{-1}]**	**Pb [ng g^{-1}]**
Minima	185.40	0.20	2.00	1.40	53.70
Maxima	648.90	48.00	566.50	203.20	647.50
average value	413.04	18.83	141.91	53.17	248.22

Tab. 42 Elemental concentrations in tooth enamel

A correlation between the Sr and Rb concentrations of soil and water samples with the isotope packages and underlying geology was not observed. The Sr concentrations of the soil samples belonging to the first isotope package with the geologic substrates loess, silt, clay and sand show a great variation in their values and range between 1.99 and 5.93 µg g^{-1}. The highest Sr concentration of 6.58 µg g^{-1} was found in the soil sample taken at Kirchberg with Böhmische Masse as geologic system. The location Grafenberg with the highest Sr isotope

ratio shows the lowest Sr concentration in soil of 1.89 µg g^{-1}. The Rb concentrations of the soil samples of the first isotope package range between 1.99 and 441.53 ng g^{-1}.

The Sr concentrations of animal tooth enamel show values between 11.2 and 132.7 µg g^{-1}. A correlation between the Sr concentrations and the possible origin of the animals was not observed. Horse tooth enamel samples tend to exhibit higher Sr concentrations than cattle enamel. 11 of 12 investigated horses and only 3 of 18 cattle show Sr concentrations between 70 and 135 µg g^{-1}. The tooth enamel samples of the three human individuals display lower Sr concentrations between 11.2 and 18.1 µg g^{-1} than animal enamel. The Sr concentration of dentine material of the human individual with the inventory number R7-14-3-3-51 is with 33.1 µg g^{-1} higher than the corresponding value of the enamel with 18.1 µg g^{-1}.

The Sr/Ca ratios have the potential to serve as dietary indicators (see chapter 1.2.). The Sr*1000/Ca ratios of cattle, horse and human tooth enamel and dentine excavated at Roseldorf are given in the Appendix 7.2.4. and illustrated in Figure 43. The values of the animals range between 0.50 and 1.73. A correlation between the Sr/Ca ratios and local/non-local animals was not observed. The cattle tend to exhibit lower Sr/Ca ratios than the horses but there is an overlap of values. Human enamel samples display values between 0.32 and 0.44 and thus, distinct lower Sr*1000/Ca ratios than horse and cattle enamel. This observation indicates a meat consummation of the human individuals at Roseldorf. The results correlate with the fact that carnivores exhibit lower Sr/Ca ratios than herbivores (Burton et al. 1999). The higher Sr/Ca ratio of dentine can be explained with the presence of diagenetic Sr.

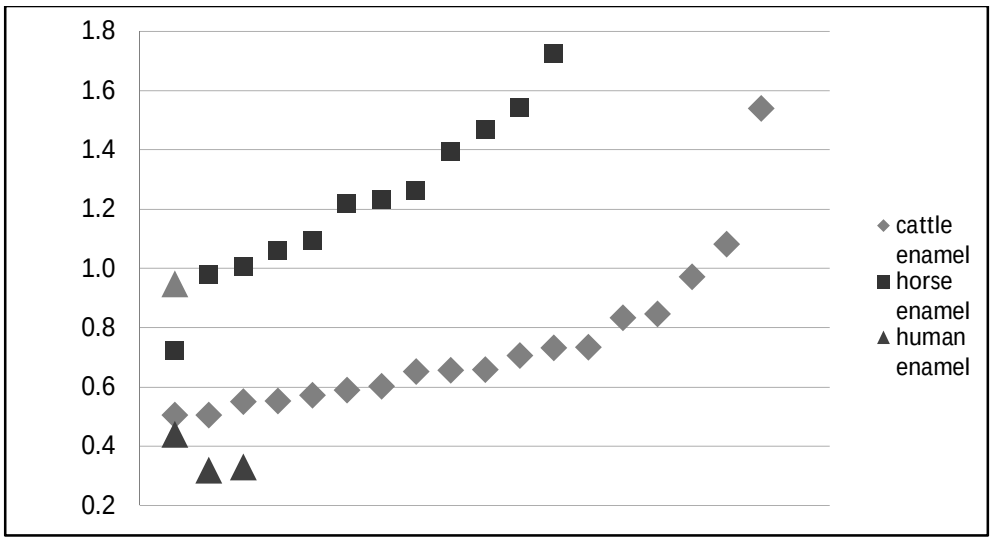

Fig. 43 Sr*1000/Ca ratios of animal and human tooth material

4. Summary and Conclusion

4.1. Diagenesis study of tooth and bone matrices

The applied sequential leaching method removed diagenetic Sr from the dental and skeletal tissues as a decrease in the values of elemental and isotopic ratios could be observed. The fractions containing biogenic Sr are indicated by stable elemental ratios of Sr/Ca and Ca/P which are in agreement with the range for biogenic hydroxyapatite reported in literature (Nelson 1981; Woodward 1962; Sponheimer et al. 2005b). The biogenic compartment was attributed to the fractions 10-20 which is in accordance to the results obtained by Sillen (1986) identifying the biogenic fraction in leachates 7-25 (Sillen 1986) and to the observations made by Schultheiss (2003) finding the biogenic apatite fraction in leachates 12-15 (Schultheiss 2003).

The investigated tooth and bone material was recovered from the same archaeological site of Gars Thunau. As a consequence, it seems to be likely that it underwent the same diagenetic trajectories. The macroscopic observations of the analysed materials lead to the assumption that the investigated jaw bones are more affected by the influence of the surrounding burial environment compared to the tooth samples. The analysed sheep jaw bones show a more porous structure than the dentine with a white and hard surface after the elimination of the cementum. Further investigations on the microscopic scale are needed for the estimation of the preservation state of the different hard tissues (see chapter 5.1).

The observed decrease in the Ca/P ratio in leachates 1-3 of both human enamel samples could be explained by the presence of adherent organic, soft tissues on the surface of enamel. The stable Sr isotopic ratios of leached human tooth enamel indicate that enamel is resistant to diagenetic alteration which is explained by its hard and dense structure (Dauphin and Williams 2004). The hard tissues of the different species show similar patterns in their elemental ratios but a difference in the initial values. The sheep tissues exhibit the highest Ca/P ratios with values of 43.0 and 8.3 for jaw bone and 9.6 and 4.1 for tooth dentine. Moreover, both sheep dentine samples show a sharper decline than human, horse and cattle dentine in the elemental ratios. In contrast to the Sr/Ca ratios of leached human, cattle and horse dentine the values do not approach a stable value for the sheep tissues.

One explanation could be a different preservation state of the analysed objects. But it is also possible that sheep jaw bone is more affected by diagenetic alteration than sheep dentine and sheep dentine more than human dentine. Horse and cattle dentine can be compared with the human tissues in their elemental patterns and values.

4.2. Sr turnover in sheep hard tissues

A uniform distribution of $^{87}Sr/^{86}Sr$ ratios along the right lower jaw bone of the sheep Stronzi was observed. The average value of the obtained Sr isotope ratios corresponds with the results of the ingested water and hay and the underlying soil of the grassland where Stronzi lived (Gölles in prep.). The bone material reflects the $^{87}Sr/^{86}Sr$ ratios of the ingested food and water of the current life span. It was proved that an incorporation of the ^{86}Sr spike into the right lower jaw bone of the ^{86}Sr spiked sheep Anja took place expressed by $^{87}Sr/^{86}Sr$ and $^{86}Sr/^{88}Sr$ ratios significantly different from the naturally possible Sr isotopic values (provided by the IUPAC). The Sr isotope ratios of the jaw bone differ significantly at different sampling positions. Thus, a metabolic turnover of the original Sr isotope composition took place at different extents in different parts of the bone. In regions of the bone which are under higher tension the highest $^{86}Sr/^{88}Sr$ values were observed underlining the fact that the rates of bone remodelling correlate with physical tension.

4.3. The Celtic excavation site Roseldorf

The distinct regional disparity in geology and the observed significant variation in $^{87}Sr/^{86}Sr$ ratios of the mapped region enabled the establishment of an $^{87}Sr/^{86}Sr$ isotope map of the north-western part of the Weinviertel in Lower Austria. Soil and water samples proved to be reliable proxy materials in terms of representing the biologically available Sr fraction of this region. The obtained Sr isotope packages equate to the underlying geologic systems and rock types. This allows an extrapolation from the obtained $^{87}Sr/^{86}Sr$ ratios to areas in this region with the same geological background. The $^{87}Sr/^{86}Sr$ ratios of the sampling locations in the Weinviertel demonstrate that the sampling density plays an important role for the establishment of ‘reliable’ Sr isotope maps. Even one specific geological substrate covers a wide range of $^{87}Sr/^{86}Sr$ values. As a consequence, attempts to estimate $^{87}Sr/^{86}Sr$ packages for regions of a specific geological system from only one obtained value of a proxy material are not favourable. A proper sampling strategy should include a representative number of

environmental samples including soil, water and cereals from different locations with the same underlying bedrock lithology as proposed by Evans et al., 2010. This diploma thesis showed the importance of the combination of archaeological, archaeozoological and geological data for the choice of sampling locations when the aim of the study is to elucidate historical questions. In this diploma thesis possible grasslands for animals in the Celtic period were chosen due to archaeozoological informations. Environmental samples were taken from the excavation site itself and from other archaeological places which are suspected to be in contact with Roseldorf in the Latène period.

Conclusions about human migration processes and the structure of the Celtic society at the settlement site Roseldorf are limited by the number of recovered human remains. Burial grounds have not been found so far at Roseldorf (Holzer 2009). One of three analysed human individuals shows a Sr isotope signature which is not in conjunction with any of the obtained $^{87}Sr/^{86}Sr$ ratios of the environmental material in the sampled region of the Weinviertel.

The cattle population in Roseldorf consisted of 70–80 per cent of bullocks which were used for working purposes and as food source. Due to the expected birth rate of 50 per cent female and 50 per cent male cattle, the Celtic settlement site Roseldorf must have been supplied with agricultural products including animals by the surrounding rural area. The composition of the cattle population points to an urban structure of Roseldorf (Lauermann and Trebsche 2008). 12 of 18 analysed cattle showed a Sr isotope signal corresponding to the geological background loess which means that they could have browsed at the excavation site itself but also on areas around the Sandberg. These results support the hypothesis of cattle supply from the hinterland of Roseldorf and indicate animal husbandry techniques.

The Sr isotope ratios of the cattle morphologically identified as Italian cattle correspond to the geological background loess. The $^{87}Sr/^{86}Sr$ values of the tooth enamel are in agreement with the local Sr isotope signature of the Celtic excavation site Roseldorf and the surrounding grasslands. Therefore, it seems likely that the Italian cattle are autochthonous. A possible explanation for their presence in Roseldorf could be that the recovered animals do not represent the first generation of this kind of cattle. This would indicate animal husbandry techniques practised by the Celtic settlers of Roseldorf. It has to be taken in

account that their origin could be a place with the same Sr isotope signature. Roseldorf was populated by the Celtic tribe Boii (Holzer 2009).The Boii had their settlement area in the regions of former Bohemia and Moravia and also in the Po Valley in Northern Italy in the so called 'Ager Gallicus' (Demandt 2001). The lithological components of the Ager Gallicus, including todays cities of Ancona and Rimini, can be compared with the geological system 'Molasse' and the background of loess, clay, silt and sand in the Weinviertel. It is mainly composed of sand, clay, limestone and maritime deposits. The geological formations originate from the Pleistocene and Holocene in the Quaternary. The presence of 'young' bedrock lithologies in the Po Valley compared to e.g. Böhmische Masse indicates relatively low $^{87}Sr/^{86}Sr$ ratios. This means that there is the possibility that the Italian cattle showing a local Sr isotope signal of the Sandberg originated from the Ager Gallicus in Northern Italy.

Higher amounts of radiogenic Sr in environmental and dental samples resulting in higher $^{87}Sr/^{86}Sr$ values point to their northern provenance in the areas of former Bohemia and Moravia where the geological background system is formed by Böhmische Masse. The Sr isotope ratios of three cattle and three horses show that they browsed in such geological regions. These results indicate contacts between the Celtic settlers in Roseldorf and the Celtic tribe Boii in the northern parts of Roseldorf such as the Celtic site Mitterretzbach (see chapter 3.3.3.2)

Current archaeological theory claims the correlation of specific settlement structure identified as sanctuaries with ritual practices of the Celtic settlers at Roseldorf (see chapter 1.7.1.). The composition of the faunal assemblage of the sanctuary Object 1 shows a tendency to old animals and not to a high quality meat which would be expected for religious ceremonies in form of banquets. Celts are known to sacrifice horses from their enemies. In Object 1 young stallions used in war contribute only to 20 per cent to the amount of horses (Holzer 2009). In Object 1 sixty per cent of the horses are of non-local origin. Non-autochthonous cattle, in contrast contribute with thirty per cent to the analysed cattle in Object 1. Five of six investigated animals do not show an autochthonous character in the settlement.

5. Future perspectives

5.1. Diagenesis study of teeth and bone matrices

The modification of the sequential leaching procedure in order to reduce the time-consuming and labour-intensive working steps could be a future perspective. The method should be adapted to its applicability on large populations. The number of samples could be reduced by a selection of dentine samples from individuals of special interest due to archaeological or anthropological observations. As there is often a lack of such information, Sr isotope ratio measurements and multielemental analysis could be restricted to the biogenic compartment such as e.g. leaching fractions 15-20. The method should be repeated including drying of the residue between the leaching steps to observe the impact of the drying procedure on the results and solubility of the Sr.

The use of chemical imaging and spectroscopic techniques for diagenetically altered hard tissues is required to gain more information on the extent of contamination due to the interaction of the investigated object with the surrounding burial matrix as successfully used in several diagenesis studies (Schultheiss 2003; Sillen 1986; Hedges et al. 1995; Lebon et al. 2011; Novotny et al. 2003). Scanning electron microscopy (SEM) to observe histological changes, X-ray diffraction analysis for the determination of the crystallinity index and FT-IR spectroscopy could be used as indication of the biological integrity of archaeological bones and teeth (Kuczumow et al. 2010; Lebon et al. 2011; Lebon et al. 2010).

5.2. Investigation of Sr turnover in sheep hard tissues

As the Sr isotope ratios of the jaw bone of the sheep Stronzi and the ingested food and water are known, other tissues of Stronzi could be analysed. The spiking of the sheep Anja was performed with an enriched solution of ^{86}Sr by an intramuscular injection. An ^{86}Sr spike could be administered to a sheep via food and water in order to test if differences in the Sr turnover rate occur in the tissues compared to the injection method. The current investigation of further bones of Anja will lead to a distribution of the ^{86}Sr spike over the whole skeleton.

5.3. The Celtic excavation site Roseldorf

In this pilot study about the Celtic settlement site Roseldorf first steps including the establishment of a local Sr range of the excavation site and the creation of an $^{87}Sr/^{86}Sr$ isotope map of the north-western part of the Weinviertel have already been performed. Further effort can be taken in the expansion of the environmental mapping of Roseldorf's surroundings taking into account the geological diversity and possible grasslands for animals. The dimension of the Sr isotope map can be extended to a larger scale concerning the eastern and southern regions of Roseldorf. Taking into account the geological background, the regions south of Roseldorf to the river Danube could be a possible place of origin of the non-local animals. This could render it possible to unravel the origin of the animal and human individuals exhibiting Sr isotope ratios under the lower $^{87}Sr/^{86}Sr$ limit. Moreover, the determination of a Sr isotope ratio range for the region of the Po Valley in Northern Italy should be considered in order to investigate if the Italian cattle found at the Celtic site Roseldorf could possibly be from there.

The results of the multielemental measurements have to be evaluated statistically in more detail. The use of multivariate data analysis could serve as a tool to establish elemental patterns of the environmental material and certain regions and geological substrates of the Weinviertel.

More animal tooth samples recovered from the settlement and the different sanctuaries could provide a more detailed overview about the animal mobility and the trading contacts of Roseldorf. An increase of the sample set would be important to get a more representative overview about the composition of the faunal assemblages of the different finding places. Especially the predominance of non-local animals, which were recovered from the settlement needs a further investigation by more analysed animals.

Concerning the human individuals an enlargement of the set of tooth samples is required for a deeper insight in human migration processes, society structures and the ritual and/or burial practices performed by the Celtic settlers in Roseldorf. The collection of more data could also lead to a better understanding of the function of Roseldorf's sanctuaries.

6. Bibliographies

Albarède, F., P. Telouk, J. Blichert-Toft, M. Boyet, A. Agranier, and B. Nelson. 2004. Precise and accurate isotopic measurements using multiple-collector ICPMS. *Geochimica et Cosmochimica Acta* 68 (12):2725-2744.

Anbar, A. D., J. E. Roe, J. Barling, and K. H. Nealson. 2000. Nonbiological fractionation of iron isotopes. *Science* 288:126-128.

Andrushko, V. A., M. R. Buzon, A. Simonetti, and R. A. Creaser. 2009. Strontium isotope evidence for prehistoric migration at Chokepukio, Valley of Cuzco, Peru. *Latin American Antiquity* 20 (1):57-75.

Anne Katzenberg, M., and R. G. Harrison. 1997. What's in a Bone? Recent advances in archaeological bone chemistry. *Journal of Archaeological Research* 5 (3):265-293.

Asahara, Y., H. Ishiguro, T. Tanaka, K. Yamamoto, K. Mimura, M. Minami, and H. Yoshida. 2006. Application of Sr isotopes to geochemical mapping and provenance analysis: The case of Aichi Prefecture, central Japan. *Applied Geochemistry* 21 (3):419-436.

Balasse, M., S. H. Ambrose, A. B. Smith, and T. D. Price. 2002. The seasonal mobility model for prehistoric herders in the south-western Cape of South Africa assessed by isotopic analysis of sheep tooth enamel. *Journal of Archaeological Science* 29 (9):917-932.

Balcaen, L., L. Moens, and F. Vanhaecke. 2010. Determination of isotope ratios of metals (and metalloids) by means of inductively coupled plasma-mass spectrometry for provenancing purposes - A review. *Spectrochimica Acta - Part B Atomic Spectroscopy* 65 (9-10):769-786.

Bendrey, R., T. E. Hayes, and M. R. Palmer. 2009. Patterns of iron age horse supply: An analysis of strontium isotope ratios in teeth. *Archaeometry* 51 (1):140-150.

Bentley, R. A. 2006. Strontium isotopes from the earth to the archaeological skeleton: A review. *Journal of Archaeological Method and Theory* 13 (3):135-187.

Bentley, R. A., H. R. Buckley, M. Spriggs, S. Bedford, C. J. Ottley, G. M. Nowell, C. G. Macpherson, and D. G. Pearson. 2007. Lapita migrants in the pacific's oldest cemetery: Isotopic analysis at teouma, vanuatu. *American Antiquity* 72 (4):645-656.

Bentley, R. A., and C. Knipper. 2005. Geographical patterns in biologically available strontium, carbon and oxygen isotope signatures in prehistoric SW Germany. *Archaeometry* 47 (3):629-644.

Blum, J. D., and Y. Erel. 1997. Rb-Sr isotope systematics of a granitic soil chronosequence: The importance of biotite weathering. *Geochimica et Cosmochimica Acta* 61 (15):3193-3204.

Boeckx, P., M. Van Meirvenne, F. Raulo, and O. Van Cleemput. 2006. Spatial patterns of δ13C and δ15N in the urban topsoil of Gent, Belgium. *Organic Geochemistry* 37 (10):1383-1393.

Boulyga, S. F., U. Klötzli, G. Stingeder, and T. Prohaska. 2007. Optimization and Application of ICPMS with Dynamic Reaction Cell for Precise Determination of 44Ca/40Ca Isotope Ratios. *Anal. Chem.* 79:7753-7760.

Bowen, G. J. 2010. Isoscapes: Spatial Pattern in Isotopic Biochemistry. *Annual Review of Earth and Planetary Sciences* 38:161-187.

Brätter, P., D. Gawlik, J. Lausch, and U. Rösick. 1977. On the distribution of trace elements in human skeletons. *Journal of Radioanalytical Chemistry* 37:393-403.

Britton, K., V. Grimes, J. Dau, and M. P. Richards. 2009. Reconstructing faunal migrations using intra-tooth sampling and strontium and oxygen isotope analyses: a case study of modern caribou (Rangifer tarandus granti). *Journal of Archaeological Science* 36 (5):1163-1172.

Britton, K., V. Grimes, L. Niven, T. E. Steele, S. McPherron, M. Soressi, T. E. Kelly, J. Jaubert, J.-J. Hublin, and M. P. Richards. 2011. Strontium isotope evidence for migration in late Pleistocene Rangifer: Implications for Neanderthal hunting strategies at the Middle Palaeolithic site of Jonzac, France. *Journal of Human Evolution* 61 (2):176-185.

Brunner, M. 2007. Determination of geographical origin of agricultural products via isotopic and elemental analysesby Inductively coupled plasma mass spectrometry (ICP-MS) on the exampleof Asparagus officinalis. *Master thesis,Univ.f.Bodenkultur, Wien*.

Budd, P., J. Montgomery, B. Barreiro, and R. G. Thomas. 2000. Differential diagenesis of strontium in archaeological human dental tissues. *Applied Geochemistry* 15 (5):687-694.

Burton, J. H., and T. D. Price. 1990. The ratio of barium to strontium as a paleodietary indicator of consumption of marine resources. *Journal of Archaeological Science* 17 (5):547-557.

Burton, J. H., T. D. Price, and W. D. Middleton. 1999. Correlation of bone Ba/Ca and Sr/Ca due to biological purification of Calcium. *Journal of Archaeological Science* 26 (6):609-616.

Buzon, M. R., A. Simonetti, and R. A. Creaser. 2007. Migration in the Nile Valley during the New Kingdom period: a preliminary strontium isotope study. *Journal of Archaeological Science* 34 (9):1391-1401.

Capo, R. C., B. W. Stewart, and O. A. Chadwick. 1998. Strontium isotopes as tracers of ecosystem processes: theory and methods *Geoderma* 82:197-225.

Cavazzini, G. 2005. A method for determining isotopic composition of elements by thermal ionization source mass spectrometry - Application to Sr. *International Journal of Mass Spectrometry* 240:17-26.

Chenery, C., H. Eckardt, and G. Müldner. 2011. Cosmopolitan Catterick? Isotopic evidence for population mobility on Rome's Northern frontier. *Journal of Archaeological Science* 38 (7):1525-1536.

Chenery, C., G. Müldner, J. Evans, H. Eckardt, and M. Lewis. 2010. Strontium and stable isotope evidence for diet and mobility in Roman Gloucester, UK. *Journal of Archaeological Science* 37 (1):150-163.

Conlee, C. A., M. R. Buzon, A. N. Gutierrez, A. Simonetti, and R. A. Creaser. 2009. Identifying foreigners versus locals in a burial population from Nasca, Peru: an investigation using strontium isotope analysis. *Journal of Archaeological Science* 36 (12):2755-2764.

Copeland, S. R., M. Sponheimer, P. J. Le Roux, V. Grimes, J. A. Lee-Thorp, D. J. De Ruiter, and M. P. Richards. 2008. Strontium isotope ratios (87Sr/86</Sr) of tooth enamel: A comparison of solution and laser ablation multicollector inductively coupled plasma mass spectrometry methods. *Rapid Communications in Mass Spectrometry* 22 (20):3187-3194.

Cox, K. J., R. A. Bentley, N. Tayles, H. R. Buckley, C. G. Macpherson, and M. J. Cooper. 2011. Intrinsic or extrinsic population growth in Iron Age northeast Thailand? The evidence from isotopic analysis. *Journal of Archaeological Science* 38 (3):665-671.

Dahl, S. G., P. Allain, P. J. Marie, Y. Mauras, G. Boivin, P. Ammann, Y. Tsouderos, P. D. Delmas, and C. Christiansen. 2001. Incorporation and distribution of strontium in bone. *Bone* 28 (4):446-453.

Dauphin, Y., and C. T. Williams. 2004. Diagenetic trends of dental tissues. *Comptes Rendus - Palevol* 3 (6-7 SPEC.ISS.):583-590.

Demandt, A. 2001. Die Kelten. *C.H. Beck Wissen*.

Denk, E., D. Hillegonds, J. Vogel, A. Synal, C. Geppert, K. Wendt, K. Fattinger, C. Hennessy, M. Berglund, R. F. Hurrel, and T. Walczyk. 2006. Labeling the human skeleton with 41Ca to assess changes in bone calcium metabolism. *Anayl. Bioanal. Chemistry* 386:1587-1602.

EIChrom. 2007. Product description of Sr specific resin: http://www.eichrom.com/products/info/sr_resin.cfm

Evans, J. A., J. Montgomery, and G. Wildman. 2009. Isotope domain mapping of 87Sr/86Sr biosphere variation on the Isle of Skye, Scotland. *Journal of the Geological Society* 166 (4):617-631.

Evans, J. A., J. Montgomery, G. Wildman, and N. Boulton. 2010. Spatial variations in biosphere 87Sr/86Sr in Britain. *Journal of the Geological Society* 167:1-4.

Evans, J. A., S. Tatham, S. R. Chenery, and C. A. Chenery. 2007. Anglo-Saxon animal husbandry techniques revealed though isotope and chemical variations in cattle teeth. *Applied Geochemistry* 22 (9):1994-2005.

Featherstone, J. D. B., S. Pearson, and R. Z. LeGeros. 1984. An Infrared method for quantification of carbonate in carbonated apatites. *Caries Research* 18:63-66.

Fox, J. L., P. J. Spooner, and A. V. Katdare. 1983. Dissolution rate behavior of hydroxyapatite-fluorapatite mixtures. *Caries Research* 17:289-296.

Frei, K. M., and R. Frei. 2011. The geographic distribution of strontium isotopes in Danish surface waters - A base for provenance studies in archaeology, hydrology and agriculture. *Applied Geochemistry* 26 (3):326-340.

Gölles, D. in prep. Strontium isotope ratio and trace element analysis of body tissues of a sheep as an animal model and its habitat by means of inductively coupled plasma mass spectrometry. *Bachelor thesis, Univ. f. Bodenkultur, Wien*.

Grupe, G. 1988. Impact of the choice of bone samples on trace element data in excavated human skeletons. *Journal of Archaeological Science* 15:123-129.

Haverkort, C. M., A. Weber, M. A. Katzenberg, O. I. Goriunova, A. Simonetti, and R. A. Creaser. 2008. Hunter-gatherer mobility strategies and resource use based on strontium isotope (87Sr/86Sr) analysis: a case study from Middle Holocene Lake Baikal, Siberia. *Journal of Archaeological Science* 35 (5):1265-1280.

Hedges, R. E. M. 2002. Bone diagenesis: An overview of processes. *Archaeometry* 44 (3):319-328.

Hedges, R. E. M., A. R. Millard, and A. W. G. Pike. 1995. Measurements and Relationships of Diagenetic Alteration of Bone from Three Archaeological Sites. *Journal of Archaeological Science* 22 (2):201-209.

Hedman, K. M., B. B. Curry, T. M. Johnson, P. D. Fullagar, and T. E. Emerson. 2009. Variation in strontium isotope ratios of archaeological fauna in the Midwestern United States: a preliminary study. *Journal of Archaeological Science* 36 (1):64-73.

Heumann, K. G., S. M. Gallus, G. Radlinger, and J. Vogl. 1998. Precision and accuracy in isotope ratio measurements by plasma source mass spectrometry. *J. Anal. At. Spectrom.* 13:1001-1008.

Hillson, S. 1997. *Dental Anthropology* Cambridge University Press, Cambridge.

Hoddell, D. A., R. L. Quinn, M. Brenner, and G. Kamenov. 2004. Spatial variation of strontium isotopes (87Sr/86Sr) in the Maya region: a tool for tracking ancient human migration. *Journal of Archaeological Science* 31:585-601.

Holzer, V. 2006. Roseldorf/Sandberg (Österreich) - Ein keltisches Heiligtum nach dem Modell von Gournay-sur-Aronde. *Blut und Wein. Keltisch-römische Kultpraktiken*:77-90.

———. 2007. Le sanctuaire Céltique de Roseldorf-Sandberg (Autriche). *Presses universitaires de Franche-Comté*:849-854.

———. 2008. Ein latènezeitlicher Getreidespeicher aus der keltischen Großsiedlung am Sandberg in Roseldorf (Niederösterreich). *Germania* 86:135-179.

———. 2009. Roseldorf - Interdisziplinäre Forschungen zur größten keltischen Zentralsiedlung Österreichs. *Schriftenreihe der Forschung im Verbund* 102.

Hoppe, K. A., and P. L. Koch. 2007. Reconstructing the migration patterns of late Pleistocene mammals from northern Florida, USA. *Quaternary Research* 68 (3):347-352.

Hoppe, K. A., S. M. Stover, J. R. Pascoe, and R. Amundson. 2004. Tooth enamel biomineralization in extant horses: Implications for isotopic microsampling. *Palaeogeography, Palaeoclimatology, Palaeoecology* 206 (3-4):355-365.

Horsky, M. 2010. Determination of the provenance of prehistoric wood by isotopic fingerprinting. *Diploma thesis, Univ.f. Bodenkultur, Wien*.

Huemer, C. 2008. Migration studies of humans by isotopic fingerprints using inductively coupled plasma mass spectrometry (ICP-MS). Master thesis, Univ. f. Bodenkultur, Wien.

Irrgeher, J., A. Zitek, M. Teschler-Nicola, and T. Prohaska. 2010. Anwendung von Strontium-Isotopensignaturen für Mobilitäts- und Migrationsstudien. *Journal of Alpine Geology* 52 (147 ff.).

Kazaki, M. O., V. Moriwaki, T. Aoba, V. Doi, and J. Takahashi. 1981. Solubility behaviour of carbonate apatites in relation to crystallinity. *Caries Research* 15:477-483.

Knudson, K. J. 2008. Tiwanaku influence in the South Central Andes: Strontium isotope analysis and middle horizon migration. *Latin American Antiquity* 19 (1):3-23.

Knudson, K. J., and J. E. Buikstra. 2007. Residential mobility and resource use in the Chiribaya polity of southern Peru: Strontium isotope analysis of Archaeological tooth enamel and bone. *International Journal of Osteoarchaeology* 17 (6):563-580.

Knudson, K. J., and T. A. Tung. 2011. Investigating regional mobility in the southern hinterland of the Wari empire: Biogeochemistry at the site of Beringa, Peru. *American Journal of Physical Anthropology* 145 (2):299-310.

Kohn, M. J., M. J. Schoeninger, and J. W. Valley. 1998. Variability in oxygen isotope compositions of herbivore teeth: reflections of seasonality or developmental physiology? *Chemical Geology* 152 (1-2):97-112.

Kuczumow, A., E. Cukrowska, A. Stachniuk, R. Gaweda, R. Mroczka, W. Paszkowicz, K. Skrzypiec, R. Falkenberg, and L. Backwell. 2010. Investigation of chemical changes in bone material from South African fossil hominid deposits. *Journal of Archaeological Science* 37 (1):107-115.

Kusaka, S., T. Nakano, T. Yumoto, and M. Nakatsukasa. 2011. Strontium isotope evidence of migration and diet in relation to ritual tooth ablation: A case study from the Inariyama Jomon site, Japan. *Journal of Archaeological Science* 38 (1):166-174.

Lachniet, M. S., and W. P. Patterson. 2009. Oxygen isotope values of precipitation and surface waters in northern Central America (Belize and Guatemala) are dominated by temperature and amount effects. *Earth and Planetary Science Letters* 284 (3-4):435-446.

Latkoczy, C., T. Prohaska, G. Stingeder, and M. Teschler-Nicola. 1998. Strontium isotope ratio measurements in prehistoric human bone samples by means of HR-ICP-MS. *J. Anal. At. Spectrom.* 13 (6):561-566.

Lauermann, E. 2001. Archäologische Forschungen, Mitterretzbach 1999-2001. 1-4/2001.

Lauermann, E., and P. Trebsche. 2008. Opfer und Rituale bei den Kelten.

Leach, S., M. Lewis, C. Chenery, G. Müldner, and H. Eckardt. 2009. Migration and diversity in Roman Britain: A multidisciplinary approach to the identification of immigrants in Roman York, England. *American Journal of Physical Anthropology* 140 (3):546-561.

Lebon, M., K. Müller, J. J. Bahain, F. Fröhlich, C. Falguères, L. Bertrand, C. Sandt, and I. Reiche. 2011. Imaging fossil bone alterations at the microscale SR-FTIR microspectroscopy. *J. Anal. At. Spectrom.* 26:922-929.

Lebon, M., I. Reiche, J. J. Bahain, C. Chadefaux, A. M. Moigne, F. Fröhlich, F. Sémah, H. P. Schwarcz, and C. Falguères. 2010. New parameters for the characterization of diagenetic alterations and heat-induced changes of fossil bone mineral using Fourier transform infrared spectrometry. *Journal of Archaeological Science* 37 (9):2265-2276.

LeGeros, R. Z., and M. S. Tung. 1983. Chemical stability of carbonate- and fluoride-containing apatites. *Caries Research* 17 (5):419-429.

Lippert, H. 2000. Lehrbuch Anatomie. *Urban&Fischer Verlag München*.

Longinelli, A. 1984. Oxygen isotopes in mammal bone phosphate: a new tool for paleohydrological and paleoclimatological research? *Geochimica et Cosmochimica Acta* 48:385-390.

Lucas, P., P. Constantino, B. Wood, and B. Lawn. 2008. Dental enamel as dietary indicator in mammals. *BioEssays* 30:374-385.

Maréchal, C. N., P. Télouk, and F. Albarède. 1999. Precise analysis of copper and zinc isotopic compositions by plasma-source mass spectrometry. *Chemical Geology* 156 (1-4):251-273.

Mitchell, P. D., and A. R. Millard. 2009. Migration to the medieval Middle East with the crusades. *American Journal of Physical Anthropology* 140 (3):518-525.

Moens, L., F. Vanhaecke, D. R. Bandura, V. I. Baranov, and S. D. Tanner. 2001. Elimination of isobaric interferences in ICP-MS, using ion-molecule reaction chemistry: Rb/Sr age determination of magmatic rocks, a case study. *J. Anal. At. Spectrom.* 16:991-994.

Montgomery, J. 2010. Passports from the past: Investigating human dispersals using strontium isotope analysis of tooth enamel. *Annals of Human Biology* 37 (3):325-346.

Montgomery, J., J. A. Evans, D. Powlesland, and C. A. Roberts. 2005. Continuity or colonization in Anglo-Saxon England? Isotope evidence for mobility, subsistence practice, and status at West Heslerton. *American Journal of Physical Anthropology* 126 (2):123-138.

Müldner, G., C. Chenery, and H. Eckardt. 2011. The 'Headless Romans': Multi-isotope investigations of an unusual burial ground from Roman Britain. *Journal of Archaeological Science* 38 (2):280-290.

Nafplioti, A. 2008. "Mycenaean" political domination of Knossos following the Late Minoan IB destructions on Crete: negative evidence from strontium isotope ratio analysis. *Journal of Archaeological Science* 35 (8):2307-2317.

———. 2011. Tracing population mobility in the Aegean using isotope geochemistry: A first map of local biologically available 87Sr/86Sr signatures. *Journal of Archaeological Science* 38 (7):1560-1570.

Nehlich, O., J. Montgomery, J. Evans, S. Schade-Lindig, S. L. Pichler, M. P. Richards, and K. W. Alt. 2009. Mobility or migration: a case study from the Neolithic settlement of Nieder-Mörlen (Hessen, Germany). *Journal of Archaeological Science* 36 (8):1791-1799.

Nelson, B. K., M. J. Deniro, M. J. Schoeninger, D. J. De Paolo, and P. E. Hare. 1986. Effects of diagenesis on strontium, carbon, nitrogen and oxygen concentration and isotopic composition of bone. *Geochimica et Cosmochimica Acta* 50 (9):1941-1949.

Nelson, D. G. A. 1981. The influence of carbonate on the atomic structure and reactivity of hydroxyapatite. *Journal of Dental Research* 60:1621-1629.

Nickel, R., A. Schummer, and E. Seiferle. 1995. Lehrbuch der Anatomie der Haustiere. *Blackwell Wissenschafts-Verlag, Berlin, Wien* II:77-100.

Nielsen-Marsh, C. M., C. I. Smith, M. M. E. Jans, A. Nord, H. Kars, and M. J. Collins. 2007. Bone diagenesis in the European Holocene II: taphonomic and environmental considerations. *Journal of Archaeological Science* 34 (9):1523-1531.

Niu, H., and R. S. Houk. 1996. Fundamental aspects of ion extraction in inductively coupled plasma mass spectrometry *Spectrochimica Acta - Part B* 51:779-815.

Novotny, F., M. Teschler-Nicola, T. Prohaska, C. Latkoczy, and G. Stingeder. 2003. Diagenetic alterations in archaeological human skeletal remains via light microscopy and their implications. *Am. J. Phy. Anthrop. Suppl.* 36:159.

NuInstruments. 2007. Nu Plasma Manual, Nu Instruments Ltd., Wrexham, UK.

Pellegrini, M., R. E. Donahue, C. Chenery, J. Evans, J. Lee-Thorp, J. Montgomery, and M. Mussi. 2008. Faunal migration in late-glacial central Italy: Implications for human resource exploitation. *Rapid Communications in Mass Spectrometry* 22 (11):1714-1726.

Perry, M. A., D. Coleman, and N. Delhopital. 2008. Mobility and exile at 2nd century A.D. Khirbet edh-Dharih: Strontium isotope analysis of human migration in Western Jordan. *Geoarchaeology* 23 (4):528-549.

Perry, M. A., D. S. Coleman, D. L. Dettman, and A. H. Al-Shiyab. 2009. An isotopic perspective on the transport of byzantine mining camp laborers into southwestern Jordan. *American Journal of Physical Anthropology* 140 (3):429-441.

Pike, A., C. M. Nielsen-Marsh, and R. E. M. Hedges. 2001. Bone dissolution and hydrology. *Proceedings of Archaeological Sciences 1997, British Archaeological Reports. Archaeopress, Oxford*:127-132.

Price, T. D., J. H. Burton, and R. A. Bentley. 2002. The characterization of biologically available strontium isotope ratios for the study of prehistoric migration. *Archaeometry* 44 (1):117-135.

Price, T. D., J. H. Burton, R. J. Sharer, J. E. Buikstra, L. E. Wright, L. P. Traxler, and K. A. Miller. 2010. Kings and commoners at Copan: Isotopic evidence for origins and movement in the Classic Maya period. *Journal of Anthropological Archaeology* 29 (1):15-32.

Price, T. D., J. H. Burton, and J. B. Stoltman. 2007. Place of origin of prehistoric inhabitants of Aztalan, Jefferson Co., Wisconsin. *American Antiquity* 72 (3):524-538.

Price, T. D., and H. Gestsdóttir. 2006. The first settlers of Iceland: An isotopic approach to colonisation. *Antiquity* 80 (307):130-144.

Price, T. D., V. Tiesler, and J. H. Burton. 2006a. Early African Diaspora in colonial Campeche, Mexico: Strontium isotopic evidence. *American Journal of Physical Anthropology* 130 (4):485-490.

Price, T. D., J. Wahl, and R. A. Bentley. 2006b. Isotopic evidence for mobility and group organization among neolithic farmers at Talheim, Germany, 5000. *European Journal of Archaeology* 9 (2-3):259-284.

Prohaska, T., J. Irrgeher, and M. Teschler-Nicola. 2010. Bestimmung des 87Sr/86Sr Isotopenverhältnisses mittels MC-ICP-MS in historischen Zahnproben am Beispiel des frühmittelalterlichen Gräberfeldes der Schanze von Gars/Thunau am Kamp (~900-1000 n.Chr.). *Journal of Alpine Geology* 52:205 ff.

Prohaska, T., C. Latkoczy, G. Schultheis, M. Teschler-Nicola, and G. Stingeder. 2002. Investigation of Sr isotope ratios in prehistoric human bones and teeth using laser ablation ICP-MS and ICP-MS after Rb/Sr separation. *Journal of Analytical Atomic Spectrometry* 17 (8):887-891.

Pucher, E., and M. Schmitzberger. 2003. Zur Differenzierung heimischer und importierter Rinder in den römischen Donauprovinzen. *Beiträge zur Archäologie und prähistorischen Anthropologie* IV:60-74.

Quillfeldt, P., J. F. Masello, R. A. R. McGill, M. Adams, and R. W. Furness. 2010. Moving polewards in winter: A recent change in the migratory strategy of a pelagic seabird? *Frontiers in Zoology* 7.

Radloff, F. G. T., L. Mucina, W. J. Bond, and P. J. Le Roux. 2010. Strontium isotope analyses of large herbivore habitat use in the Cape Fynbos region of South Africa. *Oecologia* 164 (2):567-578.

Richards, M., K. Harvati, V. Grimes, C. Smith, T. Smith, J. J. Hublin, P. Karkanas, and E. Panagopoulou. 2008. Strontium isotope evidence of Neanderthal mobility at the site of Lakonis, Greece using laser-ablation PIMMS. *Journal of Archaeological Science* 35 (5):1251-1256.

Rodrigues, C., C. Máguas, and T. Prohaska. 2011. Strontium and oxygen isotope fingerprinting of green coffee beans and its potential to proof authenticity of coffee. *European Food Research and Technology* 232 (2):361-373.

Schroeder, H., T. C. O'Connell, J. A. Evans, K. A. Shuler, and R. E. M. Hedges. 2009. Trans-atlantic slavery: Isotopic evidence for forced migration to barbados. *American Journal of Physical Anthropology* 139 (4):547-557.

Schultheiss, G. 2003. Analysis of isotope ratios in anthropological and archaeological samples by high resolution inductively coupled plasma mass spectrometry (HR-ICP-MS). PhD thesis, Univ. f. Bodenkultur, Wien.

Schumacher, G. H., H. Schmidt, and W. Richter. 1983. Anatomie und Biochemie der Zähne. Gustav Fischer Verlag, Stuttgart, New York.

Schweissing, M. M., and G. Grupe. 2003. Stable strontium isotopes in human teeth and bone: A key to migration events of the late Roman period in Bavaria. *Journal of Archaeological Science* 30 (11):1373-1383.

Shaw, B., H. Buckley, G. Summerhayes, D. Anson, S. Garling, F. Valentin, H. Mandui, C. Stirling, and M. Reid. 2010. Migration and mobility at the Late Lapita site of Reber-Rakival (SAC), Watom Island using isotope and trace element analysis: a new insight into Lapita interaction in the Bismarck Archipelago. *Journal of Archaeological Science* 37 (3):605-613.

Shaw, B. J., G. R. Summerhayes, H. R. Buckley, and J. A. Baker. 2009. The use of strontium isotopes as an indicator of migration in human and pig Lapita populations in the Bismarck Archipelago, Papua New Guinea. *Journal of Archaeological Science* 36 (4):1079-1091.

Sillen, A. 1986. Biogenic and diagnetic Sr/Ca in Plio-Pleistocene fossils of the Omo Shungura Formation (Ethiopia). *Paleobiology* 12 (3):311-323.

Sillen, A., and J. C. Sealy. 1995. Diagenesis of Strontium in Fossil Bone: A Reconsideration of Nelsonet al.(1986). *Journal of Archaeological Science* 22 (2):313-320.

Smith, C. I., C. M. Nielsen-Marsh, M. M. E. Jans, and M. J. Collins. 2007. Bone diagenesis in the European Holocene I: patterns and mechanisms. *Journal of Archaeological Science* 34 (9):1485-1493.

Smith, J., J. Lee-Thorp, S. Prevec, S. Hall, and A. Späth. 2010. Pre-colonial herding strategies in the Shashe-Limpopo basin, southern Africa, based on strontium isotope analysis of domestic fauna. *Journal of African Archaeology* 8 (1):83-98.

Smits, E., A. R. Millard, G. Nowell, and D. G. Pearson. 2010. Isotopic investigation of diet and residential mobility in the Neolithic of the Lower Rhine Basin. *European Journal of Archaeology* 13 (1):5-31.

Sponheimer, M., D. de Ruiter, J. Lee-Thorp, and A. SpÃ¤th. 2005a. Sr/Ca and early hominin diets revisited: New data from modern and fossil tooth enamel. *Journal of Human Evolution* 48 (2):147-156.

Sponheimer, M., D. de Ruiter, J. Lee-Thorp, and A. Späth. 2005b. Sr/Ca and early hominin diets revisited: New data from modern and fossil tooth enamel. *Journal of Human Evolution* 48 (2):147-156.

Sponheimer, M., and J. A. Lee-Thorp. 1999. Oxygen Isotopes in Enamel Carbonate and their Ecological Significance. *Journal of Archaeological Science* 26 (6):723-728.

Steiger, R. H., and E. Jaeger. 1977. Subcommission on geochronology: Convention on the use of decay constants in geo- and cosmochronology. *Earth and Planetary Science Letters* 36:359-362.

Strobl, J. 2010. Tracer studies: Sr turnover studies in animal and human hard tissues. Bachelor thesis, Univ. f. Bodenkultur, Wien.

Sturm, M. 2008. Migration studies of fish by measurement of strontium isotope ratios and multi-elemental patterns in otoliths using LA-ICP-MS. *Master thesis,Univ.f.Bodenkultur, Wien*.

Teschler-Nicola, M., F. Gerold, M. Bujatti-Narbeshuber, T. Prohaska, C. Latkoczy, G. Stingeder, and M. Watkins. 1999. Evidence of genocide 7000 BP - Neolithic paradigm and geo-climatic reality. *Collegium Antropologicum* 23 (2):437-450.

Teschler-Nicola, M., T. Prohaska, and E. M. Wild. 2005. Der Fundkomplex von Schletz und seine Bedeutung für den aktuellen Diskurs endlinearbandkeramischer Phänomene in Zentraleuropa. *Collegium Anthropologicum*.

Thesleff, I., and P. Nieminen. 1996. Tooth morphogenesis and cell differentiation. *Current Opinion in Cell Biology* 8:844-850.

Thomas, R. 2001a. A Beginner's Giude to ICP-MS - Part II: The sample introduction system. *Spectroscopy* 16 (5):56-60.

———. 2001b. A Beginner's Guide to ICP-MS - Part III: The plasma source. *Spectroscopy* 16 (6):26-30.

———. 2001c. A Beginner's Guide to ICP-MS - Part IV: The interface region. *Spectroscopy* 16 (7):26-28.

———. 2001d. Beginner's Guide to ICP-MS - Part VI: The mass analyzer. *Spectroscopy* 16 (10):44-48.

———. 2002a. A Beginner's Guide to ICP-MS - Part X: Detectors. *Spectroscopy* 17 (4):34-39.

———. 2002b. A Beginner's Guide to ICP-MS - Part XII: A Review of Interferences. *Spectroscopy* 17 (10):24-31.

———. 2002c. A Beginner's Guide to ICP-MS: Part IX-Mass Analyzers: Collision/Reaction Cell Technology. *Spectroscopy* 17 (2):42-48.

Tiefengraber, G., B. Kavur, and A. Gaspari. 2009. Druideninsignie und Götterfigur.Zeugen keltischer Rituale in Roseldorf/Niederösterreich. *Keltske Studije II, Studies in Celtic Archaeology*:173-184.

Towers, J., J. Montgomery, J. Evans, M. Jay, and M. P. Pearson. 2010. An investigation of the origins of cattle and aurochs deposited in the Early Bronze Age barrows at Gayhurst and Irthlingborough. *Journal of Archaeological Science* 37 (3):508-515.

Trueman, C. N., M. R. Palmer, J. Field, K. Privat, N. Ludgate, V. Chavagnac, D. A. Eberth, R. Cifelli, and R. R. Rogers. 2008. Comparing rates of recrystallisation and the potential for preservation of biomolecules from the distribution of trace elements in fossil bones. *Comptes Rendus - Palevol* 7 (2-3):145-158.

Tung, T. A., and K. J. Knudson. 2011. Identifying locals, migrants, and captives in the Wari Heartland: A bioarchaeological and biogeochemical study of human remains from Conchopata, Peru. *Journal of Anthropological Archaeology* 30 (3):247-261.

Velasco-Vásquez, J., M. Arnay-de-la-rosa, E. González-reimers, and O. Hernández-torres. 1997. Paleodietary analysis on the prehistoric population of El Hierro (Canary Islands). *Biological Trace Element Research* 59 (1-3):207-213.

Viner, S., J. Evans, U. Albarella, and M. Parker Pearson. 2010. Cattle mobility in prehistoric Britain: Strontium isotope analysis of cattle teeth from Durrington Walls (Wiltshire, Britain). *Journal of Archaeological Science* 37 (11):2812-2820.

Walton, M. S., A. Shortland, S. Kirk, and P. Degryse. 2009. Evidence for the trade of Mesopotamian and Egyptian glass to Mycenaean Greece. *Journal of Archaeological Science* 36 (7):1496-1503.

Wassenaar, L. I., S. L. Van Wilgenburg, K. Larson, and K. A. Hobson. 2009. A groundwater isoscape (δD, δ18O) for Mexico. *Journal of Geochemical Exploration* 102 (3):123-136.

Weiss, D. J., B. Kober, A. Dolgopolova, K. Gallagher, B. Spiro, G. Le Roux, T. F. D. Mason, M. Kylander, and B. J. Coles. 2004. Accurate and precise Pb isotope ratio measurements in environmental samples by MC-ICP-MS. *International Journal of Mass Spectrometry* 232 (3):205-215.

Werner, R. A., and W. A. Brand. 2001. Referencing strategies and techniques in stable isotope ratio analysis. *Rapid Communications in Mass Spectrometry* 15 (7):501-519.

West, J. B., G. J. Bowen, T. E. Dawson, and K. P. Tu. 2010. Isoscapes. Understanding movement, pattern, and process on Earth through isotope mapping. *Springer Verlag, Dordrecht, Heidelberg, London, New York*.

White, T. D., and A. Folkens. 2005. *The human bone manual* 1st edition, Elsevier.

White, W. M., F. Albarède, and P. Télouk. 2000. High-precision analysis of Pb isotope ratios by mulit-collector ICP-MS. *Chemical Geology* 167:257-270.

Woodward, H. Q. 1962. *Health Physics* 1062 (8):513-517.

Wright, L. E. 2005. Identifying immigrants to Tikal, Guatemala: Defining local variability in strontium isotope ratios of human tooth enamel. *Journal of Archaeological Science* 32 (4):555-566.

Wright, L. E., J. A. Valdés, J. H. Burton, T. Douglas Price, and H. P. Schwarcz. 2010. The children of Kaminaljuyu: Isotopic insight into diet and long distance interaction in Mesoamerica. *Journal of Anthropological Archaeology* 29 (2):155-178.

Zitek, A., M. Sturm, H. Waidbacher, and T. Prohaska. 2010. Discrimination of wild and hatchery trout by natural chronological patterns of elements and isotopes in otoliths using LA-ICP-MS. *Fisheries Management and Ecology* 17 (5):435-445.

7. Appendix

7.1 Certificates of Analysis

National Institute of Standards & Technology

Certificate of Analysis

Standard Reference Material® 987

Strontium Carbonate
(Isotopic Standard)

This Standard Reference Material (SRM) is certified for use as an isotopic reference material for the calibration of mass spectrometers. The material consists of highly purified strontium carbonate of high homogeneity. A unit of SRM 987 consists of 1 g of powder.

Certified Values: The certified values for the absolute strontium isotopic abundance ratios and the atom fractions of ^{88}Sr, ^{87}Sr, ^{86}Sr and ^{84}Sr are listed in Table 1. A NIST-certified value is a value for which NIST has the highest confidence in its accuracy, in that all known or suspected sources of bias have been investigated or accounted for by NIST. A certified value is the present best estimate of the true value based on the results of analyses performed at NIST and cooperating laboratories. Value assignment categories are based on the definition of terms and modes used at NIST for chemical reference materials [1]. The uncertainties listed with the values are expanded uncertainties (95 % confidence interval) and are calculated according to the methods in the ISO and NIST Guides [2].

Table 1. Certified Values for SRM 987 Strontium Carbonate

Absolute Abundance Ratios	$^{88}Sr/^{86}Sr = 8.378\,61 \pm 0.003\,25$
	$^{87}Sr/^{86}Sr = 0.710\,34 \pm 0.000\,26$
	$^{84}Sr/^{86}Sr = 0.056\,55 \pm 0.000\,14$
that yield atom percents of:	$^{88}Sr = 82.584\,5 \pm 0.006\,6$
	$^{87}Sr = 7.001\,5 \pm 0.002\,6$
	$^{86}Sr = 9.856\,6 \pm 0.003\,4$
	$^{84}Sr = 0.557\,4 \pm 0.001\,5$

This material was used as the reference sample in a determination of the absolute abundance ratios and atomic weight of strontium [3]. The atomic weight of strontium calculated from the absolute abundance ratios is 87.616 81 ± 0.000 12.

Expiration of Certification: The certification of this SRM is deemed to be indefinite within the stated uncertainties. However, certification is nullified if the SRM is contaminated or otherwise altered.

Maintenance of Certified Values: NIST will monitor this SRM and, if substantive changes occur in the certified values, NIST will notify the purchaser. Registration (see attached sheet) will facilitate notification.

Stephen A. Wise, Chief
Analytical Chemistry Division

Gaithersburg, MD 20899
Certificate Issue Date: 19 June 2007
See Certificate Revision History on Last Page

Robert L. Watters, Jr., Chief
Measurement Services Division

The overall direction and coordination of the technical measurements leading to the certification of this SRM were performed under the chairmanship of I.L. Barnes and W.R. Shields of the NIST Analytical Chemistry Division.

The characterization of this SRM was performed by G. Marinenko, E.E. Etz, D.G. Friend, I.L. Barnes, L.J. Moore, T.C. Rains, T.A. Rush, L.A. Machlan, T.J. Murphy, and P.J. Paulsen, all of the NIST Analytical Chemistry Division.

The support aspects involved in the preparation of this SRM were coordinated through the NIST Measurement Services Division. The current revised certificate was coordinated by Robert D. Vocke, Jr. of the Analytical Chemistry Division.

Storage and Handling: There are no special storage or handling instructions. While strontium carbonate is slightly hygroscopic (absorbing approximately 0.02 % moisture at 90 % humidity), this has no effect on the isotopic abundances.

The strontium carbonate used for this SRM was obtained from Spex Industries, Inc[1]. of Metuchen, NJ. The material, when received, was of high purity in relation to cationic impurities but assayed only 99.0 % due to moisture and other volatile impurities. The impurities reported in the strontium carbonate material are lithium, 4 mg/kg; sodium, 6 mg/kg; potassium, < 1 mg/kg; magnesium, < 2 mg/kg; calcium, 5 mg/kg; barium, < 15 mg/kg; copper, < 3 mg/kg; iron, < 3 mg/kg; aluminum, < 1 mg/kg; and silicon, < 1 mg/kg.

REFERENCES

[1] May, W.E.; Parris, R.M.; Beck II, C.M.; Fassett, J.D.; Greenberg, R.R.; Guenther, F.R.; Kramer, G.W.; Wise; S.A.; Gills, T.E.; Colbert, J.C.; Gettings, R.J.; MacDonald, B.S.; *Definitions of Terms and Modes Used at NIST for Value-Assignment of Reference Materials for Chemical Measurements*; NIST Spec. Pub. 260-136, U.S. Government Printing Office: Washington, DC (2000).

[2] ISO; *Guide to the Expression of Uncertainty in Measurement*; ISBN 92-67-10188-9, 1st ed., International Organization for Standardization: Geneva, Switzerland (1993); see also Taylor, B.N.; Kuyatt, C.E.; *Guidelines for Evaluating and Expressing the Uncertainty of NIST Measurement Results*; NIST Technical Note 1297, U.S. Government Printing Office: Washington, DC (1994); available at http://physics.nist.gov/Pubs/.

[3] Moore, L.J.; Murphy, T.J.; Barnes, I.L.; Paulsen, P.J.; *Absolute Isotopic Abundance Ratios and Atomic Weight of a Reference Sample of Strontium*, J. of Res. (NBS) Vol. 87, No. 1, pp. 1–8 (1982).

Certificate Revision History: 19 June 2007 (Editorial change); 14 June 2007 (Editorial changes and revised as isotopic standard only); 01 May 2000 (Editorial changes); 01 October 1982 (Revision of certified values); 06 March 1972 (Editorial changes); 08 November 1971 (Original certificate date).

Users of this SRM should ensure that the certificate in their possession is current. This can be accomplished by contacting the SRM Program at: telephone (301) 975-6776; fax (301) 926-4751; e-mail srminfo@nist.gov; or via the Internet at http://www.nist.gov/srm.

[1]Certain commercial equipment, instrumentation, or materials are identified in this certificate to specify adequately the experimental procedure. Such identification does not imply recommendation or endorsement by the NIST, nor does it imply that the materials or equipment identified are necessarily the best available for the purpose.

7.2. Measurement results

7.2.1. Diagenesis study of teeth and bone matrices

7.2.1.1. Elemental ratios and element data

leachate	Ca/P	Sr*1000/Ca	Sr [ng g^{-1}]	Ca [ng g^{-1}]]	P [ng g^{-1}]	Ba [ng g^{-1}]
A_1	2.4773	2.5863	108.92	42116.32	17000.78	70.71
A_2	1.9201	2.1511	61.84	28747.03	14971.74	50.76
A_3	1.8576	1.8478	50.38	27262.47	14676.41	45.96
A_4	1.8295	1.6288	38.64	23725.13	12968.16	38.33
A_5	1.8471	1.4341	32.85	22905.28	12400.94	33.78
A_6	1.8344	1.2991	29.09	22391.39	12206.67	30.69
A_7	1.8326	1.2047	27.16	22543.38	12301.44	27.77
A_8	1.8237	1.1247	25.07	22290.52	12222.50	25.87
A_9	1.8399	1.0704	21.83	20396.47	11085.93	22.31
A_10	1.8281	1.0581	21.03	19878.68	10873.91	20.84
A_11	1.8456	1.0331	22.64	21909.72	11871.16	21.18
A_12	1.8584	1.0165	19.90	19576.14	10533.85	18.33
A_13	1.8743	1.0130	18.16	17926.32	9564.29	16.75
A_14	1.8651	0.9746	12.26	12582.57	6746.36	11.10
A_15	1.8752	0.9588	18.55	19350.98	10319.68	15.68
A_16	1.8391	0.9370	14.60	15578.97	8471.13	13.20
A_17	1.8515	0.9089	13.98	15378.33	8305.78	12.18
A_18	1.8567	0.8307	5.71	6873.76	3702.22	5.05
A_19	1.8565	0.8581	12.15	14164.44	7629.71	9.96
A_20	1.8871	0.8348	11.54	13823.27	7325.24	9.45
A_21	2.2288	1.1677	19.97	23971.65	7675.33	11.45
A_22	2.1099	1.0103	18.07	25067.34	8475.07	12.34
A_23	2.0416	0.9146	14.52	22231.96	7776.07	8.54
A_24	2.0403	0.8538	12.52	20527.21	7189.82	7.12

A_25	2.0580	0.8173	11.56	19777.30	6870.16	6.33
A_26	2.0427	0.8140	10.49	18000.42	6306.27	5.60
A_27	2.0557	0.7829	10.25	18294.87	6367.56	5.12
A_28	2.0750	0.7418	9.39	17677.30	6097.89	4.42
A_29	2.0603	0.7317	8.22	15665.76	5450.71	3.67
A_30	2.0572	0.7368	8.88	16822.08	5856.50	3.80

leachate	Ca/P	Sr*1000/Ca	Sr [ng g^{-1}]	Ca [ng g^{-1}]	P [ng g^{-1}]	Ba [ng g^{-1}]
B_1	9.5775	2.4240	183.43	75671.69	7900.96	92.49
B_2	3.5544	2.2586	117.63	52081.53	14652.80	78.00
B_3	2.8592	2.0652	93.43	45240.14	15822.40	70.43
B_4	2.8418	1.9332	78.95	40839.76	14371.27	65.30
B_5	2.6065	1.8047	70.98	39332.54	15090.35	60.81
B_6	2.3664	1.7402	62.56	35951.49	15192.47	56.55
B_7	2.1709	1.6734	55.11	32929.79	15169.01	50.39
B_8	2.0805	1.6290	50.85	31215.41	15003.64	47.28
B_9	2.0679	1.5986	49.63	31045.01	15012.48	45.06
B_10	2.0336	1.5844	46.50	29350.42	14432.48	42.23
B_11	2.0698	1.6032	48.40	30187.23	14584.26	42.14
B_12	2.0229	1.5587	49.11	31510.90	15576.99	41.50
B_13	2.0354	1.5476	43.86	28339.06	13922.78	36.74
B_14	2.0302	1.5295	44.17	28878.62	14224.74	35.64
B_15	2.0366	1.5240	42.26	27732.14	13616.65	33.27
B_16	2.0084	1.5105	39.58	26204.95	13047.81	30.83
B_17	2.0177	1.4921	39.46	26445.34	13106.70	29.72
B_18	2.1347	1.4745	33.59	22778.68	10670.79	25.43
B_19	2.1348	1.4685	33.89	23080.69	10811.47	24.89
B_20	2.1728	1.4475	32.95	22761.78	10475.66	23.85
B_21	3.6608	1.8256	40.11	30787.99	6002.18	21.47
B_22	2.6351	1.6064	35.70	31138.39	8432.46	20.33
B_23	2.4080	1.5465	31.57	28585.25	8477.79	17.75
B_24	2.2893	1.5077	36.13	33605.42	10468.83	21.47
B_25	2.2446	1.4309	35.60	34900.99	11085.42	20.15

B_26	2.2066	1.3852	30.81	31167.23	10079.25	17.61
B_27	2.2042	1.3387	28.20	29502.39	9555.65	15.57
B_28	2.2019	1.3246	28.30	29930.23	9703.32	15.55
B_29	2.1793	1.3111	26.06	27821.20	9119.33	14.32
B_30	2.1508	1.2983	26.04	28085.50	9326.93	15.13

leachate	Ca/P	Sr*1000/Ca	Sr [ng g^{-1}]	Ca [ng g^{-1}]	P [ng g^{-1}]	Ba [ng g^{-1}]
C_1	2.4989	1.1529	79.72	69149.36	27671.96	41.47
C_2	2.1598	0.9706	49.35	50842.48	23540.18	34.09
C_3	2.1285	0.8444	38.54	45641.94	21442.79	29.29
C_4	2.0567	0.7215	31.89	44200.73	21491.28	25.66
C_5	2.0110	0.6725	28.22	41955.40	20863.11	23.02
C_6	2.0318	0.6200	24.71	39853.81	19615.35	20.19
C_7	2.0301	0.5886	22.21	37729.23	18584.59	17.33
C_8	2.0218	0.5636	20.53	36428.81	18018.05	15.76
C_9	2.0487	0.5157	17.31	33571.09	16386.25	13.29
C_10	2.0373	0.5240	17.59	33567.21	16476.13	12.79
C_11	2.0470	0.5079	16.20	31891.33	15579.19	11.32
C_12	2.0503	0.4652	12.94	27823.30	13570.32	8.73
C_13	2.0467	0.4849	13.35	27536.44	13453.99	8.48
C_14	2.0367	0.4572	11.23	24563.97	12060.89	6.95
C_15	2.0371	0.4465	10.35	23189.41	11383.82	6.50
C_16	2.0474	0.4427	10.14	22899.99	11184.93	6.32
C_17	2.0444	0.4262	9.14	21451.32	10492.89	5.52
C_18	2.0457	0.4399	9.00	20469.44	10006.15	6.47
C_19	2.0283	0.4413	9.06	20534.84	10124.40	5.14
C_20	2.0299	0.4197	7.71	18381.96	9055.44	4.33
C_21	2.1856	0.5574	7.55	18963.23	6200.34	2.55
C_22	2.1536	0.4818	5.10	14777.31	4917.24	1.35
C_23	2.0444	0.4471	4.34	13521.25	4745.02	0.94
C_24	2.0773	0.4509	3.93	12124.05	4194.15	0.88
C_25	2.0848	0.4265	3.30	10749.81	3712.51	0.55
C_26	2.0744	0.4181	3.40	11293.36	3916.67	0.48

C_27	2.1006	0.4170	2.63	8732.88	3005.26	0.17
C_28	2.0718	0.4030	3.57	12346.50	4281.24	0.53
C_29	2.0630	0.3923	2.93	10383.04	3626.10	0.19
C_30	2.1122	0.3954	2.62	9188.71	3141.51	0.22

leachate	Ca/P	Sr*1000/Ca	Sr [ng g^{-1}]	Ca [ng g^{-1}]	P [ng g^{-1}]	Ba [ng g^{-1}]
D_1	2.8443	2.2516	84.02	37314.34	13119.04	67.52
D_2	2.2765	1.9239	61.21	31816.98	13976.41	59.51
D_3	2.2118	1.7527	51.24	29237.30	13218.51	53.45
D_4	2.1947	1.6550	45.41	27435.78	12500.78	49.82
D_5	2.0782	1.6661	39.72	23842.34	11472.39	44.26
D_6	2.1002	1.5988	39.82	24904.75	11858.21	43.94
D_7	2.1049	1.5891	40.08	25223.54	11983.37	43.70
D_8	2.1162	1.5728	34.82	22135.37	10459.99	37.29
D_9	2.0984	1.5513	28.40	18306.41	8724.08	29.96
D_10	2.1029	1.5540	31.35	20173.11	9593.05	32.01
D_11	2.1137	1.5479	30.65	19801.90	9368.53	31.28
D_12	2.1267	1.5083	18.40	12196.47	5734.99	19.11
D_13	2.1256	1.5134	15.94	10531.40	4954.66	16.54
D_14	2.1172	1.5217	12.36	8125.29	3837.69	13.74
D_15	2.0979	1.4709	9.57	6509.07	3102.73	10.15
D_16	2.0869	1.5259	11.09	7265.68	3481.51	11.61
D_17	2.2417	1.4341	8.03	5597.38	2496.93	8.47
D_18	2.0812	1.5282	8.77	5738.81	2757.51	9.35
D_19	2.0898	1.5180	7.27	4786.45	2290.40	8.12
D_20	2.0285	1.4552	3.23	2216.46	1092.66	3.94
D_21	2.4133	1.5227	2.98	2658.40	810.78	2.17
D_22	2.2133	1.4524	2.46	2283.25	764.13	1.72
D_23	2.2023	1.4261	2.25	2122.77	716.39	1.46
D_24	2.1031	1.4589	2.41	2227.71	785.47	1.64
D_25	2.1148	1.3836	1.78	1709.94	607.90	1.06
D_26	2.1195	1.3547	1.51	1471.13	526.82	1.14
D_27	2.0766	1.3361	1.05	1008.33	380.01	0.51

D_28	2.2935	1.3802	3.01	2973.14	950.24	1.94
D_29	2.0522	1.3503	1.28	1234.21	462.41	0.63
D_30	2.4952	1.3462	1.44	1404.79	428.69	1.94

leachate	Ca/P	Sr*1000/Ca	Sr [ng g^{-1}]	Ca [ng g^{-1}]	P [ng g^{-1}]	Ba [ng g^{-1}]
E_1	2.7442	2.3104	124.92	54066.40	19701.82	159.21
E_2	2.2388	1.8153	91.03	50142.83	22396.92	128.92
E_3	2.1159	1.5324	67.69	44171.76	20875.88	98.88
E_4	2.1146	1.2721	53.46	42024.79	19873.55	78.88
E_5	2.0972	1.1755	46.02	39145.95	18665.87	65.66
E_6	2.1311	1.0745	42.42	39474.14	18522.97	57.06
E_7	2.1170	1.0189	37.05	36359.45	17174.91	47.39
E_8	2.1045	1.0113	40.64	40188.99	19096.47	49.94
E_9	2.1217	0.9521	31.59	33179.45	15638.29	37.95
E_10	2.1134	0.9386	30.83	32849.17	15543.07	35.92
E_11	2.1117	0.9122	28.20	30918.74	14641.93	31.51
E_12	2.1099	0.8728	21.91	25098.63	11895.86	24.27
E_13	2.1301	0.8838	26.97	30516.75	14326.47	28.22
E_14	2.1164	0.8316	22.14	26629.49	12582.23	22.05
E_15	2.1107	0.8742	23.37	26731.22	12664.34	23.42
E_16	2.1153	0.8383	20.46	24410.50	11539.82	20.30
E_17	2.1221	0.8224	17.51	21290.84	10032.98	17.06
E_18	2.1036	0.8293	12.71	15322.26	7283.84	12.28
E_19	2.1498	0.8481	15.32	18058.96	8400.29	14.23
E_20	2.1080	0.8158	9.97	12216.10	5795.18	9.37
E_21	2.3851	1.1209	10.53	13080.33	3939.29	7.63
E_22	2.1936	1.1149	10.89	13611.05	4454.33	23.99
E_23	2.1828	0.9132	8.91	13582.91	4467.26	6.42
E_24	2.1499	0.9149	7.43	11281.56	3778.23	5.52
E_25	2.1771	0.9331	6.80	10105.53	3348.81	5.08
E_26	2.1156	0.8925	8.24	12845.33	4362.55	6.05
E_27	2.1191	0.8520	4.48	7231.75	2480.95	2.90
E_28	2.1199	0.8760	5.05	7941.98	2717.02	3.52

E_29	2.1433	0.8678	4.59	7275.24	2467.25	3.24
E_30	2.1527	0.8177	4.57	7694.70	2594.34	3.07

leachate	Ca/P	Sr*1000/Ca	Sr [ng g^{-1}]	Ca [ng g^{-1}]	P [ng g^{-1}]	Ba [ng g^{-1}]
F_1	3.4551	0.7886	40.10	50849.40	14717.11	6.60
F_2	2.2786	0.6266	29.25	46675.85	20484.83	5.88
F_3	2.1948	0.5437	25.76	47375.17	21585.56	5.98
F_4	2.1657	0.4615	19.63	42532.67	19639.05	5.85
F_5	2.1617	0.4321	17.24	39900.70	18457.90	5.72
F_6	2.0928	0.3810	12.96	34030.22	16260.41	4.98
F_7	2.0921	0.3868	10.81	27955.64	13362.56	4.29
F_8	2.1619	0.4052	15.50	38247.65	17691.78	5.92
F_9	2.1013	0.3758	12.14	32314.53	15378.50	5.04
F_10	2.1030	0.3562	10.00	28075.59	13350.26	4.05
F_11	2.1063	0.3368	7.29	21638.10	10272.88	3.04
F_12	2.0962	0.3171	3.34	10519.52	5018.40	1.40
F_13	2.1006	0.3215	3.25	10114.34	4815.09	1.39
F_14	2.0963	0.3264	3.46	10600.51	5056.65	1.45
F_15	2.0899	0.3178	3.36	10570.33	5057.77	1.50
F_16	2.0570	0.2838	1.40	4922.79	2393.23	0.71
F_17	2.2139	0.3108	1.87	6004.65	2712.22	0.85
F_18	2.0502	0.2643	0.99	3737.97	1823.23	0.66
F_19	2.0761	0.3011	1.89	6286.54	3028.07	0.97
F_20	2.0549	0.2629	1.06	4044.06	1967.99	0.92
F_21	2.2250	0.3220	0.91	3843.92	1268.92	b.d.
F_22	2.1296	0.3114	0.67	2874.99	1003.86	b.d.
F_23	2.1221	0.2740	0.53	2570.03	905.72	b.d.
F_24	2.1264	0.2949	0.54	2447.65	863.14	b.d.
F_25	2.0310	0.2572	0.33	1680.26	636.35	b.d.
F_26	2.0838	0.3950	0.42	1355.05	509.80	b.d.
F_27	2.0124	0.2322	0.28	1541.71	593.52	b.d.
F_28	2.0883	0.2631	0.38	1915.67	698.65	b.d.
F_29	2.0052	0.2338	0.25	1360.06	531.56	b.d.

F_30	1.9929	0.2650	0.33	1592.29	617.31	b.d.

leachate	Ca/P	Sr*1000/Ca	Sr [ng/g]	Ca [ng g^{-1}]	P [ng g^{-1}]
G_1	8.3073	3.3101	221.72	66984.45	8063.35
G_2	2.6954	2.6280	135.51	51561.60	19129.43
G_3	2.4189	2.2676	106.26	46861.03	19373.11
G_4	2.3321	2.0588	89.25	43350.45	18588.68
G_5	2.2740	1.7368	69.49	40012.33	17595.87
G_6	2.1570	1.4314	37.92	26494.90	12283.44
G_7	2.1783	1.4795	42.73	28881.77	13258.89
G_8	2.3012	1.7872	68.50	38325.92	16654.65
G_9	2.2488	1.6579	61.90	37336.08	16603.02
G_10	2.1064	1.4071	38.16	27120.80	12875.69
G_11	2.1311	1.2574	18.57	14767.56	6929.45
G_12	2.2735	1.2858	11.06	8598.84	3782.21
G_13	2.1400	1.3227	8.26	6245.80	2918.65
G_14	2.1565	1.2879	9.61	7462.11	3460.35
G_15	2.0850	1.2192	8.22	6739.57	3232.45
G_16	2.1220	1.1728	4.01	3421.54	1612.38
G_17	2.0778	1.2110	4.70	3884.00	1869.27
G_18	2.1357	1.1647	4.72	4053.08	1897.74
G_19	2.0684	1.1668	4.37	3742.58	1809.43
G_20	2.0529	1.1998	3.22	2687.94	1309.31
G_21	2.2520	1.1432	3.61	4321.41	1402.43
G_22	2.1882	1.0645	2.44	3095.24	1046.83
G_23	2.1626	1.0968	1.39	1646.69	585.30
G_24	2.0682	1.0957	1.23	1439.79	541.23
G_25	2.0903	1.0864	1.10	1286.68	483.68
G_26	2.0268	1.0856	1.15	1350.33	521.05
G_27	2.0155	1.0799	0.95	1102.37	436.93
G_28	2.0478	1.0373	0.93	1124.49	437.68
G_29	2.2390	1.0196	1.09	1366.50	476.77
G_30	1.9172	1.0160	0.90	1107.01	461.04

leachate	Ca/P	Sr*1000/Ca	Sr [ng/g]	Ca [ng g^{-1}]	P [ng g^{-1}]	Ba [ng g^{-1}]
H_1	3.6420	1.8673	101.94	54590.96	14989.27	43.44
H_2	2.5268	1.6070	72.03	44822.19	17738.63	41.65
H_3	2.3283	1.3471	55.36	41097.98	17651.43	40.41
H_4	2.2541	1.1490	43.89	38201.67	16947.51	37.28
H_5	2.1467	1.0135	32.76	32321.72	15056.29	32.48
H_6	2.1403	0.9849	30.95	31425.51	14682.42	30.64
H_7	2.2358	0.9291	26.28	28290.95	12653.51	25.65
H_8	2.1662	0.9215	22.46	24371.30	11250.88	22.17
H_9	2.1740	0.9265	25.34	27355.08	12582.93	24.98
H_10	1.7716	0.8047	0.40	494.91	279.36	1.03
H_11	2.2270	0.8484	35.89	42302.24	18994.75	34.46
H_12	2.1444	0.8094	8.66	10701.83	4990.52	8.11
H_13	2.1497	0.8137	8.24	10127.19	4710.87	7.62
H_14	2.1565	0.8403	11.12	13231.13	6135.34	9.87
H_15	2.1517	0.8635	8.57	9927.64	4613.87	7.48
H_16	2.1733	0.7979	4.57	5722.48	2633.05	4.23
H_17	2.1558	0.8331	6.62	7939.87	3683.03	6.06
H_18	2.1356	0.8591	4.54	5285.43	2474.87	4.17
H_19	2.0858	0.8582	3.53	4112.72	1971.73	3.34
H_20	2.0845	0.8427	4.19	4969.30	2383.99	3.95
H_21	2.6129	1.0441	3.03	3984.00	1112.48	1.47
H_22	2.2811	0.9649	2.35	3313.34	1066.31	0.98
H_23	2.1802	0.8734	2.00	3110.36	1049.78	0.93
H_24	2.1525	0.8829	2.50	3877.57	1315.43	1.21
H_25	2.1212	0.8435	1.93	3106.10	1077.56	0.83
H_26	2.1520	0.8238	1.95	3221.24	1099.95	0.89
H_27	2.0685	0.8102	1.05	1710.35	627.57	0.22
H_28	2.1188	0.8310	1.50	2427.30	852.10	0.54
H_29	2.1373	0.8156	1.45	2381.85	829.65	0.47
H_30	2.3316	0.8095	1.87	3136.71	989.58	0.71

leachate	Ca/P	Sr*1000/Ca	Sr [ng g^{-1}]	Ca [ng g^{-1}]	P [ng g^{-1}]	Ba [ng g^{-1}]
l_1	42.8473	2.4873	489.35	196739.96	4591.65	260.84
l_2	9.7037	2.3583	328.28	139202.42	14345.36	212.73
l_3	6.7785	2.2738	362.54	159440.19	23521.60	261.88
l_4	3.7623	2.2417	203.58	90815.49	24138.11	169.04
l_5	2.8032	2.2307	225.40	101043.60	36045.62	206.36
l_6	2.6109	2.2393	205.61	91817.13	35167.31	202.36
l_7	2.5231	2.2302	161.75	72526.22	28745.11	166.44
l_8	2.4226	2.1662	170.10	78524.32	32413.67	182.36
l_9	2.3750	2.1080	166.81	79134.73	33320.58	183.26
l_10	2.3529	2.0147	165.78	82283.16	34971.19	187.78
l_11	2.3047	1.9415	143.02	73663.05	31962.19	168.07
l_12	2.2759	1.8783	131.40	69956.29	30737.66	160.61
l_13	2.2327	1.8335	119.41	65125.79	29169.59	149.38
l_14	2.2489	1.7755	116.84	65807.41	29262.26	146.72
l_15	2.2200	1.7001	103.22	60710.97	27346.94	132.97
l_16	2.2141	1.6799	102.71	61140.91	27614.20	133.26
l_17	2.2267	1.6058	91.88	57219.77	25696.84	119.53
l_18	2.2083	1.6100	89.01	55287.23	25035.88	115.26
l_19	2.2112	1.5658	86.23	55070.24	24904.77	110.78
l_20	2.1881	1.5645	87.76	56094.32	25635.66	111.14
l_21	2.8838	1.5283	66.49	61171.76	15086.09	62.24
l_22	2.4739	1.4563	61.53	59398.15	17077.93	59.06
l_23	2.3384	1.3778	52.84	53889.11	16401.22	53.12
l_24	2.2785	1.3433	55.61	58191.57	18167.90	55.35
l_25	2.2626	1.3140	48.04	51352.95	16157.19	49.59
l_26	2.2119	1.3145	51.53	55095.20	17724.54	51.28
l_27	2.2253	1.2718	47.41	52374.56	16753.10	47.81
l_28	2.2054	1.2751	50.77	55962.18	18054.70	50.85
l_29	2.2272	1.2352	44.79	50932.16	16280.48	44.31
l_30	2.2198	1.2294	44.33	50647.48	16244.09	43.01

leachate	Ca/P	Sr*1000/Ca	Sr [ng g^{-1}]	Ca [ng g^{-1}]	P [ng g^{-1}]	Ba [ng g^{-1}]
J_1	3.1970	1.5895	109.55	68922.25	21558.21	8.84
J_2	2.2721	1.4699	84.45	57456.09	25287.12	9.89
J_3	2.1777	1.3516	67.28	49775.44	22857.17	9.41
J_4	2.1475	1.2184	51.73	42455.22	19769.18	10.37
J_5	2.1587	1.2327	53.23	43182.82	20004.14	10.25
J_6	2.1661	1.1647	48.03	41241.20	19038.97	10.37
J_7	2.1604	1.1502	43.05	37424.87	17323.29	9.73
J_8	2.0647	1.1209	37.90	33810.80	16375.44	8.85
J_9	2.0607	1.1286	37.96	33637.97	16323.92	8.26
J_10	2.0601	1.1181	40.84	36531.36	17732.49	8.96
J_11	2.0796	1.0520	19.93	18941.91	9108.53	4.92
J_12	2.0759	1.0777	20.76	19258.66	9277.24	5.26
J_13	2.1341	1.0310	18.50	17944.03	8408.10	4.20
J_14	2.2631	1.0108	17.66	17469.51	7719.40	3.93
J_15	2.1186	1.0032	12.93	12886.03	6082.40	3.03
J_16	2.0704	0.9968	11.29	11322.94	5468.85	2.62
J_17	2.0322	0.9311	4.42	4744.13	2334.44	1.19
J_18	2.0847	0.9639	9.00	9340.06	4480.27	1.99
J_19	2.2411	1.1732	12.20	10398.31	4639.91	6.05
J_20	2.0633	0.9313	7.51	8068.55	3910.43	1.43
J_21	2.1781	0.8072	1.87	3132.09	1062.71	b.d.
J_22	2.0981	0.8003	2.03	3450.12	1210.47	b.d.
J_23	2.0371	0.7938	1.84	3143.48	1140.22	b.d.
J_24	1.9980	0.7516	1.33	2365.45	887.03	b.d.
J_25	1.9760	0.7317	0.93	1659.08	643.95	b.d.
J_26	1.9761	0.7757	2.02	3534.23	1315.34	b.d.
J_27	1.9725	0.7352	0.94	1658.64	644.96	b.d.
J_28	1.9520	0.7765	1.49	2580.99	986.04	b.d.
J_29	1.9865	0.7349	1.14	2060.63	783.58	b.d.
J_30	1.8912	0.7010	0.65	1174.09	491.39	b.d.

leachate	Ca/P	Sr*1000/Ca	Sr [ng g^{-1}]	Ca [ng g^{-1}]	P [ng g^{-1}]	Ba [ng g^{-1}]
K_1	2.9697	1.3366	200.15	149747.85	50424.61	101.25
K_2	2.2241	1.0851	127.39	117401.00	52785.67	84.26
K_3	2.1476	0.9528	102.89	107989.84	50283.99	73.17
K_4	2.1449	0.8421	77.77	92357.35	43059.89	57.75
K_5	2.1083	0.8037	70.72	87998.01	41738.52	50.68
K_6	2.0997	0.7735	55.78	72113.19	34344.37	40.39
K_7	2.0980	0.7519	43.23	57496.14	27405.22	30.87
K_8	2.1394	0.7404	48.51	65510.60	30621.42	32.97
K_9	2.1846	0.7378	46.18	62601.38	28655.89	29.59
K_10	2.1227	0.7564	43.80	57907.18	27280.21	27.41
K_11	2.1064	0.7117	29.30	41175.27	19547.84	18.36
K_12	2.1001	0.7273	32.63	44868.50	21364.63	20.63
K_13	2.0754	0.6948	21.75	31302.11	15082.23	13.17
K_14	2.1041	0.7421	30.86	41583.44	19762.78	19.07
K_15	2.0864	0.7209	27.72	38450.43	18428.66	16.99
K_16	2.0584	0.7237	26.07	36030.01	17503.79	15.92
K_17	2.0766	0.7138	24.54	34371.18	16551.69	14.85
K_18	2.0750	0.7172	22.77	31741.03	15297.03	14.02
K_19	2.0831	0.7444	25.70	34529.03	16575.91	15.74
K_20	2.0858	0.7193	21.71	30178.24	14468.32	13.70
K_21	2.9399	1.0581	24.25	31975.06	7795.01	9.11
K_22	2.4025	0.9410	23.37	34681.61	10335.85	10.01
K_23	2.3146	0.8441	15.56	25647.72	7966.85	6.09
K_24	2.2629	0.8457	15.07	24777.62	7876.49	5.67
K_25	2.2261	0.8137	12.86	21920.63	7098.64	5.15
K_26	2.1477	0.7891	11.59	20351.81	6841.17	4.23
K_27	2.1525	0.7450	11.17	20781.76	6967.20	4.03
K_28	2.1208	0.7496	16.08	29911.48	10117.27	7.08
K_29	2.1122	0.6947	13.30	26637.59	9061.73	4.68
K_30	2.1442	0.6704	10.90	22556.87	7579.74	3.67

leachate	Ca/P	Sr*1000/Ca	Sr [ng g^{-1}]	Ca [ng g^{-1}]	P [ng g^{-1}]	Ba [ng g^{-1}]
L_1	4.0887	2.4726	53.82	21765.74	5323.35	32.57
L_2	2.4417	1.9740	33.84	17141.90	7020.40	32.29
L_3	2.2469	1.6668	24.56	14735.63	6558.31	30.71
L_4	2.0115	1.3645	18.31	13417.49	6670.27	29.37
L_5	2.0581	1.3154	16.65	12658.52	6150.71	27.71
L_6	1.9897	1.2035	11.14	9257.60	4652.72	20.80
L_7	1.9619	1.1214	7.00	6245.52	3183.39	13.45
L_8	1.9784	1.1403	5.89	5169.58	2613.06	11.16
L_9	1.9888	1.1155	5.20	4662.91	2344.57	10.02
L_10	1.9769	1.1731	3.45	2943.11	1488.73	7.04
L_11	1.9803	1.1530	2.82	2444.43	1234.36	5.80
L_12	1.9771	1.3397	2.41	1796.53	908.68	4.88
L_13	1.9133	1.1173	1.21	1086.16	567.67	2.89
L_14	1.9281	1.1524	1.37	1186.65	615.46	3.15
L_15	1.9186	1.0904	1.35	1234.29	643.32	3.15
L_16	1.8986	1.0506	0.97	920.75	484.97	2.48
L_17	1.8459	1.0444	0.98	939.19	508.81	2.51
L_18	1.8991	1.0400	0.78	751.41	395.66	2.03
L_19	1.9096	1.0489	0.90	860.29	450.51	2.50
L_20	1.8588	0.8956	0.47	522.43	281.05	1.35
L_21	2.3362	1.3593	0.89	845.65	281.73	1.28
L_22	2.1642	1.1669	0.70	767.12	278.45	0.88
L_23	2.0708	1.1411	0.57	616.04	239.38	0.70
L_24	2.1807	1.3444	2.44	2483.93	833.39	3.42
L_25	1.9298	1.0708	0.37	408.27	180.69	0.38
L_26	1.9668	1.0136	0.38	442.67	189.68	0.42
L_27	1.8751	0.9540	0.28	334.33	158.07	0.21
L_28	1.9306	1.0189	0.43	510.88	218.23	0.49
L_29	2.4095	0.8926	0.34	453.26	157.93	0.30
L_30	1.7845	1.0155	0.29	314.98	158.43	0.27

leachate	Ca/P	Sr*1000/Ca	Sr [ng g^{-1}]	Ca [ng g^{-1}]	P [ng g^{-1}]	Ba [ng g^{-1}]
M_1	4.2236	0.6346	12.62	19883.79	4707.78	2.94
M_2	2.4485	0.4713	8.38	17781.90	7262.33	3.67
M_3	1.8958	0.4217	6.19	14675.63	7741.26	3.20
M_4	1.9548	0.3980	5.24	13156.23	6730.12	2.82
M_5	1.9501	0.3984	4.92	12349.97	6333.00	2.76
M_6	2.0171	0.4006	4.38	10938.87	5423.09	2.39
M_7	1.9905	0.4021	3.85	9581.46	4813.62	1.90
M_8	2.0107	0.4052	3.32	8185.18	4070.76	1.39
M_9	1.9871	0.4134	3.27	7901.24	3976.24	1.28
M_10	1.9667	0.4257	2.96	6943.04	3530.36	1.00
M_11	2.0485	0.4869	2.54	5219.23	2547.84	0.75
M_12	2.0019	0.5056	3.01	5949.79	2972.11	1.13
M_13	2.0086	0.4980	2.75	5523.42	2749.91	1.05
M_14	2.0128	0.4794	2.58	5386.23	2675.98	0.94
M_15	2.0110	0.4596	2.08	4519.72	2247.51	0.62
M_16	2.0209	0.4373	1.93	4417.66	2186.01	0.53
M_17	1.9897	0.4329	1.74	4022.14	2021.51	0.46
M_18	2.0252	0.4185	1.54	3685.81	1820.02	0.33
M_19	2.0183	0.3918	1.39	3553.74	1760.75	0.26
M_20	2.0700	0.3926	1.38	3524.86	1702.80	0.24

leachate	Ca/P	Sr*1000/Ca	Sr [ng g^{-1}]	Ca [ng g^{-1}]	P [ng g^{-1}]	Ba [ng g^{-1}]
N_1	2.5750	0.4271	16.31	38180.12	14827.46	5.30
N_2	1.9763	0.3333	9.63	28899.94	14623.08	5.32
N_3	1.9974	0.3092	7.42	23994.58	12012.90	4.09
N_4	2.0029	0.2993	6.23	20827.68	10398.73	3.04
N_5	2.0358	0.2859	4.82	16870.15	8286.86	1.94
N_6	2.0349	0.2961	4.38	14777.90	7262.14	1.63
N_7	1.9953	0.2997	3.72	12428.15	6228.82	1.36
N_8	1.9965	0.3159	3.34	10573.15	5295.87	1.01
N_9	2.0317	0.3348	3.52	10509.68	5172.91	1.22
N_10	2.0279	0.3226	3.19	9886.36	4875.10	0.95

N_11	2.0645	0.4919	3.43	6975.58	3378.83	2.06
N_12	2.0288	0.3666	2.87	7837.05	3862.81	1.55
N_13	2.0180	0.3522	2.25	6402.06	3172.40	1.51
N_14	2.0211	0.3285	2.05	6235.42	3085.15	0.72
N_15	2.0675	0.3448	3.31	9604.12	4645.37	1.21
N_16	2.0482	0.3389	2.03	5977.92	2918.59	0.55
N_17	2.0119	0.3149	1.60	5065.70	2517.86	0.20
N_18	2.0219	0.2952	1.25	4239.97	2097.06	0.04
N_19	2.0454	0.2926	1.30	4431.93	2166.74	0.00
N_20	2.0210	0.2917	1.31	4480.48	2216.93	0.01

7.2.1.2. $^{87}Sr/^{86}Sr$ ratios

leached fraction	$^{87}Sr/^{86}Sr$	Stddev	leached fraction	$^{87}Sr/^{86}Sr$	Stddev	leached fraction	$^{87}Sr/^{86}Sr$	Stddev	leached fraction	$^{87}Sr/^{86}Sr$	Stddev
A_Fr_1	0.7176	0.00001	B_Fr_1	0.7153	0.00001	C_Fr_1	0.7164	0.00001	D_Fr_1	0.7153	0.00001
A_Fr_2	0.7174	0.00001	B_Fr_2	0.7143	0.00001	C_Fr_2	0.7160	0.00001	D_Fr_2	0.7151	0.00001
A_Fr_3	0.7173	0.00001	B_Fr_3	0.7132	0.00001	C_Fr_3	0.7157	0.00001	D_Fr_3	0.7150	0.00001
A_Fr_4	0.7168	0.00001	B_Fr_4	0.7124	0.00001	C_Fr_4	0.7154	0.00001	D_Fr_4	0.7151	0.00001
A_Fr_5	0.7166	0.00001	B_Fr_5	0.7121	0.00001	C_Fr_5	0.7151	0.00001	D_Fr_5	0.7150	0.00001
A_Fr_6	0.7165	0.00001	B_Fr_6	0.7121	0.00001	C_Fr_6	0.7148	0.00001	D_Fr_6	0.7151	0.00001
A_Fr_7	0.7164	0.00001	B_Fr_7	0.7119	0.00001	C_Fr_7	0.7148	0.00001	D_Fr_7	0.7151	0.00001
A_Fr_8	0.7166	0.00003	B_Fr_8	0.7139	0.00002	C_Fr_8	0.7152	0.00002	D_Fr_8	0.7150	0.00002
A_Fr_9	0.7165	0.00003	B_Fr_9	0.7133	0.00003	C_Fr_9	0.7151	0.00002	D_Fr_9	0.7150	0.00002
A_Fr_10	0.7164	0.00003	B_Fr_10	0.7130	0.00002	C_Fr_10	0.7147	0.00002	D_Fr_10	0.7149	0.00003
A_Fr_11	0.7165	0.00004	B_Fr_11	0.7127	0.00001	C_Fr_11	0.7145	0.00002	D_Fr_11	0.7152	0.00002
A_Digest	0.7157	0.00001	B_Digest	0.7125	0.00002	C_Digest	0.7146	0.00001	D_digest	0.7151	0.00001

leached fraction	$^{87}Sr/^{86}Sr$	Stddev	leached fraction	$^{87}Sr/^{86}Sr$	Stddev	leached fraction	$^{87}Sr/^{86}Sr$	Stddev	leached fraction	$^{87}Sr/^{86}Sr$	Stddev
E_Fr_1	0.7180	0.00001	F_Fr_1	0.7136	0.00001	G_Fr_1	0.7164	0.00001	H_Fr_1	0.7161	0.00001
E_Fr_2	0.7175	0.00002	F_Fr_2	0.7129	0.00002	G_Fr_2	0.7160	0.00001	H_Fr_2	0.7156	0.00001
E_Fr_3	0.7171	0.00001	F_Fr_3	0.7121	0.00001	G_Fr_3	0.7157	0.00001	H_Fr_3	0.7152	0.00001
E_Fr_4	0.7167	0.00002	F_Fr_4	0.7119	0.00002	G_Fr_4	0.7154	0.00001	H_Fr_4	0.7149	0.00002
E_Fr_5	0.7167	0.00001	F_Fr_5	0.7118	0.00001	G_Fr_5	0.7152	0.00001	H_Fr_5	0.7147	0.00001
E_Fr_6	0.7167	0.00002	F_Fr_6	0.7118	0.00001	G_Fr_6	0.7150	0.00001	H_Fr_6	0.7147	0.00001
E_Fr_7	0.7167	0.00001	F_Fr_7	0.7122	0.00002	G_Fr_7	0.7148	0.00002	H_Fr_7	0.7146	0.00001
E_Fr_8	0.7169	0.00001	F_Fr_8	-	-	G_Fr_8	0.7144	0.00001	H_Fr_8	0.7152	0.00001
E_Fr_9	0.7166	0.00001	F_Fr_9	0.7119	0.00003	G_Fr_9	-	-	H_Fr_9	0.7150	0.00001
E_Fr_10	0.7165	0.00001	F_Fr_10	0.7117	0.00005	G_Fr_10	-	-	H_Fr_10	0.7148	0.00001
E_Fr_11	0.7167	0.00002	F_Fr_11	0.7124	0.00007	G_Fr_11	-	-	H_Fr_11	0.7149	0.00001
E_Digest	0.7165	0.00001	F_Digest	0.7147	0.00001	G_Digest	0.7147	0.00001	H_Digest	0.7147	0.00001

leached fraction	$^{87}Sr/^{86}Sr$	Stddev	leached fraction	$^{87}Sr/^{86}Sr$	Stddev	leached fraction	$^{87}Sr/^{86}Sr$	Stddev	leached fraction	$^{87}Sr/^{86}Sr$	Stddev
I_Fr_1	0.7164	0.00001	J_Fr_1	0.7137	0.00001	K_Fr_1	0.7155	0.00005	L_Fr_1	0.7161	0.00001
I_Fr_2	0.7162	0.00001	J_Fr_2	0.7134	0.00001	K_Fr_2	0.7152	0.00001	L_Fr_2	0.7157	0.00001
I_Fr_3	0.7160	0.00001	J_Fr_3	0.7133	0.00001	K_Fr_3	0.7147	0.00001	L_Fr_3	0.7151	0.00001
I_Fr_4	0.7157	0.00001	J_Fr_4	0.7133	0.00001	K_Fr_4	0.7146	0.00001	L_Fr_4	0.7151	0.00001
I_Fr_5	0.7153	0.00001	J_Fr_5	0.7131	0.00001	K_Fr_5	0.7141	0.00003	L_Fr_5	0.7152	0.00002
I_Fr_6	0.7150	0.00001	J_Fr_6	0.7131	0.00001	K_Fr_6	0.7144	0.00001	L_Fr_6	0.7151	0.00001
I_Fr_7	0.7148	0.00001	J_Fr_7	0.7130	0.00001	K_Fr_7	0.7144	0.00001	L_Fr_7	0.7150	0.00001
I_Fr_8	0.7150	0.00001	J_Fr_8	-	-	K_Fr_8	0.7154	0.00000	L_Fr_8	0.7153	0.00002
I_Fr_9	0.7148	0.00001	J_Fr_9	0.7117	0.00004	K_Fr_9	0.7150	0.00001	L_Fr_9	0.7154	0.00001
I_Fr_10	0.7146	0.00000	J_Fr_10	0.7120	0.00002	K_Fr_10	0.7150	0.00001	L_Fr_10	0.7152	0.00003
I_Fr_11	0.7144	0.00001	J_Fr_11	0.7128	0.00001	K_Fr_11	0.7147	0.00000	L_Fr_11	0.7152	0.00003
I_Fr_Digest	0.7143	0.00001	J_Digest	0.7128	0.00001	K_Digest	0.7141	0.00002	L_Digest	0.7150	0.00001

leached fraction	$^{87}Sr/^{86}Sr$	Stddev	leached fraction	$^{87}Sr/^{86}Sr$	Stddev
M_Fr_1	0.7158	0.00001	N_Fr_1	0.7123	0.00001
M_Fr_2	0.7157	0.00001	N_Fr_2	0.712	0.00001
M_Fr_3	0.7157	0.00001	N_Fr_3	0.7121	0.00001
M_Fr_4	0.7158	0.00001	N_Fr_4	0.7128	0.00001
M_Fr_5	0.7161	0.00001	N_Fr_5	0.7137	0.00002
M_Fr_6	0.7159	0.00001	N_Fr_6	0.7126	0.00001
M_Fr_7	0.7157	0.00003	N_Fr_7	0.7125	0.00002
M_Digest	0.7154	0.00001	N_Digest	0.7106	0.00001

7.2.1.3 Figures of leached hard tissues

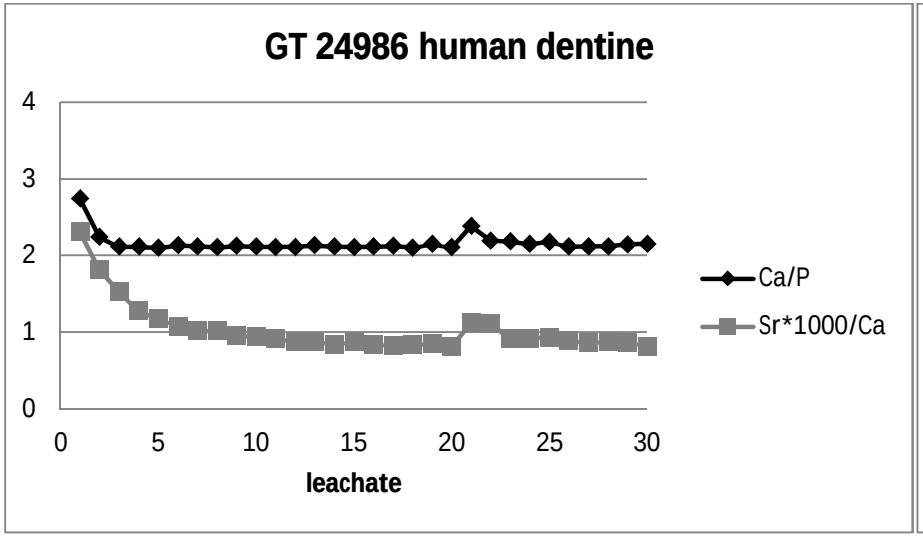

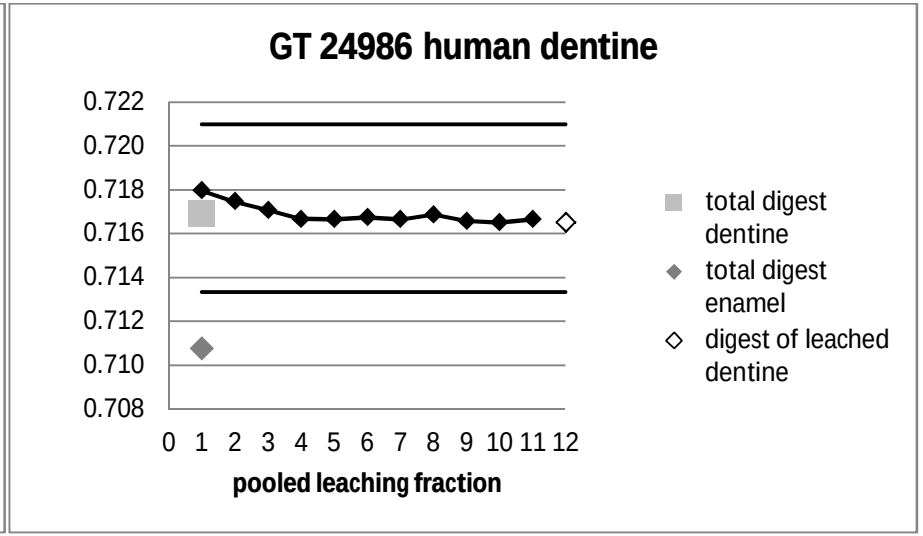

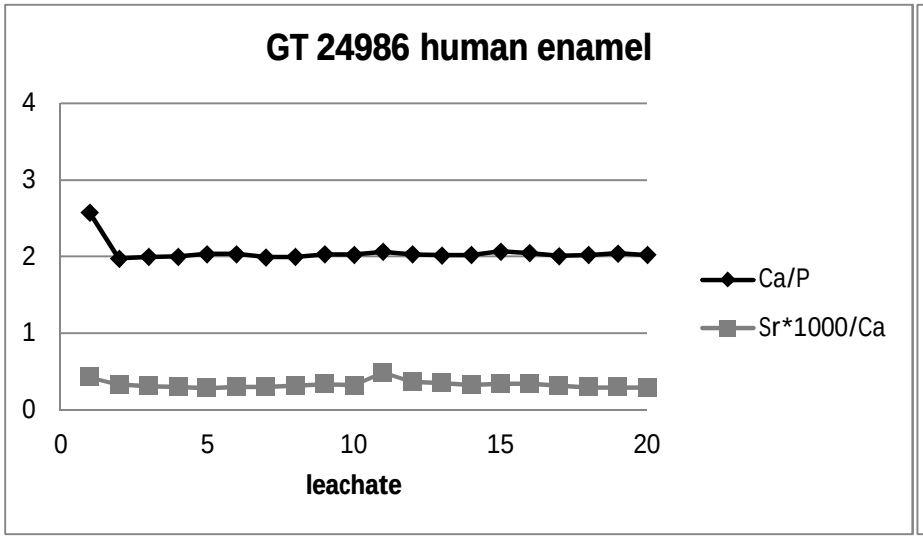
GT 24986 human enamel
4
3
2
1
0
0
5
10
15
20
leachate
Ca/P
Sr*1000/Ca

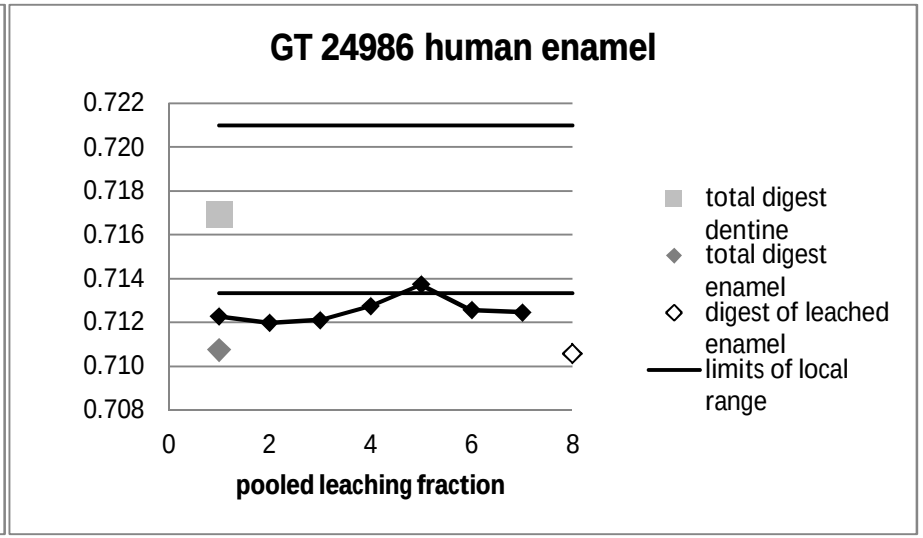
GT 24986 human enamel
0.722
0.720
0.718
0.716
0.714
0.712
0.710
0.708
0
2
4
6
8
pooled leaching fraction
total digest dentine
total digest enamel
digest of leached enamel
limits of local range

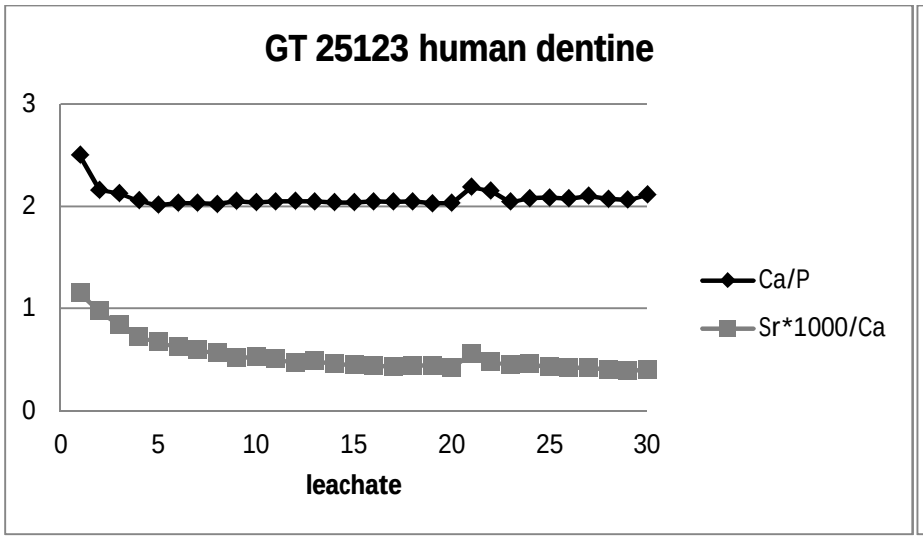
GT 25123 human dentine
3
2
1
0
0
5
10
15
20
25
30
leachate
Ca/P
Sr*1000/Ca

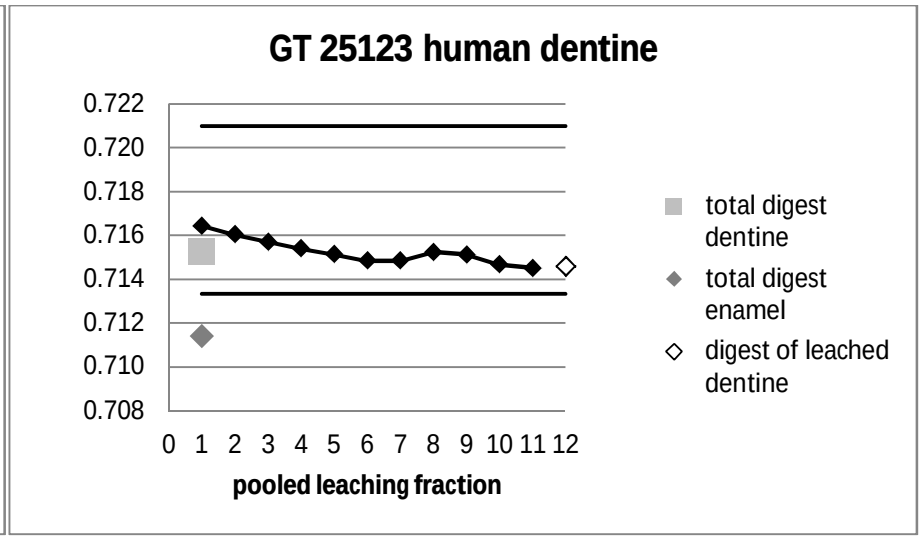
GT 25123 human dentine
0.722
0.720
0.718
0.716
0.714
0.712
0.710
0.708
0 1 2 3 4 5 6 7 8 9 10 11 12
pooled leaching fraction
total digest dentine
total digest enamel
digest of leached dentine

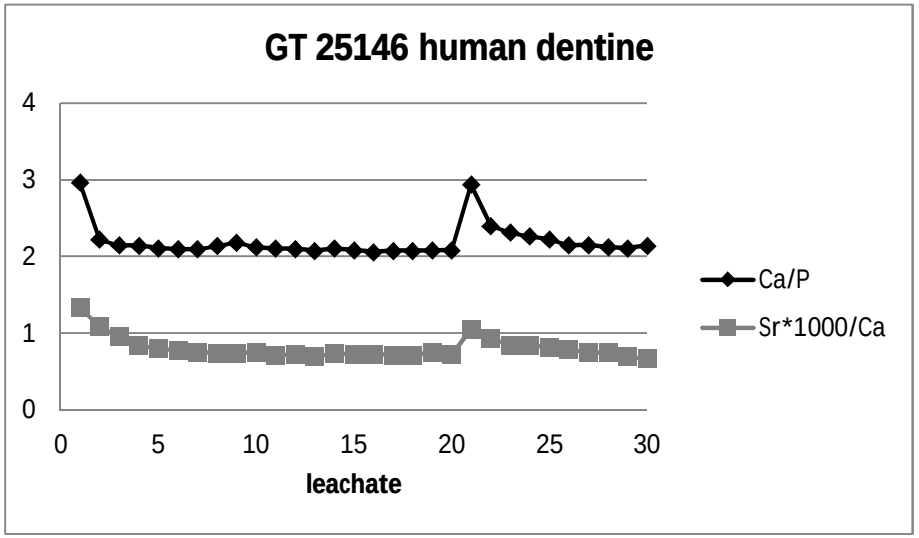
GT 25146 human dentine
4
3
2
1
0
0
5
10
15
20
25
30
leachate
Ca/P
Sr*1000/Ca

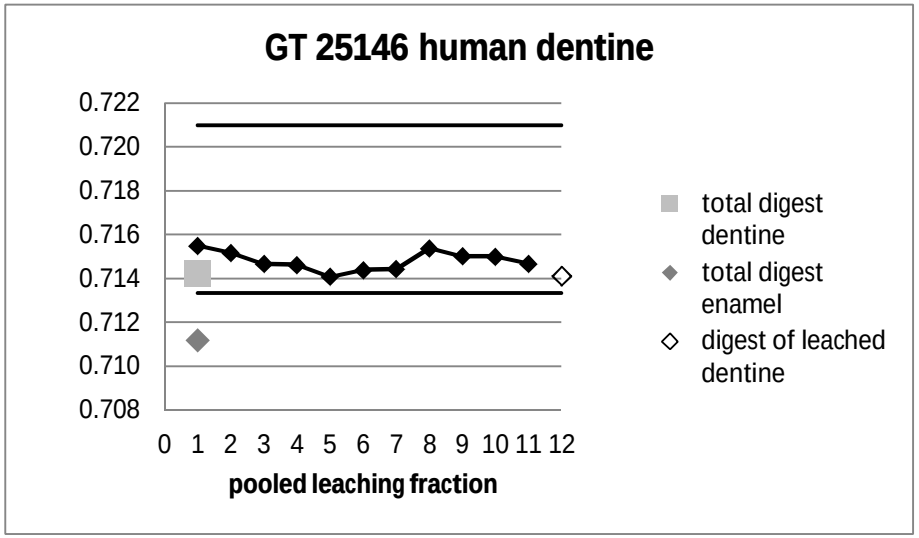
GT 25146 human dentine
0.722
0.720
0.718
0.716
0.714
0.712
0.710
0.708
0 1 2 3 4 5 6 7 8 9 10 11 12
pooled leaching fraction
total digest dentine
total digest enamel
digest of leached dentine

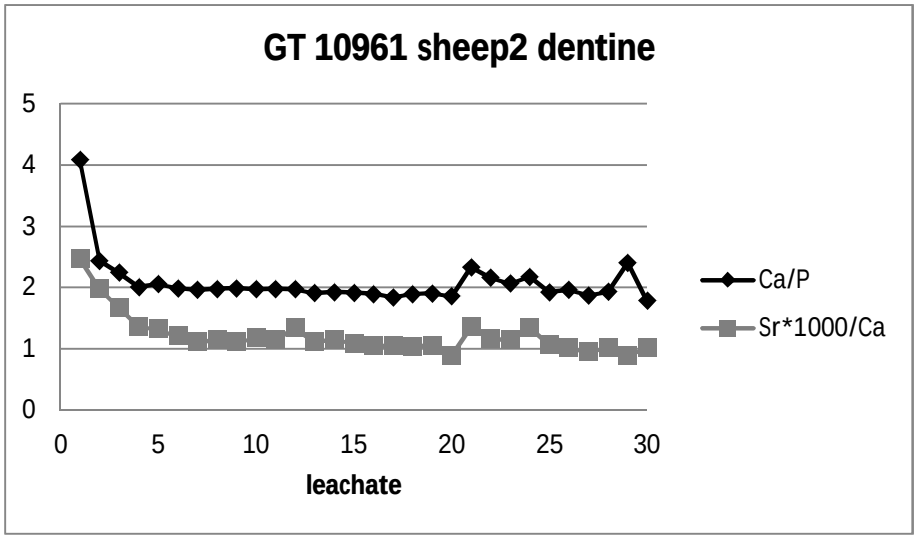
GT 10961 sheep2 dentine
5
4
3
2
1
0
0
5
10
15
20
25
30
leachate
Ca/P
Sr*1000/Ca

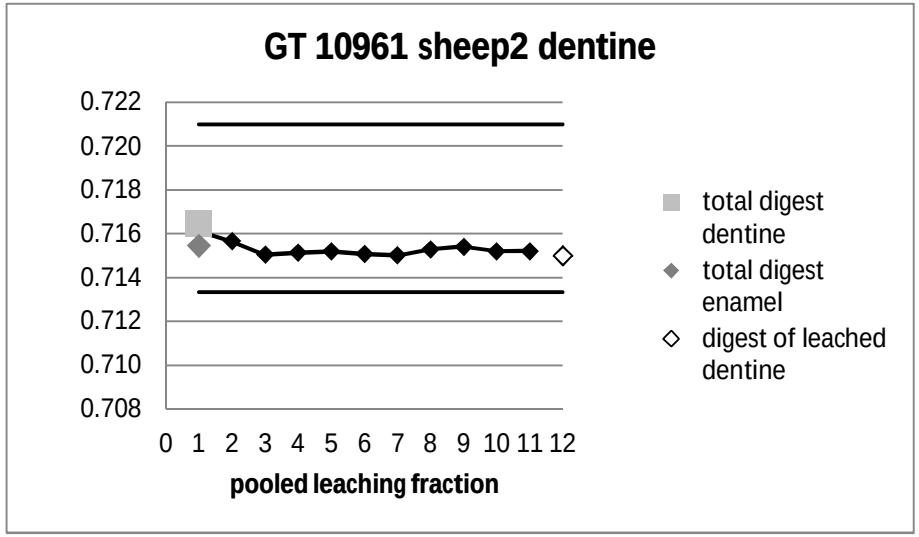
GT 10961 sheep2 dentine
0.722
0.720
0.718
0.716
0.714
0.712
0.710
0.708
0 1 2 3 4 5 6 7 8 9 10 11 12
pooled leaching fraction
total digest dentine
total digest enamel
digest of leached dentine

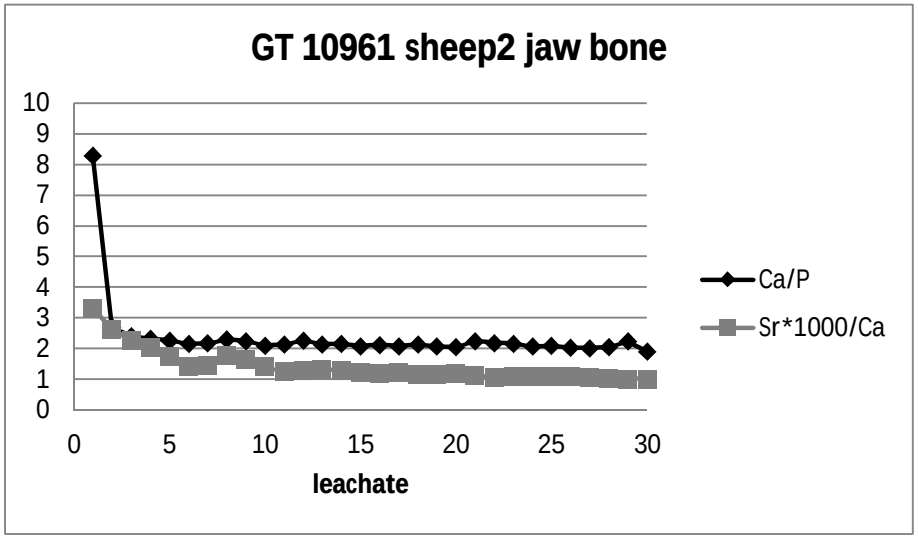
GT 10961 sheep2 jaw bone
10
9
8
7
6
5
4
3
2
1
0
0
5
10
15
20
25
30
leachate
Ca/P
Sr*1000/Ca

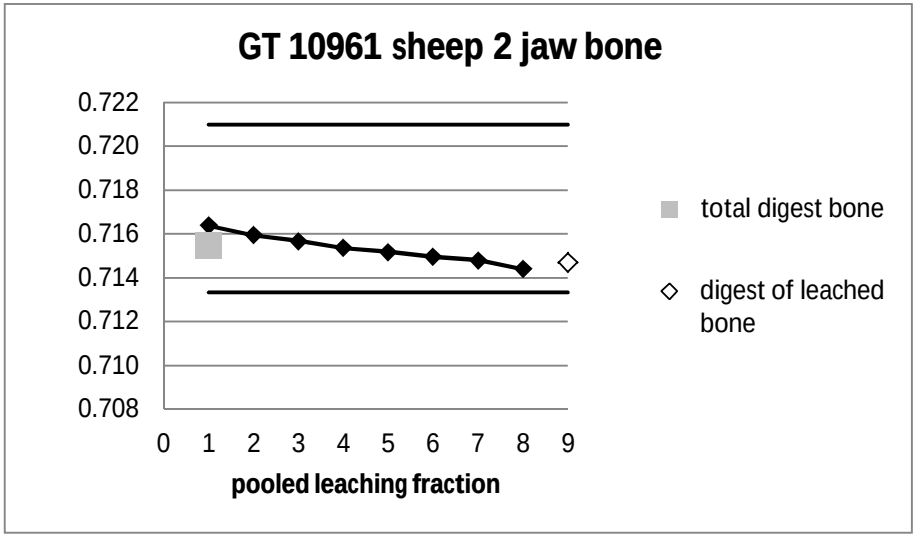
GT 10961 sheep 2 jaw bone
0.722
0.720
0.718
0.716
0.714
0.712
0.710
0.708
0 1 2 3 4 5 6 7 8 9
pooled leaching fraction
total digest bone
digest of leached bone

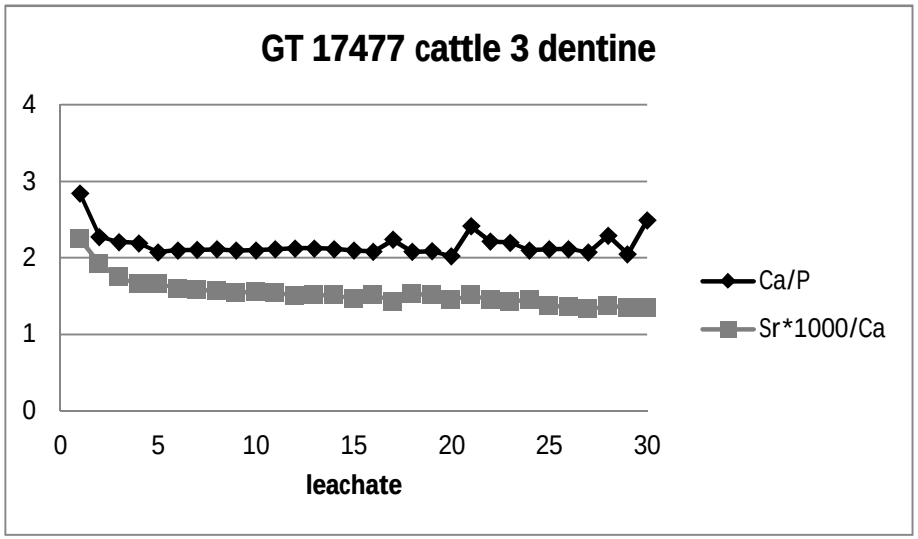
GT 17477 cattle 3 dentine
4
3
2
1
0
0
5
10
15
20
25
30
leachate
Ca/P
Sr*1000/Ca

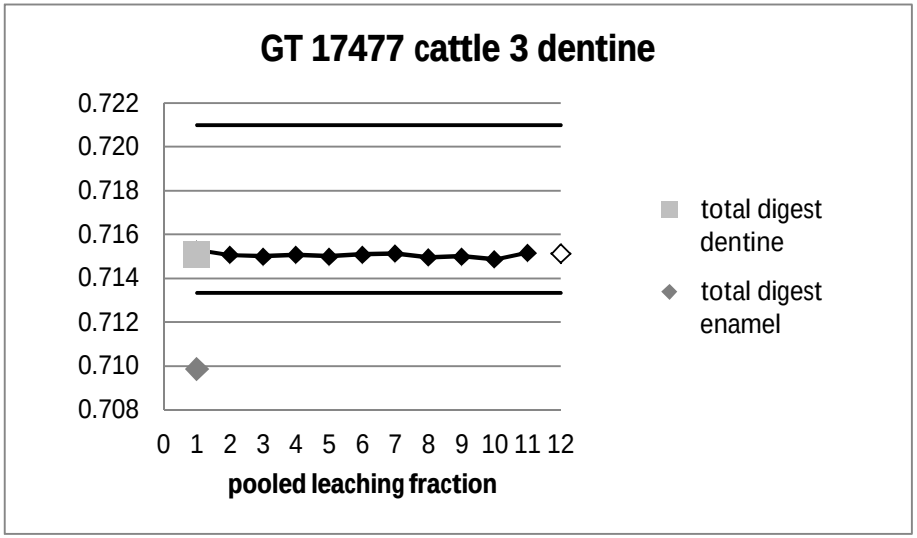
GT 17477 cattle 3 dentine
0.722
0.720
0.718
0.716
0.714
0.712
0.710
0.708
0 1 2 3 4 5 6 7 8 9 10 11 12
pooled leaching fraction
total digest dentine
total digest enamel

7.2.2. $^{87}Sr/^{86}Sr$ ratios of sheeps

7.2.2.1. Right lower jaw bone of sheep 'Stronzi'

inside			outside		
sample code	$^{87}Sr/^{86}Sr$	Stddev	sample code	$^{87}Sr/^{86}Sr$	Stddev
1A	0.7086	0.00001	1B	0.7086	0.00001
2A	0.7087	0.00001	2B	0.7086	0.00001
3A	0.7085	0.00001	3B	0.7087	0.00001
4A	0.7087	0.00001	4B	0.7087	0.00001
5A	0.7086	0.00001	5B	0.7090	0.00003
6A	0.7086	0.00001	6B	0.7087	0.00001
7A	0.7087	0.00001	7B	0.7087	0.00001
8A	0.7086	0.00001			

7.2.2.2. Right lower jaw bone of sheep 'Anja'

sample code	$^{87}Sr/^{86}Sr$	$^{86}Sr/^{88}Sr$	sample code	$^{87}Sr/^{86}Sr$	$^{86}Sr/^{88}Sr$
0A	0.6771	0.1251	0B	0.5331	0.1565
1A	0.5952	0.1427	1B	0.6467	0.1285
2A	0.6181	0.1373	2B	0.6343	0.1310
3A	0.6265	0.1354	3B	0.5693	0.1492
4A	0.6384	0.1328	4B	0.5901	0.1412
5A	0.6495	0.1281	5B	0.6319	0.1341
6A	-	-	6B	0.6331	0.1339
7A	-	-	7B	0.4800	0.1777
8A	0.6673	0.1269	8B	0.6655	0.1273

7.2.3. $^{87}Sr/^{86}Sr$ ratios Roseldorf

7.2.3.1. Water samples

sample code	sample number	location name	x coordinate	y coordinate	$^{87}Sr/^{86}Sr$	stddev	rock type	geological age
RD_W_1	5	Sandberg	15.967800	48.658580	0.7101	0.00001	loess, clay, silt	Pleistocene, Miocene
RD_W_2	8	Sandberg	15.967800	48.658580	0.7104	0.00001	loess, clay, silt	Pleistocene, Miocene
RD_W_3	13	Sandberg	15.967800	48.655560	0.7104	0.00003	loess, clay, silt	Pleistocene, Miocene
RD_W_4	15	Sulzbach	48.675530	15.972090	0.7103	0.00002	clay, silt	Miocene
RD_W_5	17	Sulzgraben	15.974920	48.691540	0.7101	0.00001	clay, silt, sand	Pleistocene
RD_W_6	18	Zellerndorf	15.952550	48.695810	0.7114	0.00001	loess, clay, silt, sand	Pleistocene, Miocene
RD_W_7	19	Pulkau	15.952360	48.697570	0.7131	0.00002	loess, clay, silt, sand	Pleistocene, Miocene
RD_W_8	21	gotic church	15.954760	48.700220	0.7107	0.00001	loess, clay, silt, sand	Pleistocene, Miocene
RD_W_9	24	Zellerndorf	15.930890	48.716760	0.7113	0.00002	biotitegranite	Palaeozoic
RD_W_10	26	Mitterretzbach	15.973890	48.783030	0.7152	0.00001	biotite, micaceous granite, loess	Palaeozoic, Pleistocene
RD_W_11	28	Thallerbach	15.847520	48.698910	0.7124	0.00003	loess, lime sand brick, biotitegranite	Pleistocene, Miocene, Palaeozoic
RD_W_12	32	Maignerbach	15.850782	48.669708	0.7127	0.00002	loess, lime sand brick, biotitegranite	Pleistocene, Miocene, Palaeozoic
RD_W_13	33	Schmida	15.849560	48.645830	0.7113	0.00002	loess, biotitegranite	Pleistocene, Palaeozoic
RD_W_14	34	Grafenbergerbach	15.852480	48.634920	0.7119	0.00002	loess	Pleistocene
RD_W_15	41	Schmida	15.932020	48.634980	0.7117	0.00002	loess	Pleistocene

7.2.3.2. Soil extracts

sample code	sample number	location name	x coordinate	y coordinate	$^{87}Sr/^{86}Sr$	Stddev	rock type	geological age
RD_1	1	Sandberg	15.967800	48.658580	0.7110	0.00015	loess, clay, silt	Pleistocene, Miocene
RD_2	2	Sandberg	15.967800	48.658580	0.7101	0.00014	loess, clay, silt	Pleistocene, Miocene
RD_3	3	Sandberg	15.967800	48.658580	0.7110	0.00016	loess, clay, silt	Pleistocene, Miocene
RD_4	4	Sandberg	15.967800	48.658580	0.7099	0.00017	loess, clay, silt	Pleistocene, Miocene
RD_5	6	Sandberg	15.967800	48.658580	0.7108	0.00016	loess, clay, silt	Pleistocene, Miocene
RD_6	7	Sandberg	15.967800	48.658580	0.7100	0.00003	loess, clay, silt	Pleistocene, Miocene
RD_7	10	Sandberg	15.967790	48.655560	0.7110	0.00006	loess, clay, silt	Pleistocene, Miocene
RD_8	11	Sandberg	15.967790	48.655560	0.7110	0.00003	loess, clay, silt	Pleistocene, Miocene
RD_9	12	Sandberg	15.967790	48.655560	0.7104	0.00005	loess, clay, silt	Pleistocene, Miocene
RD_10	20	gotic church	15.954340	48.700540	0.7111	0.00002	loess	Pleistocene
RD_11	22	Zellerndorf	15.944720	48.707660	0.7109	0.00002	loess, clay, silt, sand	Pleistocene, Miocene
RD_12	23	Zellerndorf	15.931000	48.717000	0.7122	0.00007	biotitegranite	Palaeozoic
RD_13	27	Heiliger Stein	15.970280	48.792020	0.7138	0.00004	biotite, micaceous granite	Palaeozoic
RD_14	29	Großreipersdorf	15.865170	48.692060	0.7109	0.00003	loess	Pleistocene
RD_15	30	Großreipersdorf	15.847091	48.685010	0.7114	0.00003	loess	Pleistocene
RD_16	31	Großreipersdorf	15.844516	48.675320	0.7112	0.00002	loess	Pleistocene
RD_17	35	Grafenberg	15.859530	48.640610	0.7110	0.00002	loess	Pleistocene
RD_18	36	Grafenberg	15.852940	48.626600	0.7154	0.00007	loess, biotitegranite	Pleistocene, Palaeozoic
RD_19	37	Grafenberg	15.841080	48.623230	0.7108	0.00006	loess	Pleistocene
RD_20	38	Sauberg	15.852910	48.613310	0.7114	0.00002	biotitegranite	Palaeozoic
RD_21	39	Kirchberg	15.886420	48.630410	0.7121	0.00008	biotitegranite	Palaeozoic
RD_22	40	Roseldorf	15.910060	48.645050	0.7107	0.00004	loess	Pleistocene
RD_23	42	Schmida	15.931930	48.634980	0.7114	0.00002	loess	Pleistocene
RD_24	43	Goggendorf	15.924710	48.620210	0.7103	0.00005	loess	Pleistocene
RD_25	44	Goggendorf	15.933150	48.603710	0.7103	0.00004	loess	Pleistocene

7.2.3.3. Cereals and grapes

sample code	sample number	sample type	location name	x coordinate	y coordinate	$^{87}Sr/^{86}Sr$	Stddev	rock type	geological age
RD_G1	9	cereals	Sandberg	15.967810	48.658490	0.7104	0.00006	loess, clay, silt	Pleistocene, Miocene
RD_G2	14	cereals	Sandberg	15.967880	48.655530	0.7105	0.00014	loess, clay, silt	Pleistocene, Miocene
RD_G3	16	cereals	Sulzbach	15.972090	48.675530	0.7110	0.00028	clay, silt	Miocene
RD_T1	25	grape	Zellerndorf	15.931000	48.717000	0.7130	0.00009	biotitegranite	Palaeozoic
RD_T1	25	leaf of grape	Zellerndorf	15.931000	48.717000	0.7128	0.00009	biotitegranite	Palaeozoic
RD_T1	25	branche of grape	Zellerndorf	15.931000	48.717000	0.7127	0.00001	biotitegranite	Palaeozoic
RD_T1	25	all grape components	Zellerndorf	15.931000	48.717000	0.7129	0.00012	biotitegranite	Palaeozoic

7.2.3.4. Human teeth

inventory number	sample ID	find spot	age	tooth material	$^{87}Sr/^{86}Sr$	Stddev
R7-14-3-3-51	R7-14-3-3-51_E	Object 14	adult	enamel	0.7089	0.00001
R7-14-3-3-51	R7-14-3-3-51_D	Object 14	adult	dentine	0.7103	0.00001
SENr. 48; 14/3798	Obj.14-1	Object 14	adult	enamel	0.7109	0.00001
SENr. 48; 14/3798	Obj.14-2	Object 14	adult	enamel	0.7105	0.00002
SENr. 2; 30-1031	Object 30/I_1	Object 30/I	child	enamel/Maxilla	0.7101	0.00001
SENr. 2; 30-1031	Object 30/I_2	Object 30/I	child	enamel/Maxilla	0.7099	0.00001
SENr. 2; 30-1031	Object 30/I_3	Object 30/I	child	enamel/Maxilla	0.7108	0.00003

7.2.3.5. Animal teeth

inventory number	animal type	find spot	possible origin	tooth	$^{87}Sr/^{86}Sr$	Stddev
R3-1-16-107-2548	cattle	Object 1	Celtic	Molar/Mandibula	0.7094	0.00001
R3-1-15-103-2260	cattle	Object 1	Celtic	Molar/Mandibula	0.7094	0.00002
R1-50-112	cattle	Settlement	Celtic	M3/Mandibula	0.7094	0.00004
R4-1-15-117-3735	cattle	Object 1	Celtic	M3/Mandibula	0.7100	0.00001
R5-1-15-43-4489	cattle	Object 1	Italian	M3/Mandibula	0.7101	0.00002
R1-28-13	cattle	Settlement	Italian	M3/Mandibula	0.7103	0.00003
R6-1-11-59-5614	cattle	Object 1	Celtic	Molar/Mandibula	0.7103	0.00002
R2-1-4-37-365	cattle	Object 1	Celtic	M3/Mandibula	0.7103	0.00002
R4-1-15-131-4285	cattle	Object 1	Celtic	M3/Mandibula	0.7105	0.00003
R3-1-15-103-2788	cattle	Object 1	Celtic	Molar/Mandibula	0.7106	0.00002
R3-1-1-43-2953	cattle	Object 1	Celtic	M3/Mandibula	0.7106	0.00001
R3-1-16-70-1934	cattle	Object 1	Italian	M3/Mandibula	0.7109	0.00002
R3-1-12-60-1745	cattle	Object 1	Italian	M3/Mandibula	0.7109	0.00002
R4-1-5-53-4328	cattle	Object 1	Italian	M3/Mandibula	0.7110	0.00002
R1-140-89	cattle	Settlement	Italian	M3/Mandibula	0.7111	0.00004
R1-168-102	cattle	Settlement	Celtic	M3/Mandibula	0.7114	0.00002
R2-1-12-2-858	cattle	Object 1	Celtic	M3/Mandibula	0.7118	0.00002
R2-1-14-54-607	cattle	Object 1	Celtic	M3/Mandibula	0.7124	0.00002
R1-227-209	horse	Settlement	Celtic	Premolar/Maxila	0.7091	0.00002
R1-0.Nr	horse	Settlement	Celtic	Premolar/Maxila	0.7092	0.00002
R3-1-1-43-2702	horse	Object 1	Celtic	M1-2/Maxila	0.7094	0.00002
R3-1-1-2-2027	horse	Object 1	Celtic	M1-2/Mandibula	0.7099	0.00001
R4-1-15-135-4366	horse	Object 1	Celtic	M1-2/Maxila	0.7099	0.00002
R3-1-16-43-2268	horse	Object 1	Celtic	M1-2/Maxila	0.7101	0.00003
R2-1-18-2-941	horse	Object 1	Celtic	M1-2/Mandibula	0.7101	0.00002
R6-1-10-217-5495	horse	Object 1	Celtic	M1-2/Mandibula	0.7113	0.00002
R2-1-4-2-945	horse	Object 1	Celtic	M1-2/Maxila	0.7122	0.00002
R6-1-10-217-5490	horse	Object 1	Celtic	M1-2/Mandibula	0.7156	0.00187
R2-1-4-37-951	horse	Object 1	Celtic	M1-2/Maxila	0.7166	0.00153
R2-1-12-2-454	horse	Object 1	Celtic	M1-2/Mandibula	0.7166	0.00012

7.2.4. Multielementdata Roseldorf

7.2.4.1. Water samples

	Sr [µg g^{-1}]	Rb [ng g^{-1}]	Al [µg g^{-1}]	Fe [µg g^{-1}]	Zn [ng g^{-1}]	Mg [µg g^{-1}]	Ba [µg g^{-1}]	U [ng g^{-1}]	As [ng g^{-1}]	Pb [ng g^{-1}]
RD_W_1	1.25	7.25	6.64	5.70	36.97	42.46	0.29	4.55	5.29	29.63
RD_W_2	0.11	1.21	0.29	0.37	10.47	3.70	0.02	1.28	0.84	1.43
RD_W_3	0.01	0.34	0.11	0.21	2.87	0.27	0.01	0.19	0.40	0.90
RD_W_4	1.95	0.92	0.01	0.55	1.41	131.63	0.06	54.41	2.07	0.73
RD_W_5	2.93	1.49	0.02	1.55	5.73	163.86	0.07	43.71	2.76	0.15
RD_W_6	1.79	18.82	0.07	1.25	12.57	129.61	0.13	12.70	7.25	0.79
RD_W_7	0.32	2.54	0.77	2.42	33.81	16.59	0.11	3.25	3.90	8.05
RD_W_8	4.29	192.35	0.79	6.94	94.60	100.52	1.53	10.57	131.83	8.71
RD_W_9	0.60	13.69	1.41	4.33	90.19	19.81	0.26	3.66	35.67	19.12
RD_W_10	1.65	6.98	0.35	3.56	30.78	71.78	0.28	21.00	16.86	4.24
RD_W_11	4.98	45.33	0.10	4.27	60.40	261.36	0.81	58.58	13.59	1.56
RD_W_12	4.13	22.06	1.36	7.63	124.30	191.78	0.92	43.07	19.22	16.50
RD_W_13	4.95	18.90	0.44	5.73	77.20	180.53	0.85	53.63	13.44	9.14
RD_W_14	5.07	43.97	0.25	4.19	83.66	332.24	0.81	82.04	21.08	2.02
RD_W_15	5.54	27.42	1.17	7.80	123.83	307.68	0.85	83.77	20.84	17.92
LoD [ng g^{-1}]	4.64	0.20	3.72	21.61	0.03	18.56	0.002	0.07	0.05	0.08

7.2.4.2. Soil samples

sample ID	Sr [µg g^{-1}]	Rb [ng g^{-1}]	Al [ng g^{-1}]	Fe [µg g^{-1}]	Zn [µg g^{-1}]	Mg [µg g^{-1}]	Ba [µg g^{-1}]	U [ng g^{-1}]	As [ng g^{-1}]	Pb [ng g^{-1}]
RD_1	70.87	388.30	43.28	5.74	0.22	240.44	4.88	2.67	<LoD	1.36
RD_2	70.92	271.76	1154.52	9.13	0.52	191.48	9.15	1.97	<LoD	2.34
RD_3	70.80	248.46	66.11	5.32	0.19	213.23	4.47	3.21	<LoD	0.40
RD_4	70.58	247.39	41.21	7.87	0.47	172.95	8.95	2.06	<LoD	2.83
RD_5	40.37	392.75	39.56	5.75	0.17	211.20	4.08	2.54	<LoD	1.52
RD_6	40.53	241.65	31.83	7.61	0.44	167.74	8.48	1.64	<LoD	1.30

RD_7	40.03	384.03	7.21	4.67	0.32	201.95	6.19	1.38	<LoD	0.62
RD_8	20.88	441.53	12.00	4.92	0.38	170.10	6.96	1.81	<LoD	0.62
RD_9	30.62	296.67	6.08	6.69	0.46	157.06	8.73	2.37	<LoD	0.48
RD_10	30.70	100.84	15.74	4.38	0.36	200.54	6.67	2.50	1.52	1.15
RD_11	30.51	152.25	6.10	5.80	0.58	171.41	10.59	0.98	<LoD	1.83
RD_12	30.13	155.49	18.79	4.70	0.44	150.69	8.06	1.30	<LoD	1.14
RD_13	30.18	380.76	<LoD	7.35	0.59	177.21	11.02	0.38	<LoD	<LoD
RD_14	50.93	122.38	11.36	1.92	0.12	507.98	3.34	10.22	4.23	5.47
RD_15	40.88	70.59	107.58	5.31	0.78	209.31	13.67	3.86	<LoD	1.71
RD_16	10.99	103.74	119.63	4.58	0.42	147.35	7.88	1.06	3.83	3.27
RD_17	30.21	219.31	53.76	6.37	0.92	157.64	16.20	1.24	<LoD	0.15
RD_18	10.89	54.97	198.37	2.97	0.38	190.47	3.71	0.57	<LoD	2.05
RD_19	20.63	104.89	<LoD	5.94	0.68	140.69	12.62	1.18	<LoD	0.06
RD_20	20.48	158.68	<LoD	6.12	0.64	150.38	11.81	1.29	<LoD	<LoD
RD_21	60.58	411.84	14.89	7.66	0.49	254.17	9.48	1.85	<LoD	<LoD
RD_22	30.02	215.97	24.22	6.78	0.62	163.71	11.31	0.66	<LoD	4.56
RD_23	40.70	99.54	49.04	3.72	0.39	313.44	7.23	2.15	1.77	0.22
RD_24	30.27	177.16	45.58	6.25	0.57	150.91	10.51	1.34	<LoD	<LoD
RD_25	20.66	62.74	54.61	3.77	0.32	172.13	5.68	2.63	<LoD	1.00
LoD [ng g^{-1}]	81.95	11.27	2.14	71.59	27.34	50.67	5.40	0.76	0.18	0.12

7.2.4.3. Animal and human teeth

inventory number	Sr [µg g^{-1}]	Rb [ng g^{-1}]	Al [µg g^{-1}]	Fe [µg g^{-1}]	Zn [µg g^{-1}]	Ca [mg/g]	Mg [µg g^{-1}]	Ba [µg g^{-1}]	U [ng g^{-1}]	As [ng g^{-1}]	Pb [ng g^{-1}]
R1-0.Nr	78.4	55.1	5.2	215.0	22.2	76.1	495.9	10.7	42.7	50.4	72.5
R1-28-13	39.2	53.1	9.3	246.0	16.8	81.0	345.7	24.7	29.9	<LoD	164.3
R1-50-112	80.4	106.8	18.9	264.7	41.1	76.3	379.0	37.2	21.9	<LoD	321.8
R1-140-89	49.1	144.0	29.3	277.3	12.7	78.7	591.0	26.5	30.9	129.1	136.4
R1-168-102	39.7	312.2	54.1	326.1	28.6	80.9	345.5	35.5	23.7	26.1	189.2
R1-227-209	71.3	809.6	173.3	530.6	15.2	74.7	575.4	7.5	25.6	203.2	220.6
R2-1-4-2-945	56.2	85.2	20.0	264.6	11.9	79.9	333.0	9.6	87.6	<LoD	178.0
R2-1-4-37-365	42.8	148.4	42.6	314.4	14.9	79.9	400.1	29.0	71.6	9.9	353.4

R2-1-4-37-951	117.0	88.0	14.9	256.9	13.3	79.1	369.3	22.4	202.7	13.5	108.1
R2-1-12-2-454	91.2	38.1	9.2	446.0	121.9	77.5	520.8	14.5	88.3	1.4	114.9
R2-1-12-2-858	48.3	97.6	16.0	272.9	18.2	83.8	459.4	25.6	59.8	26.7	103.1
R2-1-14-54-607	41.5	62.8	7.9	231.6	21.0	73.3	295.7	19.7	32.4	10.7	167.3
R2-1-18-2-941	89.7	48.7	9.4	266.2	29.8	74.6	374.1	19.7	501.4	<LoD	467.2
R3-1-1-2-2027	118.1	70.0	25.3	286.3	19.4	82.2	648.9	16.0	324.0	<LoD	314.9
R3-1-1-43-2702	132.7	81.3	20.3	276.5	29.1	79.1	436.2	13.8	345.4	25.5	225.5
R3-1-1-43-2953	58.5	42.9	8.8	265.5	17.1	83.8	508.0	45.7	100.9	<LoD	192.8
R3-1-12-60-1745	44.4	145.3	43.3	318.3	16.1	79.7	437.7	16.2	225.1	<LoD	230.3
R3-1-15-103-2260	57.3	504.4	135.0	449.5	20.3	80.3	464.9	21.1	29.3	5.0	254.7
R3-1-15-103-2788	78.2	71.6	14.8	269.3	19.3	82.9	488.3	23.0	42.7	<LoD	289.7
R3-1-16-43-2268	109.5	40.9	12.2	253.6	24.1	80.6	465.1	10.3	400.5	<LoD	381.3
R3-1-16-70-1934	64.9	214.8	86.5	355.3	30.2	80.0	345.4	34.3	566.5	74.5	443.6
R3-1-16-107-2548	91.5	50.3	14.7	199.9	14.5	61.2	269.4	48.0	147.1	6.9	191.9
R4-1-5-53-4328	30.1	307.8	102.3	342.6	12.6	55.8	356.5	13.7	41.5	<LoD	647.5
R4-1-15-117-3735	69.1	56.2	12.0	284.0	25.2	83.7	426.9	24.9	32.4	60.0	409.8
R4-1-15-131-4285	52.6	813.3	239.7	604.6	26.4	76.5	441.9	24.7	66.2	199.8	460.0
R4-1-15-135-4366	99.1	224.7	66.7	353.2	23.2	80.6	412.0	15.0	249.4	<LoD	252.6
R5-1-15-43-4489	28.0	147.0	44.8	201.3	15.4	43.7	185.4	14.1	106.0	<LoD	157.8
R6-1-10-217-5490	72.5	43.4	7.6	221.7	11.0	74.5	498.4	12.3	119.8	<LoD	75.6
R6-1-10-217-5495	84.8	43.4	11.3	236.5	17.7	80.0	513.0	16.0	87.1	<LoD	72.4
R6-1-11-59-5614	53.4	176.0	60.2	319.4	19.5	82.9	394.1	20.7	189.2	7.8	413.1
R7-14-3-3-51E	18.1	<LoD	31.8	132.7	7.6	40.6	380.7	0.2	b. d.	<LoD	263.2
R7-14-3-3-51D	33.1	<LoD	52.1	136.6	24.3	35.1	269.6	20.3	247.6	<LoD	294.0
Obj14	11.2	844.5	406.1	642.1	35.0	35.6	401.3	1.6	<LoD	<LoD	401.1
Obj301I_1	11.6	354.7	39.7	156.6	18.5	42.9	347.9	0.2	b. d.	<LoD	204.2
obj301I_2	14.0	18.2	10.9	129.2	17.3	43.0	360.9	1.3	b. d.	<LoD	109.4
obj301I_3	15.8	<LoD	25.8	139.9	21.6	40.0	331.4	1.8	2.0	<LoD	53.7
LoD [ng g^{-1}]	36.82	7.93	1.47	36.81	6.12	125.73	53.76	2.52	0.03	0.02	0.02

inventory number	Sr*1000/Ca	animal type/origin	$^{87}Sr/^{86}Sr$	local character
R1-168-102	0.50	cattle settlement/Celtic	0.7114	non-local
R1-28-13	0.51	cattle settlement/Italian	0.7103	local
R2-1-4-37-365	0.55	cattle object 1/Celtic	0.7103	local
R4-1-5-53-4328	0.55	cattle object 1/Italian	0.7110	local
R3-1-12-60-1745	0.57	cattle object 1/Italian	0.7109	local
R2-1-14-54-607	0.59	cattle object 1/Celtic	0.7124	non-local
R2-1-12-2-858	0.60	cattle object 1/Celtic	0.7118	non-local
R1-140-89	0.65	cattle settlement/Italian	0.7111	local
R5-1-15-43-4489	0.66	cattle object 1/Italian	0.7101	local
R6-1-11-59-5614	0.66	cattle object 1/Celtic	0.7103	local
R4-1-15-131-4285	0.71	cattle object 1/Celtic	0.7105	local
R3-1-1-43-2953	0.73	cattle object 1/Celtic	0.7106	local
R3-1-15-103-2260	0.73	cattle object 1/Celtic	0.7094	non-local
R3-1-16-70-1934	0.83	cattle object 1/Italian	0.7109	local
R4-1-15-117-3735	0.85	cattle object 1/Celtic	0.7100	local
R3-1-15-103-2788	0.97	cattle object 1/Celtic	0.7094	non-local
R1-50-112	1.08	cattle settlement/Celtic	0.7094	non-local
R3-1-16-107-2548	1.54	cattle object 1/Celtic	0.7094	non-local
R2-1-4-2-945	0.72	horse object 1/Celtic	0.7122	non-local
R1-227-209	0.98	horse settlement/Celtic	0.7091	non-local
R6-1-10-217-5490	1.00	horse object 1/Celtic	0.7156	non-local
R1-0.Nr	1.06	horse settlement/Celtic	0.7092	non-local
R6-1-10-217-5495	1.09	horse object 1/Celtic	0.7113	non-local
R2-1-12-2-454	1.22	horse object 1/Celtic	0.7166	non-local
R2-1-18-2-941	1.23	horse object 1/Celtic	0.7101	local
R4-1-15-135-4366	1.26	horse object 1/Celtic	0.7099	local
R3-1-16-43-2268	1.40	horse object 1/Celtic	0.7101	local
R3-1-1-2-2027	1.47	horse object 1/Celtic	0.7099	local
R2-1-4-37-951	1.54	horse object 1/Celtic	0.7166	non-local
R3-1-1-43-2702	1.73	horse object 1/Celtic	0.7094	non-local
R7-14-3-3-51	0.44	human enamel	0.7089	non-local
R7-14-3-3-51	0.95	human dentine	0.7103	local
Obj. 14	0.32	human enamel/object 14	0.7107	local
Obj. 30/I	0.33	human enamel/object 30/I	0.7103	local

7.4. List of Tables

Tab. 1	IUPAC isotope abundances of Sr and Rb
Tab. 2	Human migration studies based on Sr isotope ratio measurements
Tab. 3	Strategies for generating $^{87}Sr/^{86}Sr$ isoscapes
Tab. 4	Development stages of permanent human teeth
Tab. 5	Eruption time of milk teeth and change to permanent teeth
Tab. 6	Dental development stages of cattle
Tab. 7	Mineralization and growth time of horse permanent enamel
Tab. 8	Dental development stages of horses
Tab. 9	Sample list of archaeological tissues from Gars Thunau used for sequential leaching
Tab. 10	Samples from Gars Thunau used for digestion
Tab. 11	Sample list of the right lower jaw bone of the sheep 'Stronzi'
Tab. 12	Sample list of the right lower jaw bone of Anja
Tab. 13	Sample list of animal tooth enamel excavated in Roseldorf
Tab. 14	Sample list of human tooth material excavated in Roseldorf
Tab. 15	Sample list of soil material sampled at the site in Roseldorf and in surrounding areas
Tab. 16	Sample list of recent fauna sampled at the site in Roseldorf and in surrounding areas
Tab. 17	Sample list of water derived sampled at the site in Roseldorf and in surrounding areas
Tab. 18	Pooled leaching fractions
Tab. 19	Microwave program for cereals
Tab. 20	Microwave program for grapes
Tab. 21	ELAN DRC-e parameters
Tab. 22	Element concentrations in ng g^{-1} in standard solutions
Tab. 23	NuPlasma instrument settings for Sr isotope ratio measurements
Tab. 24	Faraday collector block setup

Tab. 25 Elemental ratios Ca/P and Sr/Ca of sheep hard tissues
Tab. 26 The Ca/P ratios of leached human hard tissues
Tab. 27 The Ca/P ratios of leached animal hard tissues
Tab. 28 The Sr*1000/Ca ratios of leached human hard tissues
Tab. 29 The Sr*1000/Ca ratios of leached animal hard tissues
Tab. 30 The $^{87}Sr/^{86}Sr$ ratios of leached human and animal samples
Tab. 31 The Sr isotope ratios of hay, water and soil
Tab. 32 The geological background of the Weinviertel
Tab. 33 $^{87}Sr/^{86}Sr$ ranges related to the geological background
Tab. 34 Locations belonging to the first Sr isotope package
Tab. 35 Locations belonging to the second isotope package
Tab. 36 Cattle and horses excavated at Roseldorf related to the geological background
Tab. 37 Non-autochthonous cattle and horses
Tab. 38 Cattle and horse corresponding to the second Sr isotope package
Tab. 39 Horses with the highest $^{87}Sr/^{86}Sr$ ratios and their possible place of origin
Tab. 40 Elemental concentrations in soil material
Tab. 41 Elemental concentrations in water samples
Tab. 42 Elemental concentrations in animal tooth enamel

7.5. List of Figures

Fig. 1 Tooth anatomy
Fig. 2 Human dentition
Fig. 3 Cattle dentition
Fig. 4 M_3 cattle Mandibula
Fig. 5 Horse dentition
Fig. 6 Molar horse Mandibula
Fig. 7 The location of the Celtic settlement site Roseldorf
Fig. 8 The cultic area of Roseldorf
Fig. 9 The finding complex Object 1

Fig. 10	Possible reconstruction of a sanctuary
Fig. 11	Fragmented human and animal remains
Fig. 12	Drilling positions of the right lower jaw bone of ‘Stronzi’
Fig. 13	Drilling positions of the right lower jaw bone of Anja
Fig. 15	Drilled teeth of human individuals excavated in Roseldorf
Fig. 16	Sample locations of environmental material
Fig. 17	Elemental ratios of leachates of human dentine GT 24958
Fig. 18	$^{87}Sr/^{86}Sr$ ratios of pooled leaching fractions of human dentine GT 24958
Fig. 19	Elemental ratios of leachates of human enamel GT 24958
Fig. 20	$^{87}Sr/^{86}Sr$ ratios of pooled leaching fractions of human enamel GT 24958
Fig. 21	Elemental ratios of leachates of human dentine GT 25096
Fig. 22	$^{87}Sr/^{86}Sr$ ratios of pooled leaching fractions of human dentine GT 25096
Fig. 23	Elemental ratios of leachates of sheep dentine
Fig. 24	$^{87}Sr/^{86}Sr$ ratios of pooled leaching fractions of sheep dentine
Fig. 25	Elemental ratios of leachates of sheep jaw bone
Fig. 26	$^{87}Sr/^{86}Sr$ ratios of pooled leaching fractions of sheep jaw bone
Fig. 27	Elemental ratios of leachates of horse dentine
Fig. 28	$^{87}Sr/^{86}Sr$ ratios of pooled leaching fractions of horse dentine
Fig. 29	Elemental ratios of leachates of cattle dentine
Fig. 30	$^{87}Sr/^{86}Sr$ ratios of pooled leaching fractions of cattle dentine
Fig. 31	Distribution of $^{87}Sr/^{86}Sr$ ratios on Stronzi’s right lower jaw bone
Fig. 32	Distribution of $^{86}Sr/^{88}Sr$ and $^{87}Sr/^{86}Sr$ ratios Anja’s right lower jaw bone
Fig. 33	$^{87}Sr/^{86}Sr$ and $^{86}Sr/^{88}Sr$ ratios of Anja’s jaw bone
Fig. 34	$^{87}Sr/^{86}Sr$ ratios of environmental material
Fig. 35	Spatial variation of $^{87}Sr/^{86}Sr$ ratios of environmental material
Fig. 36	Spatial distribution of Sr isotope packages
Fig. 37	Definition of the local Sr isotope range of Celtic excavation site Roseldorf

Fig. 38 $^{87}Sr/^{86}Sr$ ratios of Roseldorf's surroundings
Fig. 39 $^{87}Sr/^{86}Sr$ ratios of Roseldorf's human tooth samples
Fig. 40 $^{87}Sr/^{86}Sr$ ratios of Roseldorf's cattle and horse tooth enamel samples
Fig. 41 $^{87}Sr/^{86}Sr$ ratios of Roseldorf's cattle and horse tooth enamel samples and environmental material
Fig. 42 Places of the possible origin of horses with the highest $^{87}Sr/^{86}Sr$ ratios
Fig. 43 Sr*1000/Ca ratios of animal and human tooth material

7.6. List of Abbreviations

BC	before Christ
cps	counts per second
CRM	Certified Reference Material
DRC	Dynamic Reaction Cell
DSN	Desolvating Nebulizer
e.g.	exempli gratia
equ.	equation
eV	electron Volt
GPS	Global Positioning System
HR SF ICP MS	High Resolution Sector Field Inductively Coupled Plasma Mass Spectrometry
ICP-QMS	Inductively Coupled Plasma-Quadrupole-Mass Spectrometry
IUPAC	International Union of Pure and Applied Chemistry
LoD	Limit of Detection
MC	Multiple Collector
NIST	National Institute of Standardisation and Technology
PFA	perfluoroalkoxy
RF	Radio Frequency
SRM	Standard Reference Material
TIMS	Thermal Ionisation Mass Spectrometry